AEDC-TR-68-108

Copy No-1

INVESTIGATION OF JET BOUNDARY SIMULATION PARAMETERS FOR UNDEREXPANDED JETS IN A QUIESCENT ATMOSPHERE

R. D. Herron

ARO, Inc.

September 1968

PROPULSION WIND TUNNEL FACILITY
ARNOLD ENGINEERING DEVELOPMENT CENTER
AIR FORCE SYSTEMS COMMAND
ARNOLD AIR FORCE STATION, TENNESSEE

NOTICES

When U. S. Government drawings specifications, or other data are used for any purpose other than a definitely related Government procurement operation, the Government thereby incurs no responsibility nor any obligation whatsoever, and the fact that the Government may have formulated, furnished, or in any way supplied the said drawings, specifications, or other data, is not to be regarded by implication or otherwise, or in any manner licensing the holder or any other person or corporation, or conveying any rights or permission to manufacture, use, or sell any patented invention that may in any way be related thereto.

Qualified users may obtain copies of this report from the Defense Documentation Center.

References to named commercial products in this report are not to be considered in any sense as an endorsement of the product by the United States Air Force or the Government.

INVESTIGATION OF JET BOUNDARY SIMULATION PARAMETERS FOR UNDEREXPANDED JETS IN A QUIESCENT ATMOSPHERE

R. D. Herron
ARO, Inc.

FOREWORD

The research reported herein was sponsored by the Arnold Engineering Development Center (AEDC), Air Force Systems Command (AFSC), under Program Element 6540223F and is related to Project 8953, Task 895309.

The results of research presented in this report were obtained by ARO, Inc. (a subsidiary of Sverdrup & Parcel and Associates, Inc.), contract operator of the AEDC, AFSC, Arnold Air Force Station, Tennessee, under Contract F40600-69-C-0001. The work was performed from March 1965 to June 1967 under ARO Projects No. PW5728 and PW3517, and the manuscript was submitted for publication on April 18, 1968.

This technical report has been reviewed and is approved.

Carl E. Simmons
Captain, USAF
Research Division
Directorate of Plans
and Technology

Edward R. Feicht
Colonel, USAF
Director of Plans
and Technology

ABSTRACT

An experimental and theoretical investigation was conducted to determine the degree of jet boundary simulation obtainable for underexpanded jets exhausting into a quiescent atmosphere. Tests were conducted with nitrogen, carbon dioxide, and helium gases, and theoretical boundaries were obtained by a method-of-characteristics solution. It was determined that the method-of-characteristics solution accurately represents the experimental jet boundaries and that the matching of the parameters δ_j and M_1/γ gives good boundary simulation for a wide range of jet conditions. Also a rapid, simple method for estimating jet boundary shape is developed from the method-of-characteristics results.

CONTENTS

APPENDIXES

I. ILLUSTRATIONS

Figure

NOMENCLATURE

A_S/A^*	Nozzle spherical area ratio, $\frac{2}{1 + \cos \theta_N} \left(\frac{d_e}{d^*}\right)^2$
d_e	Nozzle exit diameter
d^*	Nozzle throat diameter
ℓ_j	Distance along the nozzle wall measured from the throat to the nozzle exit
ℓ_1	Distance measured from the nozzle exit along the inviscid jet boundary
M	Mach number
n	Distance measured normal to the inviscid jet boundary, positive outside the inviscid jet
p	Pressure
p_p	Pressure measured by the traversing probe

r	Jet radius
r_e	Nozzle exit radius
T	Temperature
V_j	Velocity at the nozzle exit
x	Distance from the nozzle exit measured along the nozzle axis, positive downstream
β	$\sqrt{M^2 - 1}$
γ	Ratio of specific heats
δ_j	Jet boundary initial angle relative to the nozzle axis
θ_N	Nozzle half-angle
μ_j	Coefficient of viscosity corresponding to static conditions at the nozzle exit
ν	Prandtl-Meyer angle
ρ	Density

SUBSCRIPTS (Reference circled symbols in sketch below)

1	Jet boundary conditions
j	Nozzle exit conditions
t	Total or stagnation conditions
∞	Atmospheric or ambient conditions

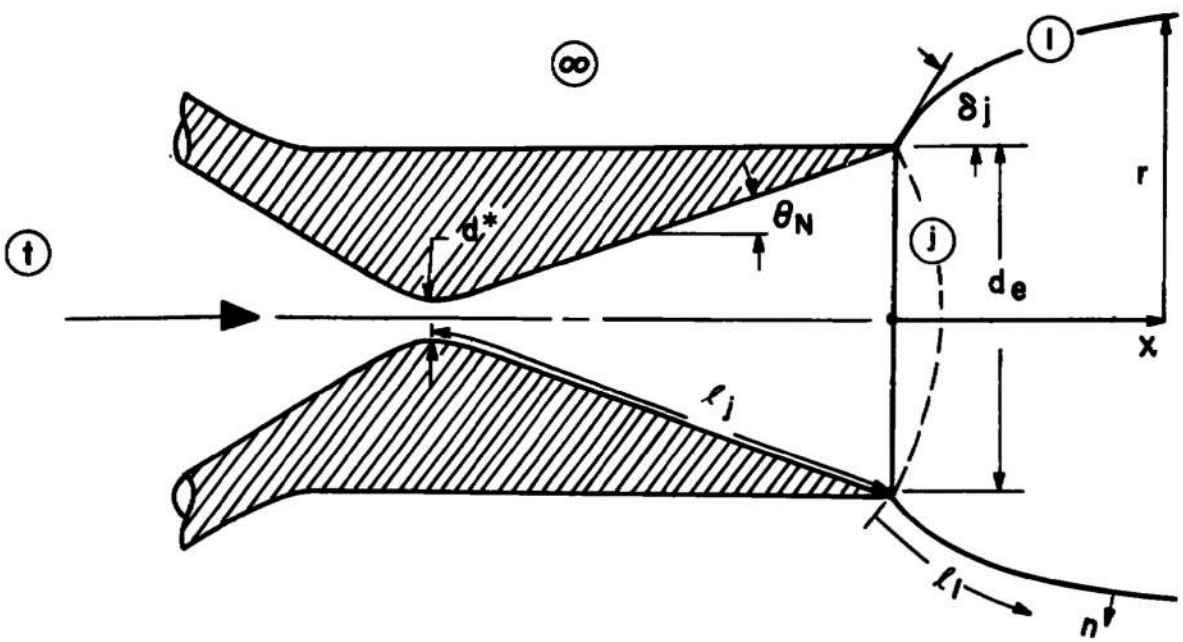

SECTION I
INTRODUCTION

In recent years, much interest has arisen in the structure and properties of highly underexpanded rocket or ramjet exhaust plumes. This interest has been created by problems such as heating and erosion of adjacent surfaces, radar and communication signal interference, separation of flow over the vehicle, and radiation emitted by the large exhaust plumes. Studies of and attempts to obtain solutions to these problems have led to the construction of high altitude test facilities and the adaptation of some existing facilities. Methods used for the experimental simulation of the full-scale jets vary in complexity from the use of small cold-gas jets to an almost exact duplication of the full-scale jets. The degree of similitude required and/or used depends on the particular problem under investigation and is discussed in Ref. 1. However the tremendous vacuum pumping capacities required and the complexity and cost of hot rocket tests frequently dictate that studies be conducted with small jets of cold gases.

One jet characteristic frequently desired is that the boundary of the experimental jet duplicates that of the full-scale jet. In an early study, Love (Ref. 2) concluded that for slightly underexpanded jets (p_j/p_∞ from 1 to 10) good boundary simulation was obtained if the initial angle, δ_j, of the jet boundary was matched. Goethert (Ref. 3) later proposed matching the parameters δ_j and $\gamma M_j^2/\beta_j$ for highly underexpanded jets. Pindzola (Ref. 4) concluded that better simulation could be obtained by matching δ_j and $\gamma M_1^2/\beta_1$ where the Mach number is now based on the jet boundary conditions rather than the nozzle exit conditions as proposed by Goethert.

The objective of the investigation reported herein was to determine the degree of jet boundary simulation obtained using Pindzola's parameters and to determine if other simulation parameters might prove more useful. The investigation included both experimental and theoretical studies of the jet boundaries. Values of the simulation parameters δ_j and $\gamma M_1^2/\beta_1$ were selected that were representative of underexpanded jet plumes, and tests were conducted with nitrogen (N_2), helium (He), and carbon dioxide (CO_2) jets at constant values of the parameters. In addition, jet boundaries were calculated for several sets of simulation parameters by an approximate method and also by a method-of-characteristics solution.

From these studies it was determined that although the parameters δ_j and $\gamma M_1^2/\beta_1$ gave good jet boundary duplication, better duplication

could be obtained by matching the parameters δ_j and M_1/γ. Also, a simple method was developed for rapidly predicting the jet boundary for a wide range of conditions.

SECTION II
THEORETICAL BOUNDARY CALCULATIONS

2.1 LATVALA'S APPROXIMATION

The approximation used by Pindzola (Ref. 4) for the original evaluation of the simulation parameters δ_j and $\gamma M_1^2/\beta_1$ was developed by Latvala in Ref. 5. Latvala's approximation is based on quasi-one-dimensional relations and the assumption of isentropic, radial flow from the nozzle. It is an adaptation of a method presented by Adamson and Nichols in Ref. 6, but uses a spherical rather than a planar area to define the flow area of the jet.

The approximate solution starts with the known initial angle of the jet, δ_j, calculated from

$$\delta_j = \nu_1 - \nu_j + \theta_N \tag{1}$$

The condition of constant pressure along the jet boundary is then used to determine the changes in jet boundary angle required to compress the flow and balance the pressure decrease caused by the one-dimensional flow area increase. The relation between turning angle and pressure change is given by the Prandtl-Meyer expansion relation

$$\frac{\Delta p}{p} = \frac{\gamma M_1^2}{\beta_1}(\Delta\nu) + \text{higher order terms in } \Delta\nu \tag{2}$$

which is identical (except for sign of $\Delta\nu$) to the expression for a compression through an oblique shock wave, up to and including the term in $(\Delta\nu)^2$. It is apparent then that two jets that have the same value of the coefficient $\gamma M_1^2/\beta_1$ could be expected to have the same pressure change-deflection angle relation within the limits of the linearization of Eq. (2). This therefore gives rise to the use of δ_j and $\gamma M_1^2/\beta_1$ as the jet boundary simulation parameters.

2.2 METHOD-OF-CHARACTERISTICS SOLUTION

The most accurate method existing for calculating the properties of an inviscid expanding jet is the method of characteristics. However, the accuracy obtained in the actual application depends on factors such

as the knowledge of the actual flow properties at the start of the calculation (the nozzle exit), the frequent assumption of neglecting the jet boundary shock, and the nonideal behavior of the gas. Also, the accuracy is limited by the computer program used because of the finite mesh size rapidly becoming larger as the solution proceeds downstream. In most applications, the effects of the viscous mixing on the jet boundary must be considered.

Application of method-of-characteristics solutions to determine the free jet boundaries have been made by several authors (Refs. 2, 5, and 7 through 12). Among these, Refs. 2, 5, and 7 included limited experimental data for sonic nozzles or low to moderately expanding jets from supersonic nozzles. Experimental determination of jet boundaries for highly underexpanded jets has been prevented by the density limitations of conventional optical instrumentation; therefore a "glow discharge" technique was used in Ref. 12. The method-of-characteristics solution was also compared in Ref. 13 with experimental data on the internal structure of jets expanding into a vacuum. In general, the above authors found the method of characteristics to reasonably predict the jet boundaries and flow properties, within its inherent limitations. A good survey of some of the exact and approximate solutions for the jet structure has been given by Adamson (Ref. 14).

The computer program used for the present calculations was developed by the Lockheed Missile and Space Corporation for use with the IBM 7090 computer. This program computes the supersonic flow properties of a gas discharging from an underexpanded nozzle into either a quiescent atmosphere or a hypersonic free stream. Ideal gas relations, oblique shock relations for the boundary shock, and the axisymmetric method of characteristics are employed. A complete description of the program is given in Ref. 15, and only the principal assumptions and the techniques used in the application of the program are given here.

Jet boundaries presented in this report were computed on an IBM 360/50 computer for the following conditions and assumptions:

1. For the case of a quiescent atmosphere only.
2. Nozzle exit flow properties were computed by the program from ideal gas, one-dimensional flow relations utilizing point source flow (spherical areas). Specific heat ratios of 1.28, 1.40, and 1.667 were used for both the nozzle and the jet flows. The value

of 1.28 used for comparison with experimental tests of CO_2 corresponds to excitation of one of the four modes of the molecular vibration.

3. The method-of-characteristics computation starts on the spherical nozzle exit surface; normally 40 points were used for the origin of the characteristic net.

4. Flow properties for the initial expansion around the nozzle lip are computed from Prandtl-Meyer relations. Approximately 1.5-deg increments were used for the Prandtl-Meyer expansion system.

Recently a new program has been developed (Ref. 16) which includes equilibrium reacting gas mixtures and a wider variety of flow field problems. A comparison of this program with some experimental data is given in Ref. 17. These comparisons include limited data from jets with sonic nozzles and with low exit pressure ratio supersonic nozzles. In general the comparisons were considered very good. This program (Ref. 16) is currently being adapted to the AEDC computer system.

2.3 JET BOUNDARY VISCOUS MIXING REGION

The velocity gradients normal to the flow direction in the interior of the jet are usually small, and therefore viscosity effects are neglected. The jet interior structure can then be calculated by the method of characteristics as described previously. However, the gradients are not negligible at the jet boundary, and effects of viscous mixing must be considered.

Ideally, the inviscid boundary can be determined and the flow properties at the inviscid boundary used to determine the corresponding mixing region flow properties. The viscid mixing solution can then be superimposed on the inviscid jet solution to define the physical jet. This procedure is probably valid if the mixing region is small compared to the jet radius and if no chemical reactions occur.

The growth of the turbulent mixing region was calculated for the conditions corresponding to the present experimental tests using the method given by Bauer in Ref. 18. The type of mixing considered is turbulent, two-dimensional, compressible, isobaric, isoenergetic, and without an initial boundary layer. It is of significance to note that for the high jet boundary Mach numbers considered in this report, the mixing region thickness and velocity distributions are almost identical for all jets. For these, the edges of the mixing regions are: $n/r_e/\ell_1/r_e = 0.13$ for the outer edge and -0.01 for the inner edge.

SECTION III
APPARATUS AND TEST PROCEDURE

3.1 TEST HARDWARE AND PROCEDURE

The experiments reported in this report were conducted in an 18-in. test cell connected to a six-stage steam ejector. The test cell installation is shown in Fig. 1, Appendix I. Test gases were heated by a resistance-type heater and expanded through conical nozzles into the test cell. Test nozzles had throat diameters of approximately 0.1 in.

Two sets of values of the simulation parameters were selected as being representative of typical underexpanded jet plumes:

$$\delta_j = 60 \text{ deg}, \ \gamma M_1^2/\beta_1 = 14$$

and

$$\delta_j = 60 \text{ deg}, \ \gamma M_1^2/\beta_1 = 18$$

These values of the simulation parameters were maintained constant, and tests were conducted with pure gases in 10- and 20-deg half-angle conical nozzles. Nitrogen, CO_2, and He gases were tested at a simulation parameter value of 14; N_2 and He were tested at a value of 18. Different values of ambient pressure and nozzle area ratio were required for each of 10 different nozzles in order to maintain the selected values of the simulation parameters.

Since each gas required a different nozzle area ratio to match the selected value of the simulation parameters, testing began with CO_2 (the largest nozzle area ratio). The nozzle exit was then cut off to give the required area ratios for N_2 and He. The configurations of the various test nozzles are shown in Fig. 2.

Possible effects of nozzle boundary layer, jet viscous mixing, gas condensation, specific heat ratio variation, and gas nonequilibrium could not be precisely evaluated beforehand; therefore, tests were conducted over a range of stagnation pressures from 100 to 400 psia; and, temperatures from 100 to 1000°F. At each test condition, cell ambient pressure was adjusted to give the required jet expansion to match the chosen values of the simulation parameters. All tests were conducted under steady-state conditions.

3.2 FLOW VISUALIZATION

A glow discharge technique was used to illuminate the jet plume so that it could be photographed, since the required test cell pressures were well below the sensitivity limit of conventional optical techniques. The glow discharge technique, previously used for jet plume studies in Ref. 12, utilized an electrically charged probe approximately 5 in. downstream of the nozzle exit. This electrical charge was supplied by Osram® ignition unit originally designed for ignition of 2000-w high-pressure xenon arc lamps. This unit is rated at 40 kv-RF at 18 ma.

Very small amounts of N_2 or CO_2 gas were bled into the upstream end of the test cell through a manifold ring. This technique, discussed in Ref. 12, provides a fine adjustment of the test cell pressure but was used primarily to give a color contrast between the jet and the ambient atmosphere. This is achieved by inbleeding CO_2 when using N_2 as the jet gas and vice versa. Although the color of the gas discharge varies somewhat with pressure level and gas temperature, the generally blue glow of the CO_2 improves the boundary contrast between the pink glow of the N_2. Carbon dioxide was also used for the inbleed gas in the tests with He. Figure 3 gives an interior view of the test cell showing the electrical probe and the gas inbleed manifold installation.

The illuminated plumes were photographed with a 35-mm camera equipped with a 50-mm lens. Ektachrome® ER-ASA160-Tungsten Balance film was used, and exposure times were normally 1/30 sec. Data were obtained at several exposure settings at each test condition, with f/4 generally giving best results. Optimum exposure varied with jet stagnation temperature and pressure. No change in boundary location could be detected as a result of a change in exposure.

Typical photographs of the jet plumes are shown in Fig. 4. Also shown in the figure are the boundary points that were selected as the experimental data as well as the theoretical method-of-characteristics solutions. The original color positives were projected, and both top and bottom boundaries were measured and averaged to give the plotted data presented later in this report.

The light emitted by the excited gas has been shown to be nearly a linear function of the gas density for the pressure range of these tests (Ref. 19). For the highly expanded plumes investigated, the gas density very rapidly decreases downstream of the nozzle exit as typically shown in Fig. 5. However, downstream at the boundary shock (which lies close to the inviscid boundary) an order-of-magnitude rise in density occurs,

giving the bright band of light. The outer edge of this band was measured as being the jet boundary. Near the nozzle exit the jet boundary tends to disappear, particularly for the CO_2 and the N_2 jets. The disappearance of the boundary may be attributed to a number of effects, including the shorter viewing path through the three-dimensional jet at the smaller axial distances, glow phenomena electrode effects, and the nozzle boundary layer.

3.3 PRESSURE PROBE TRAVERSES

To confirm that the visible boundary did in fact closely represent the physical jet, limited pressure probe traverses were made through the CO_2 and N_2 jet boundaries. These traverses were made parallel to the jet axis and do not necessarily give the pitot pressure. The probe tip was 1/8 in. in diameter and is shown in Fig. 3. Results of these tests are shown in Fig. 6. Generally good agreement is shown between the jet boundary indicated by the pressure probe traverse and that obtained with the glow discharge technique.

SECTION IV
RESULTS AND DISCUSSION

4.1 THEORETICAL JET BOUNDARIES

Jet boundaries were calculated by the Latvala approximation and by the method of characteristics for values of the simulation parameters of $\delta_j = 60$ deg and $\gamma M_1^2/\beta_1$ equal to 10, 14, 18, and 22. Boundaries were computed corresponding to nozzle half-angles of 10 and 20 deg with jet specific heat ratios of 1.667, 1.40, and 1.28. These calculations cover a very wide range of possible operating conditions, as shown in Table I (Appendix II) and in Fig. 7.

Results of the calculations by the Latvala approximation are shown in Fig. 8, and by the method of characteristics in Fig. 9. Note that since the Latvala approximation starts after the jet expansion to ambient pressure, the calculations shown in Fig. 8 are valid for all values of the nozzle half-angle, θ_N. These computations show the Latvala approximation to give almost exact boundary duplication for all conditions calculated, whereas the method of characteristics predicts substantial divergence between boundaries, especially at the lower values of $\gamma M_1^2/\beta_1$. Somewhat closer boundary duplication for

the method-of-characteristics solutions is obtained by adding the nozzle half-angle, θ_N, as an additional parameter. Also note that the boundaries with a specific heat ratio, γ, of 1.667 diverge the greatest, and that for most applications good boundary simulation would be obtained for axial distances of 10 to 15 nozzle exit radii by using air (γ = 1.4) to simulate a hot rocket (γ = 1.28).

4.2 EXPERIMENTAL RESULTS

Results of experimental tests with CO_2, N_2, and He for $\gamma M_1^2/\beta_1 = 14$ are shown in Fig. 10, and tests with N_2 and He for $\gamma M_1^2/\beta_1 = 18$ are shown in Fig. 11. Carbon dioxide was not used in the tests with $\gamma M_1^2/\beta_1 = 18$ because of the very low ambient pressures and the very large nozzle area ratios (Fig. 7) required. Data symbols are only shown for the portions of the boundaries for which a distinct boundary could be determined from the projected negatives and are shown as read, without any fairing or smoothing. Also shown are the theoretical boundaries as calculated by the method of characteristics. Since tolerances in machining the test nozzles will cause errors in the jet initial angle, δ_j, the actual initial angle is shown and the theoretical boundaries recalculated if the test value deviated more than 1 deg from the desired 60 deg. The experimental data generally lie slightly outside the method-of-characteristics solutions, as would be expected for a viscid fluid. However, little effect of gas stagnation temperature or pressure is observed, indicating little effect of nozzle boundary layer, gas condensation, or changes in the boundary viscous mixing. The exception is the data for N_2 at high stagnation pressures.

The boundary increase shown for the high stagnation pressure N_2 is real, as previously shown by the pressure probe data in Fig. 6a, and not just an apparent change caused by the flow visualization technique. Such a change could be caused by gas condensation in the test nozzles or in the jet plume. The very large rates of gas expansion in the nozzles and in the plumes would give a substantial amount of supersaturation before condensation would occur. However, as shown in Fig. 12, even equilibrium condensation in the test nozzles is possible only for the CO_2 at 300°F and condensation with the 100°F, 100-psia stagnation test conditions would occur far before condensation at the 1000°F, 500-psia conditions. The close agreement of the nitrogen boundaries at low stagnation pressure test conditions and for all conditions with CO_2 shows that gas condensation in the jet plume either does not occur or has no effect on the measured jet boundaries.

An analysis was made of the experimental N_2 data for possible effects of the nozzle boundary layer or changes in the jet boundary mixing region. The maximum change in the nozzle exit flow properties that can be caused

by the displacement thickness of a turbulent boundary layer will cause only a 0.5-deg increase in jet boundary initial angle, δj. This change is not sufficient to cause the boundary location increase shown for the high stagnation pressures. However, an analysis of the deviation of the experimental boundaries from the method-of-characteristics solutions shows excellent agreement when the data are correlated by the Reynolds number at the nozzle exit. This correlation is shown in Fig. 13, which also includes the data with He and CO_2. The Reynolds number is based on the length along the nozzle wall from the throat to the exit and the viscosity data of Ref. 20 for He and of Ref. 21 (extrapolation required for lowest temperatures) for N_2 and CO_2. The critical Reynolds number indicated in Fig. 13 is almost identical with the values given in Ref. 22 for flat plates with comparable Mach numbers. A somewhat higher critical Reynolds number would be expected for the nozzle flow because of the favorable pressure gradient; however, the choice of the proper length for nozzle flows is uncertain. Also shown in Fig. 13 are the edges of the turbulent mixing region calculated as described in Section 2.3, which gives good agreement with the data at the higher Reynolds numbers. Although it would be attractive to attribute the smaller jet boundaries at the lower Reynolds numbers to a laminar jet boundary, Ref. 23 would indicate laminar boundary thicknesses comparable to or thicker than that for a turbulent boundary. However the velocity profile assumed in Ref. 23 may not be valid at the very high Mach numbers of the experimental jet boundaries. It is significant that the inviscid method of characteristics does give a good representation of the physical jet boundary, although insufficient knowledge of the viscous mixing process and the factors affecting it may not always allow an absolute correction for the mixing.

In general, excellent agreement is obtained between the inviscid method-of-characteristics solutions and the experimental data. It is therefore believed that the validity of this program with the inputs and techniques used has been confirmed and that a comparison of simulation parameters can now be made using the method-of-characteristics calculations for the jet boundaries rather than requiring experimental measurements.

4.3 ANALYSIS OF OTHER SIMULATION PARAMETERS

Although the proposed simulation parameters δ_j and $\gamma M_1^2/\beta_1$ do provide good simulation for most cases of practical interest, they do not appear to be the completely general tool that one desires. Therefore with the method-of-characteristics program confirmed as a method of calculating the physical jet boundary, a limited analysis of

some of the other proposed simulation parameters was made. Among the parameters investigated were:

1. $\gamma M_j^2/\beta_j$ and δ_j
2. $\gamma M_j^2/\beta_j$ and p_j/p_∞ (Ref. 3)
3. $\gamma M_j^2/\beta_j$, p_j/p_∞ and δ_j (Ref. 1)

Results of this limited analysis are shown in Fig. 14. Of the sets of parameters studied none except the third set gave results as good as the $\gamma M_1^2/\beta_1$ and δ_j suggested in Ref. 4. However it should be noted that the third set requires the matching of three quantities rather than two, and is therefore a more restricted simulation.

The use of the third set of simulation parameters shown above implicitly specifies a value of θ_N. The required value of θ_N is therefore shown in Fig. 14c which presents a set of boundaries calculated for the given set of simulation parameters.

4.4 SIMULATION PARAMETERS δ_j AND M_1/γ

A rapid analysis of any other parameter in combination with δ_j can be made from the existing method-of-characteristics solutions for $\delta_j = 60$ deg. This is done by observing the variation of the jet boundary radial locations at a fixed axial station as compared to changes of the parameter under study. Ideally then, boundary locations for all calculations should give a smooth progression for the changes of the selected parameter. A summary of the calculated boundaries from which the analysis can be made is shown in Fig. 15.

The analysis described above was made on several parameters involving combinations of M_1 and γ. This analysis shows excellent correlation of the boundary location when δ_j and M_1/γ are used as the simulation parameters. A slight improvement in correlation can be gained by also duplicating θ_N as a third parameter. Sample results of this analysis are shown in Fig. 16. Excellent correlation of the boundary locations is shown.

Based on the preceding analysis, additional boundary calculations were made by the method of characteristics to determine the range of applicability of the parameters δ_j and M_1/γ. Calculations were made for the following conditions:

1. Jet boundary initial angles, δ_j, of 45, 60, and 75 deg.
2. Simulation parameter M_1/γ values of 5, 7, 10, and 13.
3. Specific heat ratio of 1.28 and 1.667.
4. Nozzle half-angle, θ_N, of 10 and 20 deg.

The very wide range of conditions covered by these calculations is shown in Table II and in Fig. 17.

Results of the calculations are shown in Figs. 18, 19, and 20. Excellent agreement between the boundaries is obtained over the very wide range of conditions investigated. Some improvement is obtained by including the nozzle half-angle, θ_N, as a third simulation parameter. Also note that the boundaries are presented for two extreme cases of the specific heat ratio, 1.28 and 1.667 only; for most practical applications using diatomic gases, the boundaries would show even better agreement.

4.5 A RAPID METHOD FOR ESTIMATING THE INVISCID BOUNDARY LOCATION

The close correlation of jet boundaries with the simulation parameters δ_j, M_1/γ, and θ_N gives rise to a very simple method of rapidly estimating the inviscid boundary location. Boundary locations at fixed axial stations are shown in Figs. 21 and 22 as a function of the jet initial angle, δ_j, and the parameter M_1/γ for nozzle half-angles of 10 and 20 deg. The estimating procedure is as follows:

1. From Eq. (1) the initial angle of the jet, δ_j, is calculated. This establishes the slope of the boundary at the nozzle exit.
2. Calculate M_1/γ from the known stagnation pressure, ambient pressure, and specific heat ratio.
3. The boundary location r/r_e can then be located at x/r_e = 5, 10, 18, and 25 from Fig. 21 for θ_N = 10 deg or Fig. 22 for θ_N = 20 deg. This provides up to five known points plus the initial angle, δ_j, and is normally enough for an accurate boundary. If desired, additional figures similar to Figs. 21 and 22 can be constructed at any x/r_e from Figs. 18, 19, and 20.
4. The small correction for other values of θ_N can be made by a comparison of the boundaries at 10 and 20 deg.

SECTION V
CONCLUDING REMARKS

The theoretical and experimental investigation of jet boundary simulation parameters for underexpanded jets in a quiescent atmosphere indicate the following conclusions:

1. Experimental jet boundaries are in excellent agreement with the inviscid jet boundaries as determined by the method of characteristics.
2. Pindzola's parameters (δ_j and $\gamma M_1^2/\beta_1$) give good boundary simulation for 10 to 15 nozzle exit radii for most applications using air ($\gamma = 1.4$) to simulate a hot rocket ($\gamma = 1.28$).
3. However, the use of δ_j and M_1/γ provides excellent boundary duplication over a wider range of conditions and to much larger axial distances. In addition, a slight improvement in the correlation can be gained by also duplicating θ_N as a third parameter.
4. A procedure developed from the method-of-characteristics solutions gives a rapid, simple method for estimating the jet boundary shape for jets with boundary initial angles from 45 to 75 deg.

REFERENCES

1. Pindzola, M. "Jet Simulation in Ground Test Facilities." AGARDograph No. 79, November 1963.
2. Love, Eugene S., Grigsby, Carl E., Lee, Louise P., and Woodling, Mildred J. "Experimental and Theoretical Studies of Axisymmetric Free Jets." NASA TR R-6, 1959.
3. Goethert, B. H. and Barnes, L. T. "Some Studies of the Flow Pattern at the Base of Missiles with Rocket Exhaust Jets." AEDC-TR-58-12 (AD302082), October 1958.
4. Pindzola, M. "Boundary Simulation Parameters for Underexpanded Jets in a Quiescent Atmosphere." AEDC-TR-65-6 (AD454770), January 1965.
5. Latvala, E. K. "Spreading of Rocket Exhaust Jets at High Altitudes." AEDC-TR-59-11 (AD215866), June 1959.

6. Adamson, T. C. Jr. and Nicholls, J. A. "On the Structure of Jets from Highly Underexpanded Nozzles into Still Air." Journal of the Aerospace Sciences, Vol. 26, No. 1, p. 16, January 1959.

7. Vick, Allen R., Andrews, Earl H. Jr., Dennard, John S., and Craidon, Charlotte B. "Comparisons of Experimental Free-Jet Boundaries with Theoretical Results Obtained with the Method of Characteristics." NASA TN D-2327, June 1964.

8. Eastman, D. W. and Radtke, L. P. "Two-Dimensional or Axially Symmetric Real Gas Flows by the Method of Characteristics, Part III: A Summary of Results from the IBM 7090 Program for Calculating the Flow Field of a Supersonic Jet." The Boeing Company, Seattle, Washington, Document No. D2-10599, December 1961.

9. Wang, C. J. and Peterson, J. B. "Spreading of Supersonic Jets from Axially Symmetric Nozzles." Jet Propulsion, Vol. 28, No. 5, p. 321, May 1958.

10. Moe, Mildred M. and Troesch, B. Andreas. "The Computation of Jet Flows with Shocks." Space Technology Laboratories, Inc., STL-TR-59-0000-00661.

11. Andrews, Earl H., Jr., Vick, Allen R., and Craidon, Charlotte B. "Theoretical Boundaries and Internal Characteristics of Exhaust Plumes from Three Different Supersonic Nozzles." NASA TN D-2650, March 1965.

12. Prunty, C. C. "Jet Spreading Characteristics at Pressure Altitudes of 180,000 to 260,000 Feet." AEDC-TR-64-95 (AD603341), August 1964.

13. Cassanova, R. A. and Stephenson, W. B. "Expansion of a Jet into Near Vacuum." AEDC-TR-65-151 (AD469041), August 1965.

14. Adamson, Thomas C., Jr. "The Structure of the Rocket Exhaust Plume without Reaction at Various Altitudes." The University of Michigan, Institute of Science and Technology, Report No. 4613-45-T (AD421447), June 1963.

15. Prozan, R. J. "PMS Jet Wake Study Program IMSC External Flow Jet Wake Program VN10." Lockheed Aircraft Corporation Report No. LMSC 919901, 9 October 1961.

16. Prozan, R. J. "Development of a Method of Characteristics Solution for Supersonic Flow of an Ideal, Frozen, or Equilibrium Reacting Gas Mixture." Lockheed Missiles and Space Company Huntsville Research and Engineering Center, Technical Report LMSC/HREC A782535, April 1966.

17. Ratliff, A. W. "Comparisons of Experimental Supersonic Flow Fields with Results Obtained by using a Method of Characteristics Solution." Lockheed Missiles and Space Company, Huntsville Research and Engineering Center, Technical Report LMSC/HREC A782592, April 1966.

18. Bauer, R. C. "Characteristics of Axisymmetric and Two-Dimensional Isoenergetic Jet Mixing Zones." AEDC-TDR-63-253 (AD426116), December 1963.

19. Muntz, E. P. and Marsden, D. J. "Electron Excitation Applied to the Experimental Investigation of Rarefied Gas Dynamics," Rarefied Gas Dynamics, Proceedings of the Third International Symposium on Rarefied Gas Dynamics, Held at the Palais De L'Unesco, Paris in 1962, Vol. II, 1963.

20. Keesom, W. H. Helium. pp. 106-110, Elsevier Publishing Company, New York, 1942.

21. Hilsenrath, Joseph, Beckett, Charles W., et al. Tables of Thermodynamic and Transport Properties of Air, Argon, Carbon Dioxide, Carbon Monoxide Hydrogen, Nitrogen, Oxygen, and Steam, p. 191 and p. 357, Pergamon Press, 1960.

22. Schlichting, Hermann. Boundary Layer Theory. Fourth Edition, p. 438. McGraw-Hill Book Company, 1960.

23. Bauer, R. C. "An Analysis of Two-Dimensional Laminar and Turbulent Compressible Mixing." AIAA Journal, Vol. 4, No. 3, March 1966, pp. 392-395.

APPENDIXES

I. ILLUSTRATIONS
II. TABLES

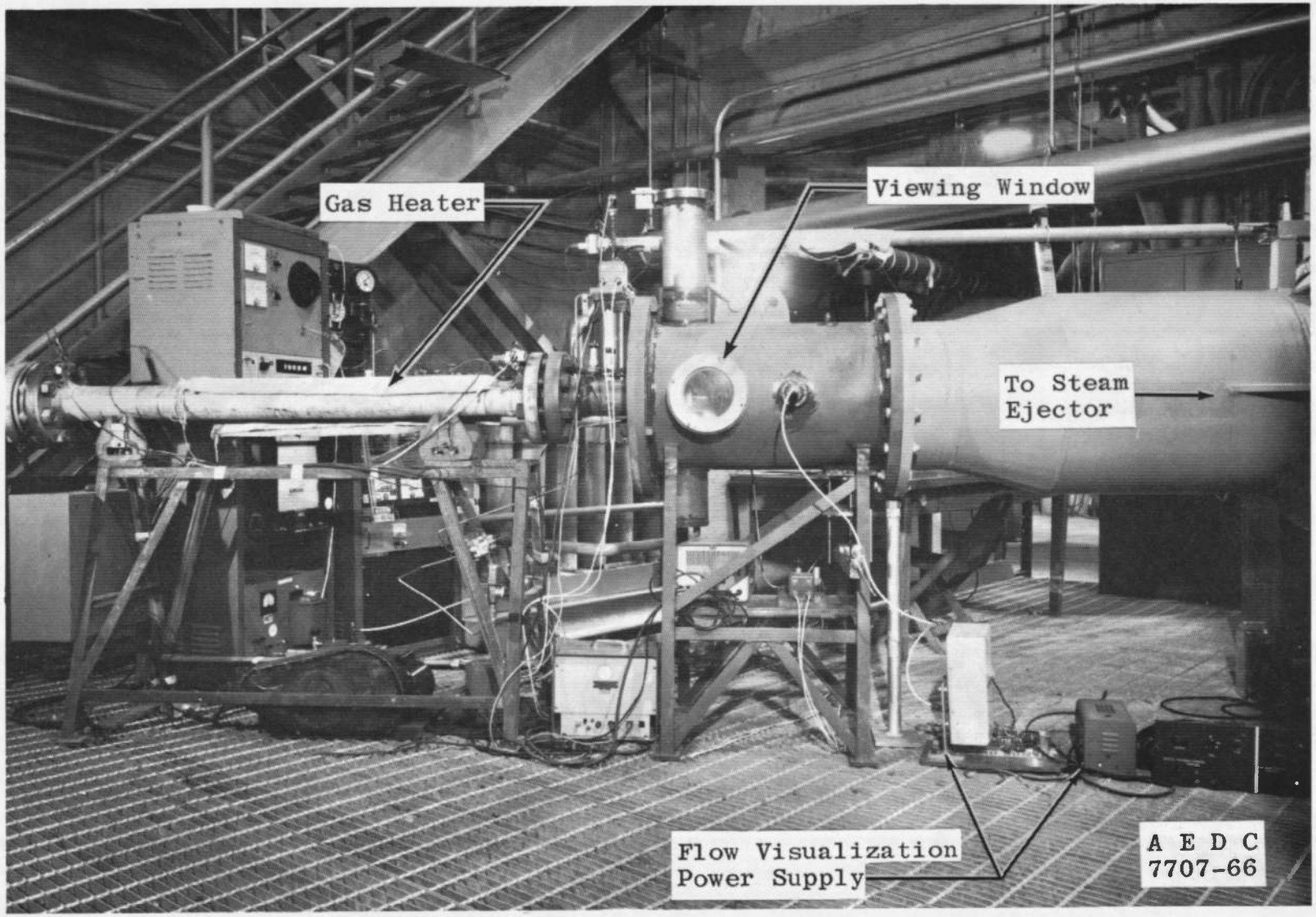

Fig. 1 18-Inch Test Cell Installation

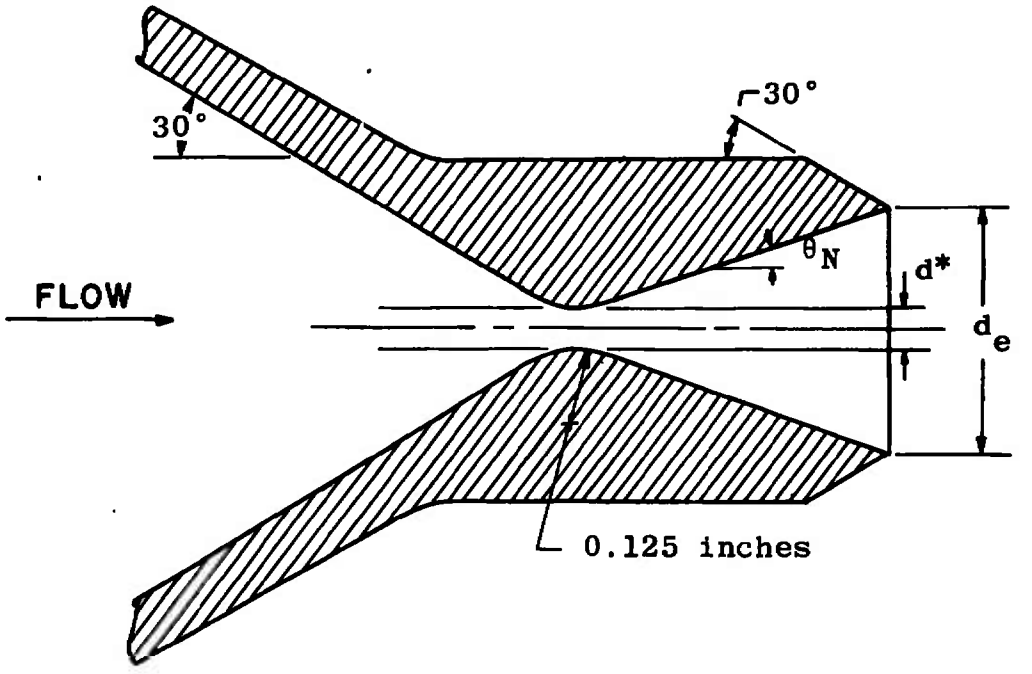

$\gamma M_1^2/\beta_1$	θ_N	Gas	d* inches	d_e inches	A_s/A^*
14	20°36'	CO_2	0.0989	0.6470	44.21
		N_2		0.2818	8.39
		He		0.1344	1.91
	10°0'	CO_2	0.1026	0.4680	20.97
		N_2		0.2181	4.55
		He		0.1254	1.51
18	20°0'	N_2	0.1039	0.3585	12.28
		He		0.1570	2.35
	10°0'	N_2	0.1026	0.2630	6.62
		He		0.1310	1.64

Fig. 2 Test Nozzle Configuration

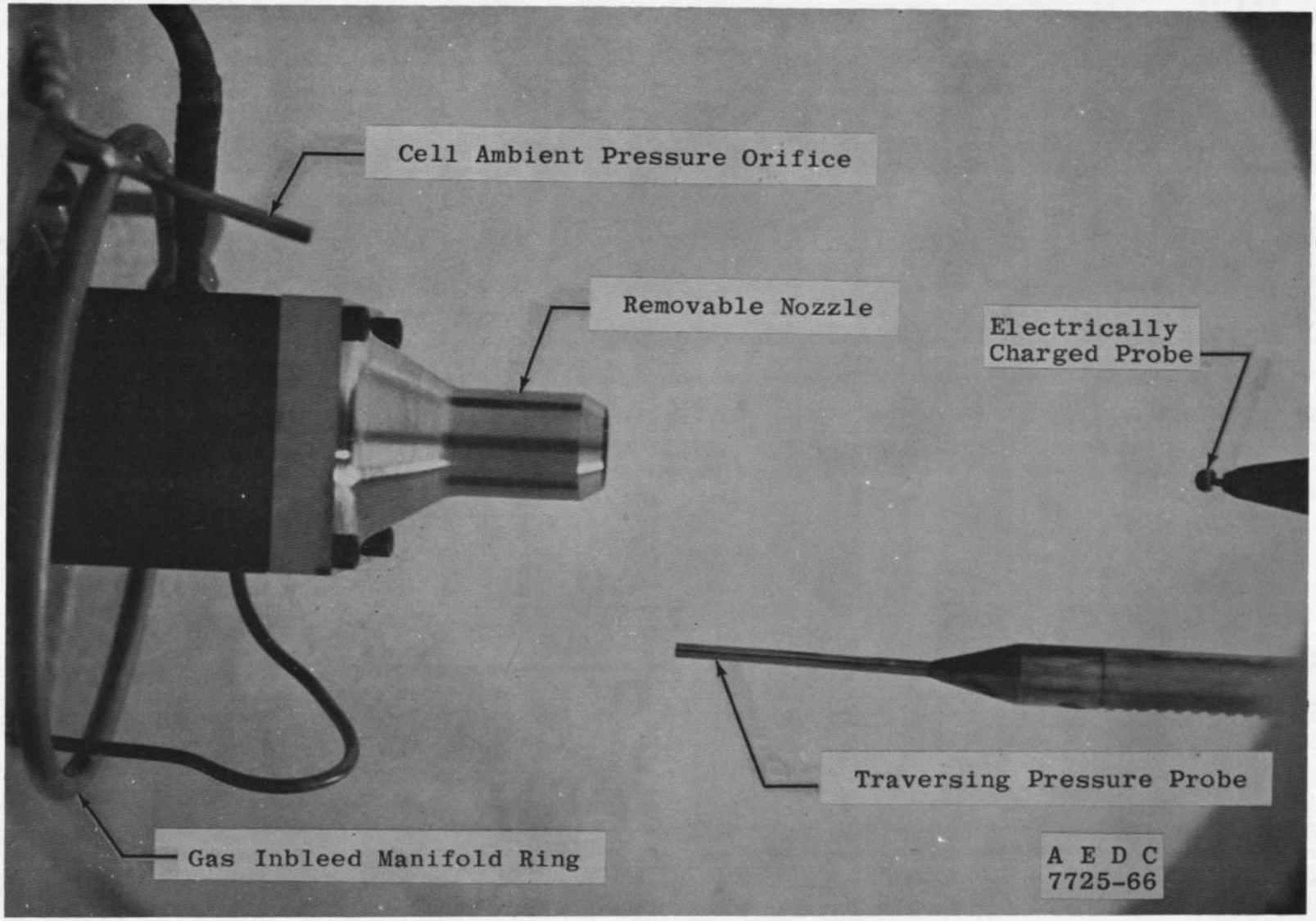

Fig. 3 Model Installation in the 18-Inch Test Cell

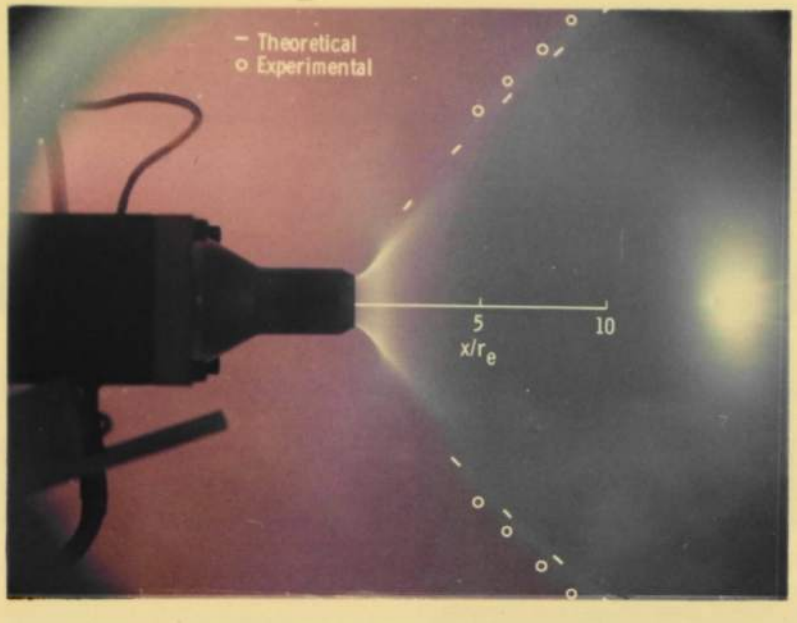

a. CO_2, δ_l = 60 deg, θ_N = 20 deg 36 min

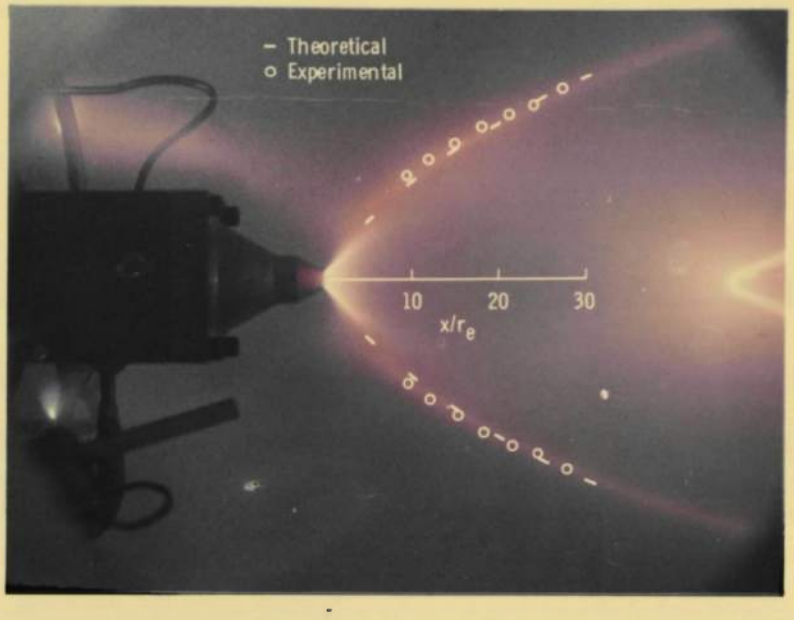

b. N_2, δ_l = 60 deg, θ_N = 10 deg

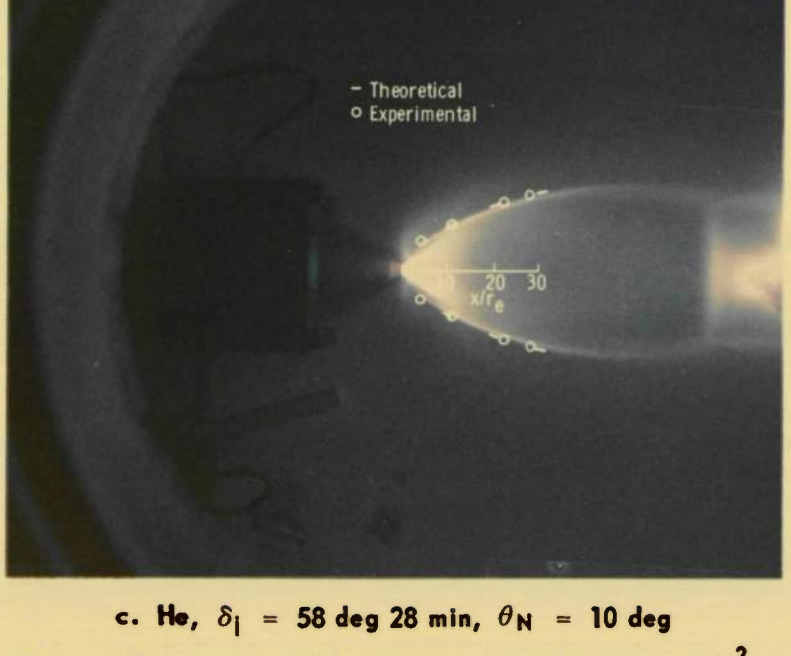

c. He, δ_l = 58 deg 28 min, θ_N = 10 deg

Fig. 4 Typical Photographs of Experimental Jet Plumes for $\gamma M_1^2/\beta_1$ = 14

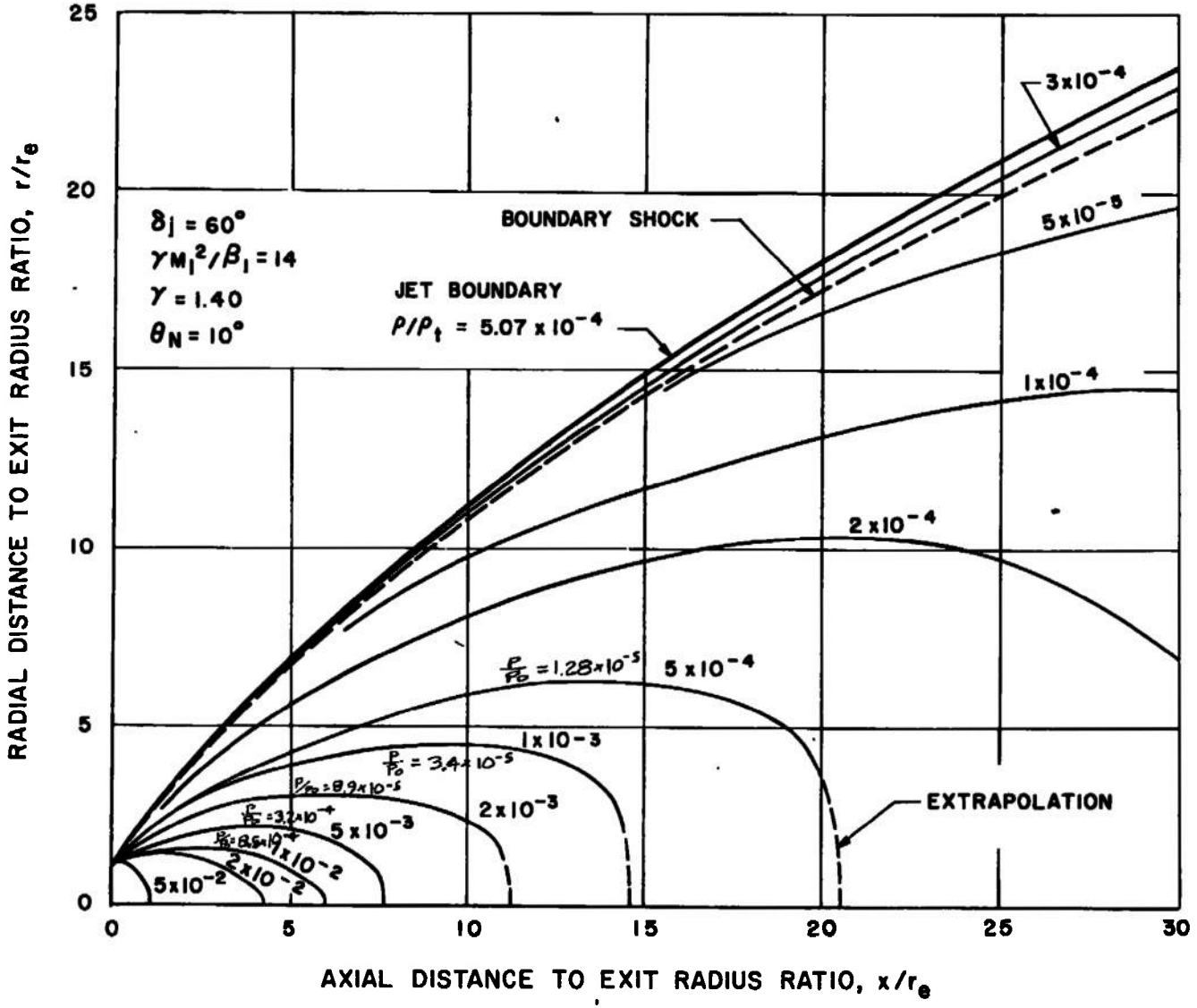

Fig. 5 Typical Jet Density Distribution

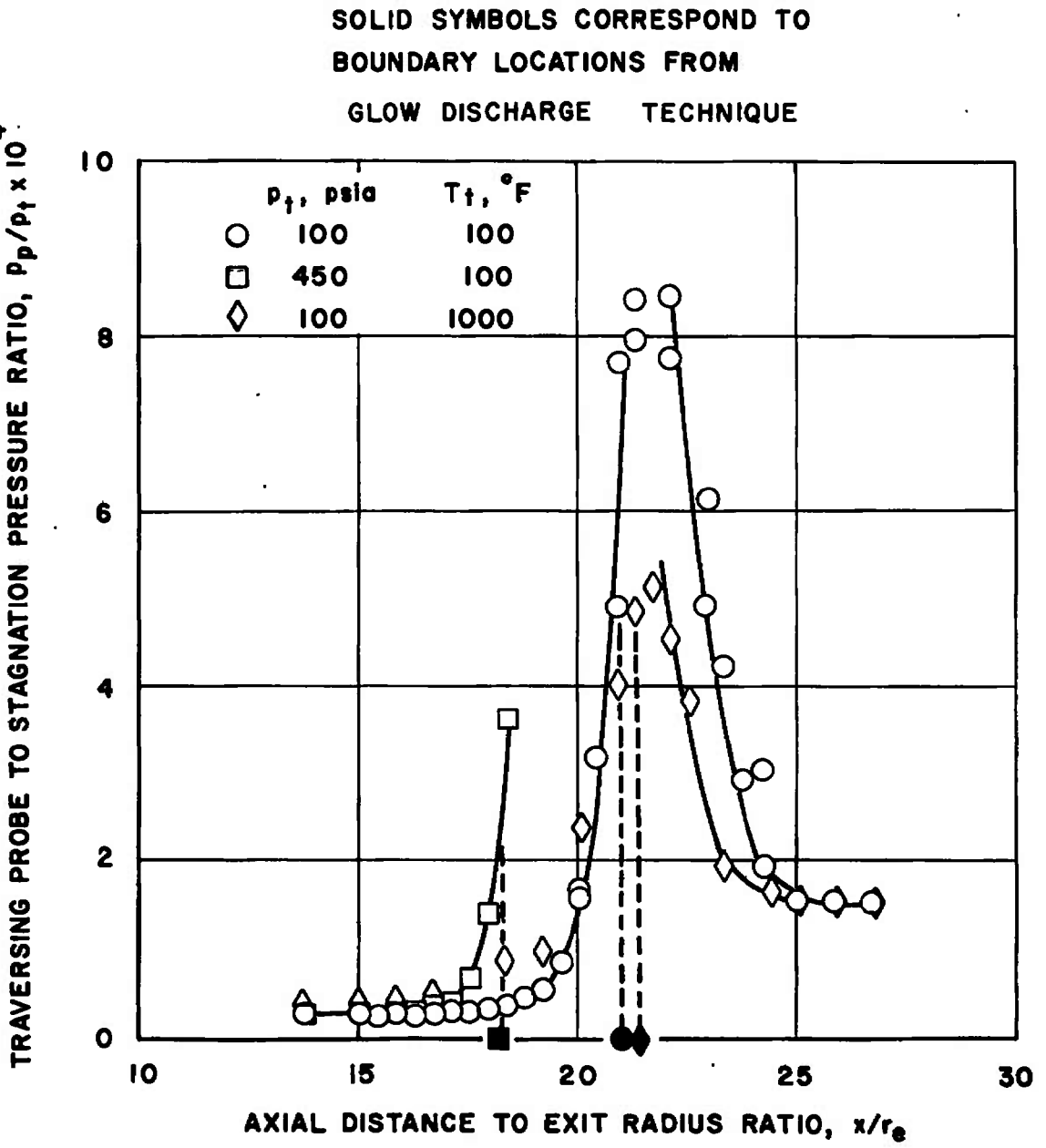

a. N_2, r/r_e = 18.22

Fig. 6 Comparison of Boundaries Determined by the "Glow Discharge" Technique with the Pressure Measured by a Traversing Probe

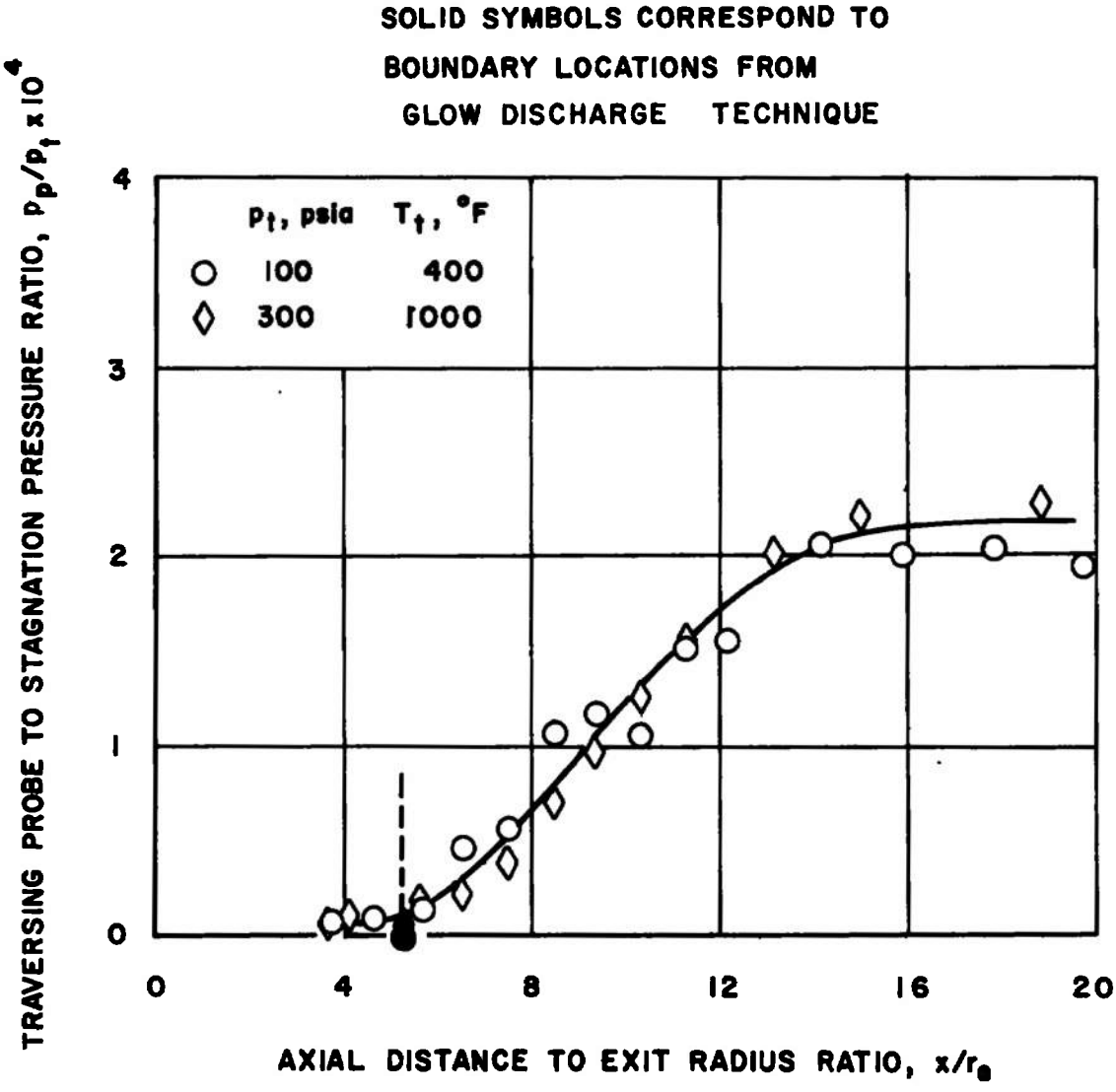

b. CO_2, $r/r_e = 8.18$

Fig. 6 Concluded

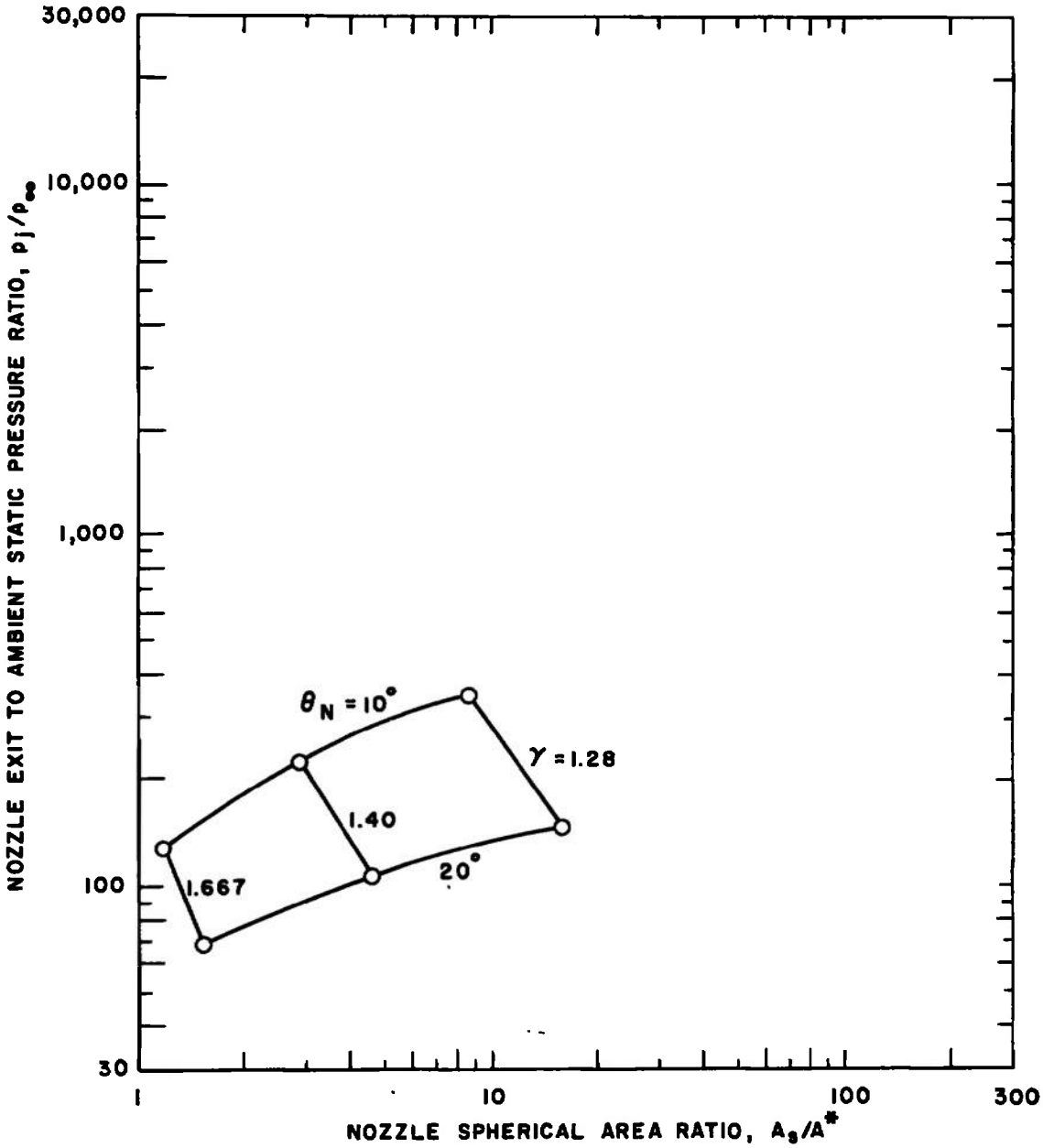

a. $\gamma M_1^2/\beta_1 = 10$

Fig. 7 Range of Nozzle Area Ratio and Exit Pressure Ratio for Jets with Constant Values of $\gamma M_1^2/\beta_1$ and $\delta_j = 60$ deg

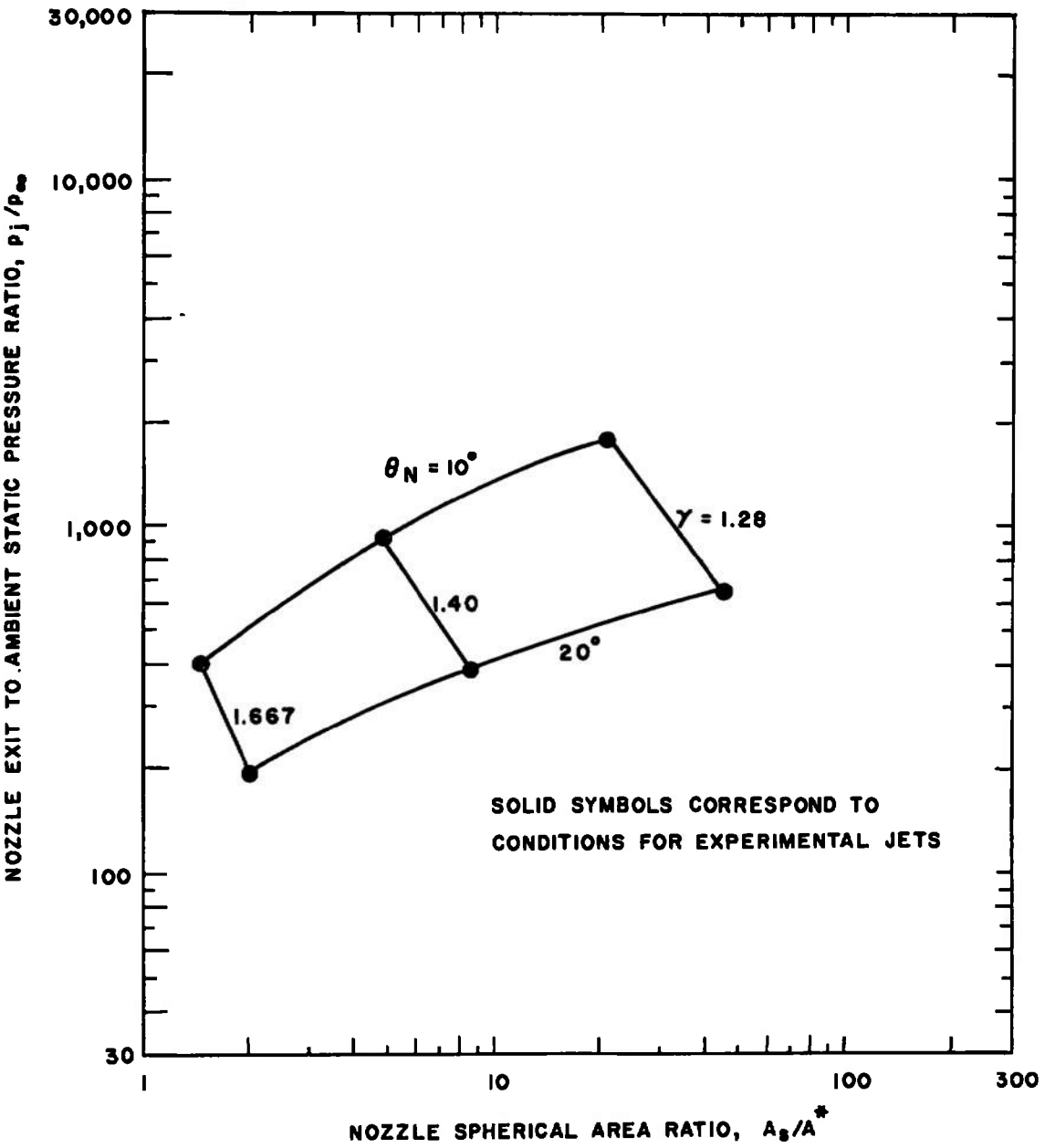

b. $\gamma M_1^2/\beta_1 = 14$

Fig. 7 Continued

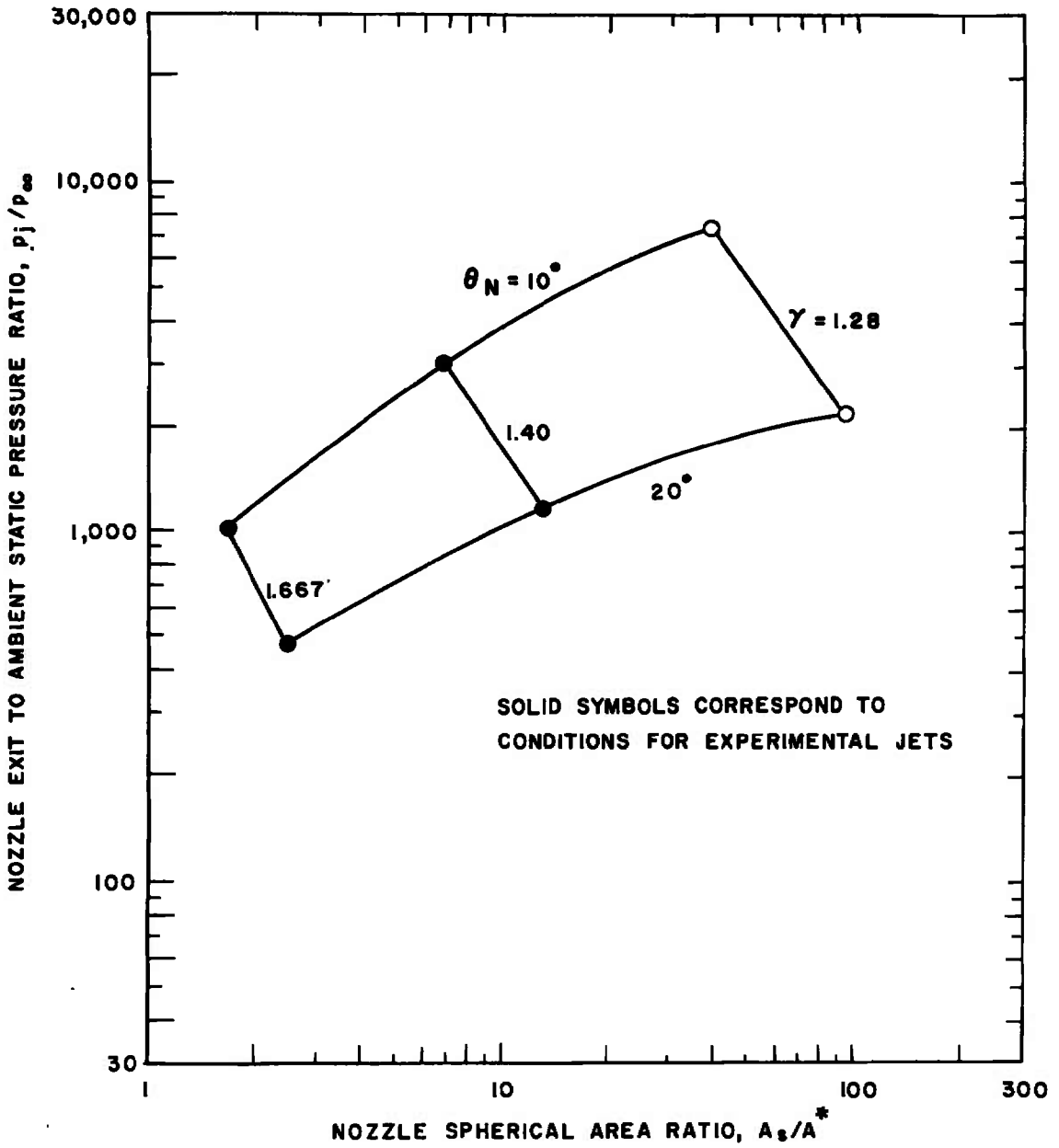

c. $\gamma M_1^2/\beta_1 = 18$

Fig. 7 Continued

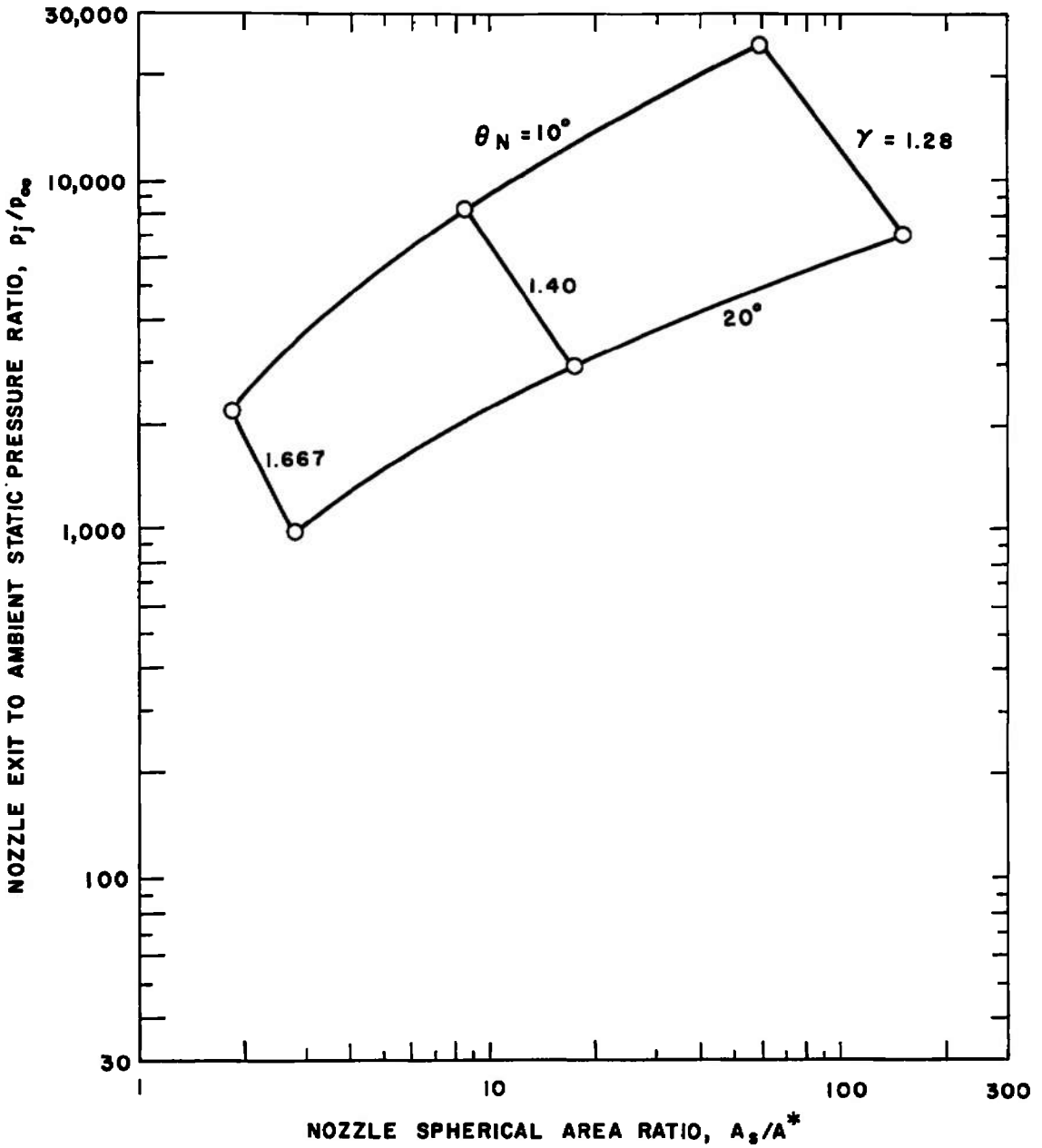

d. $\gamma M_1^2/\beta_1 = 22$

Fig. 7 Concluded

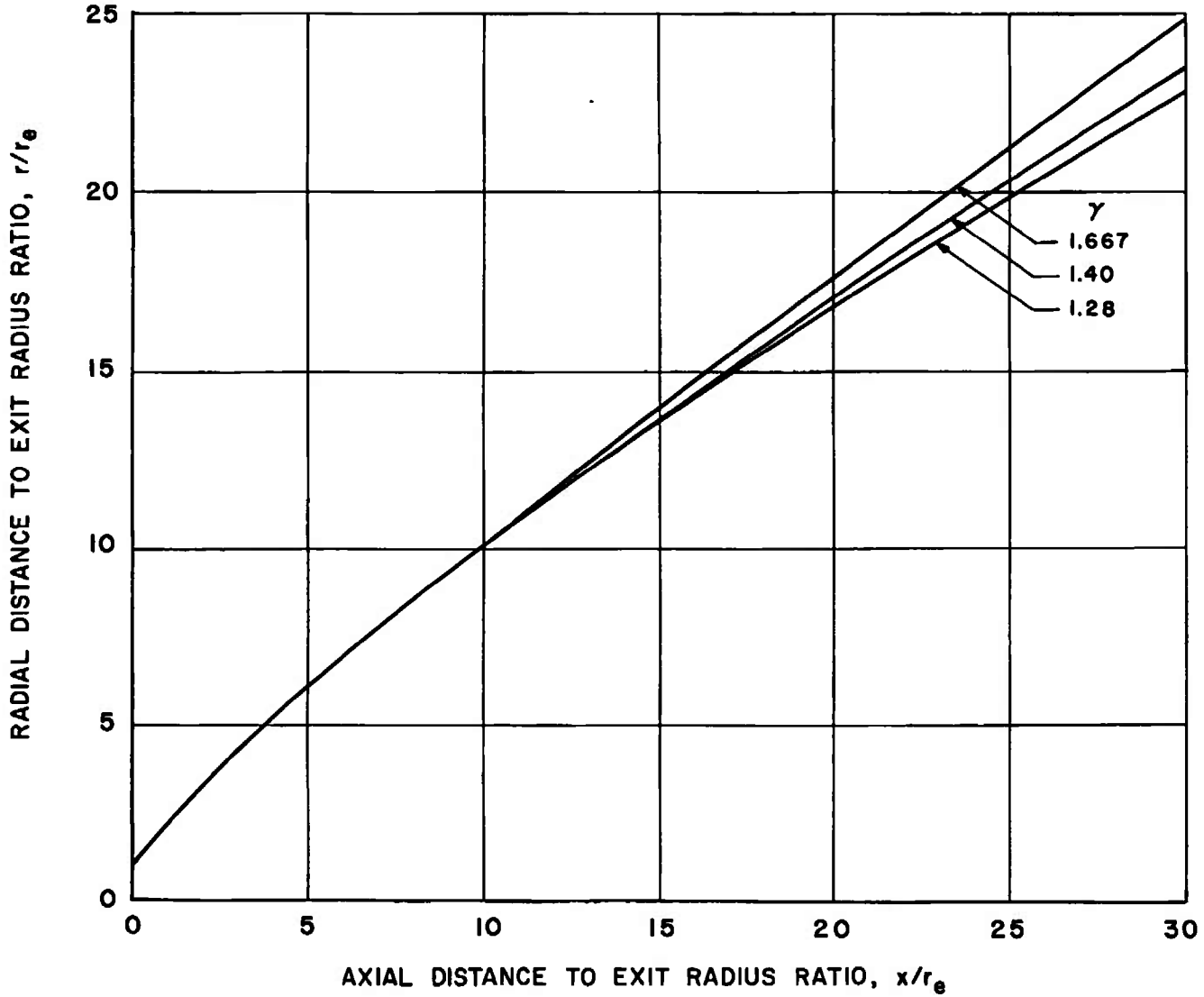

a. $\gamma M_1^2/\beta_1 = 10, \delta_i = 60$ deg

Fig. 8 Comparison of Jet Boundaries as Determined by the Latvala Approximation

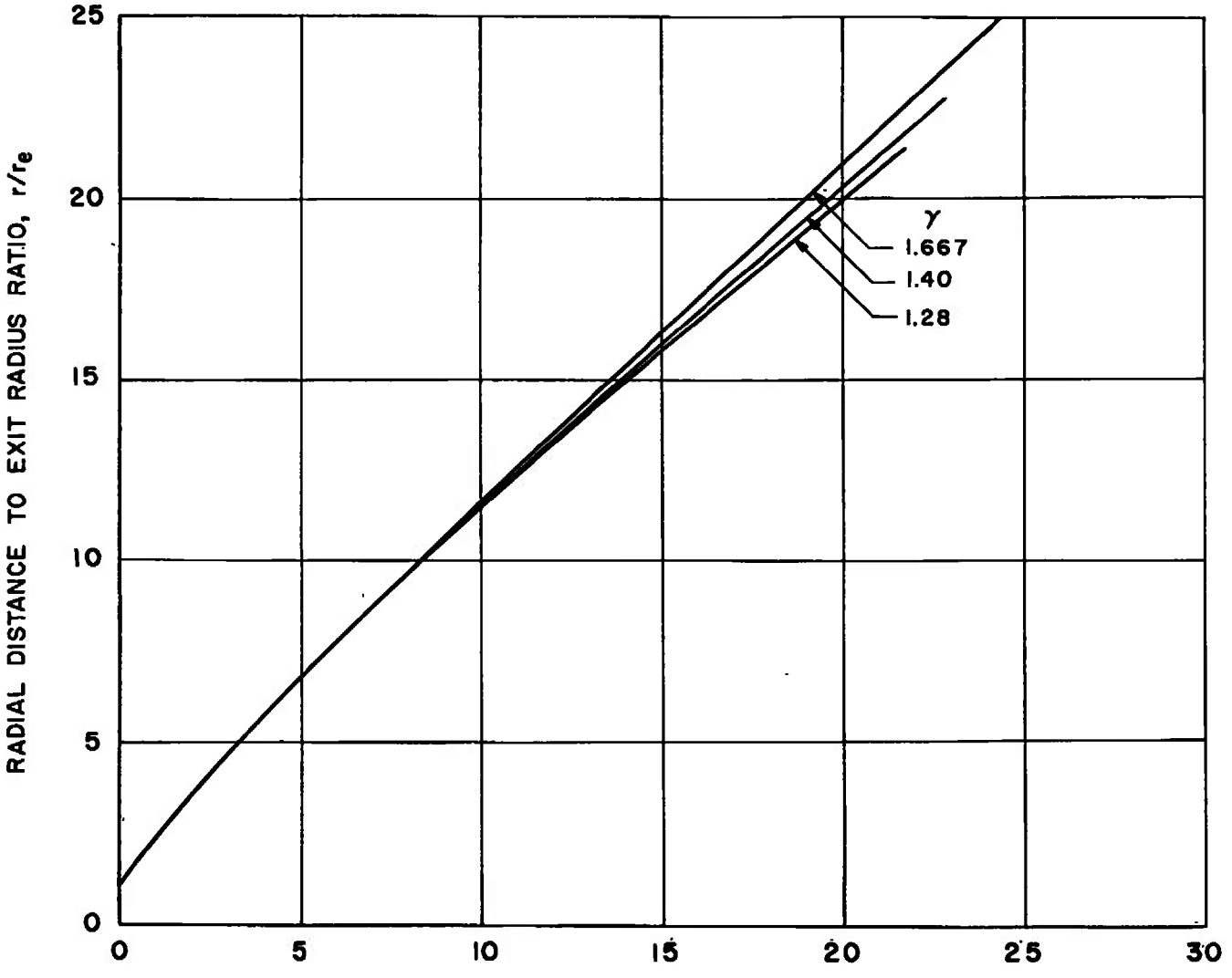

b. $\gamma M_1^2/\beta_1 = 14$, $\delta_l = 60$ deg

Fig. 8 Continued

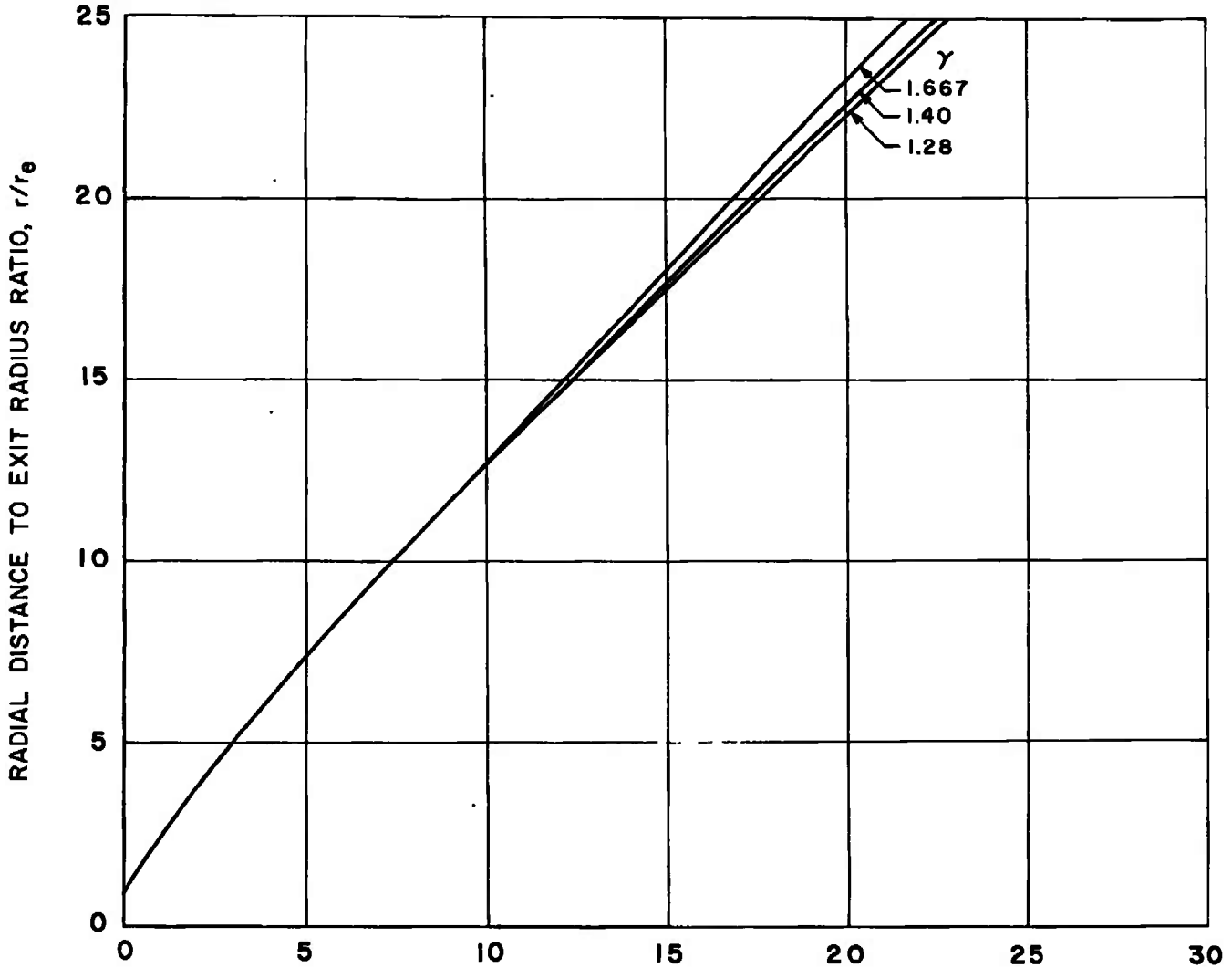

c. $\gamma M_1^2/\beta_1 = 18$, $\delta_i = 60$ deg

Fig. 8 Continued

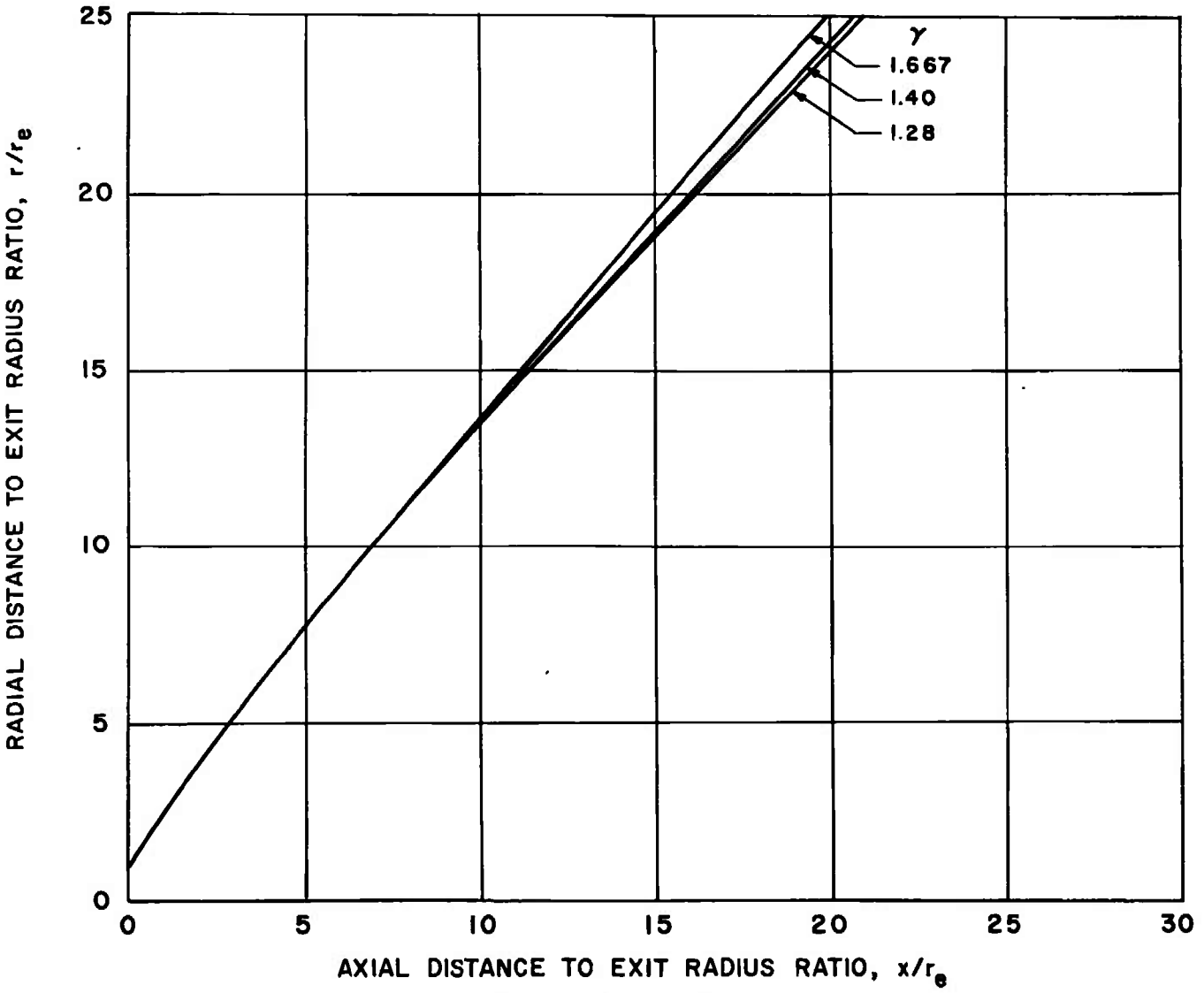

d. $\gamma M_1^2/\beta_1 = 22$, $\delta_1 = 60$ deg

Fig. 8 Concluded

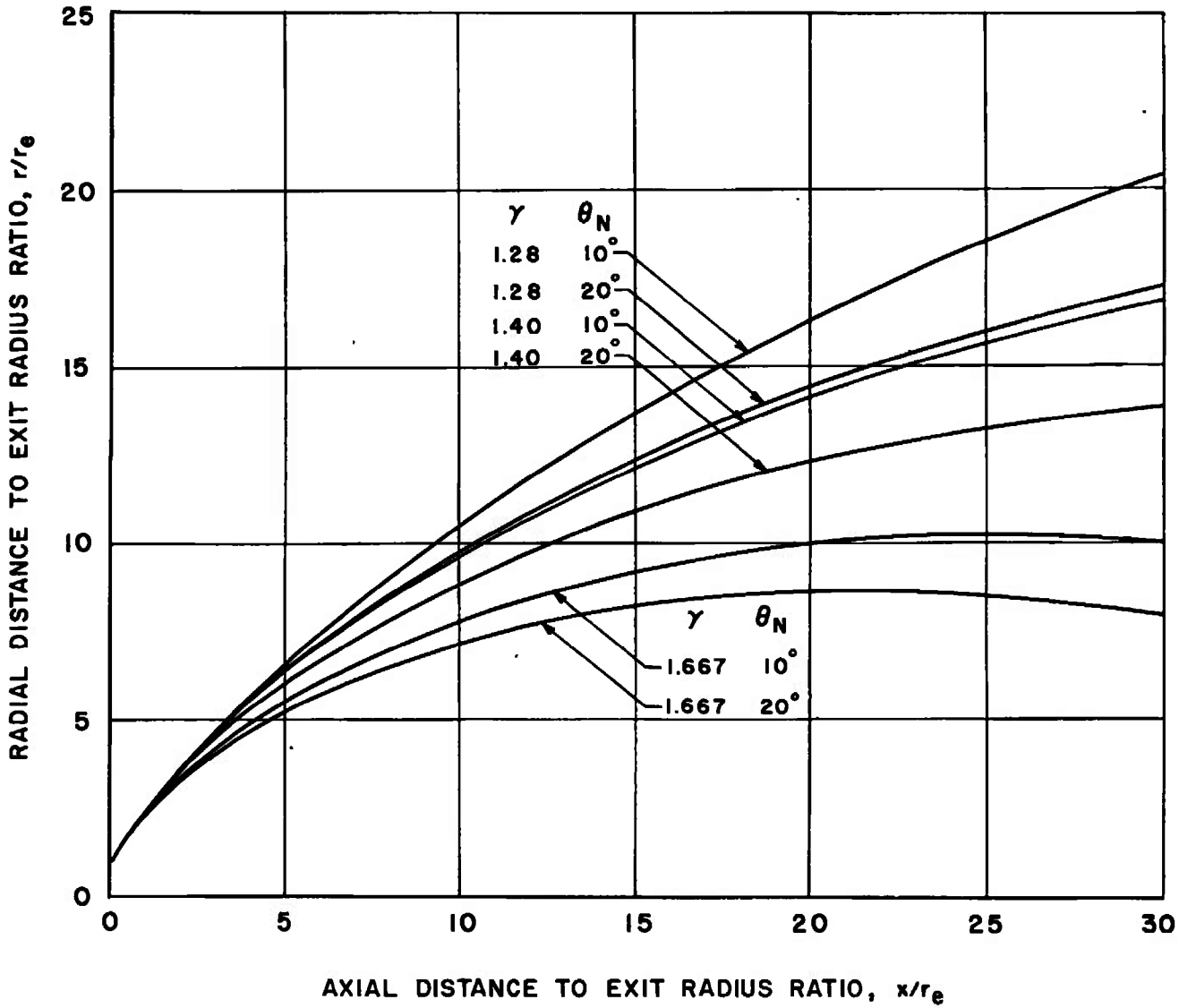

a. $\gamma M_1^2/\beta_1 = 10$, $\delta_i = 60$ deg

Fig. 9 Comparison of Jet Boundaries as Determined by a Method-of-Characteristics Solution

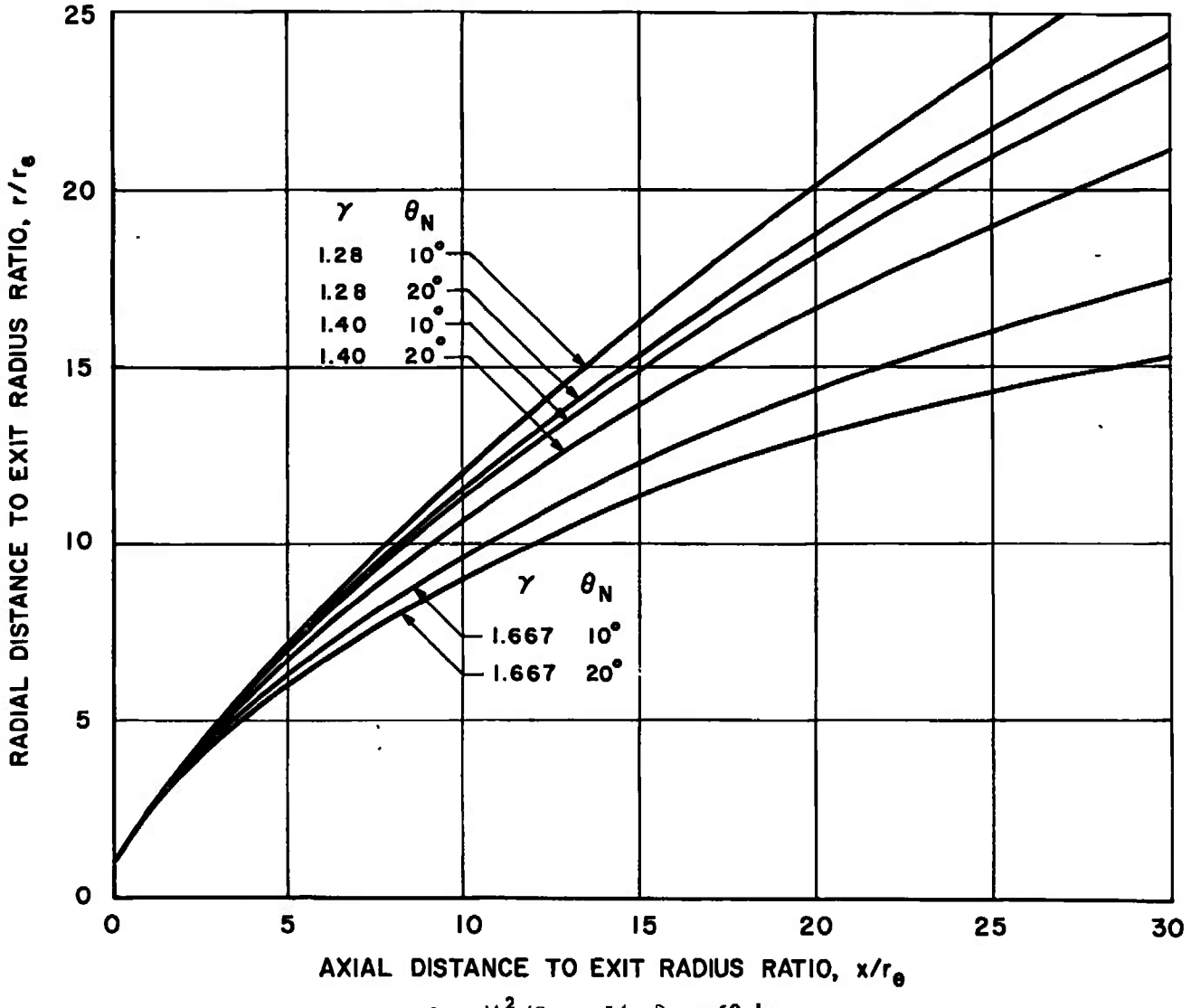

b. $\gamma M_1^2/\beta_1 = 14$, $\delta_1 = 60$ deg

Fig. 9 Continued

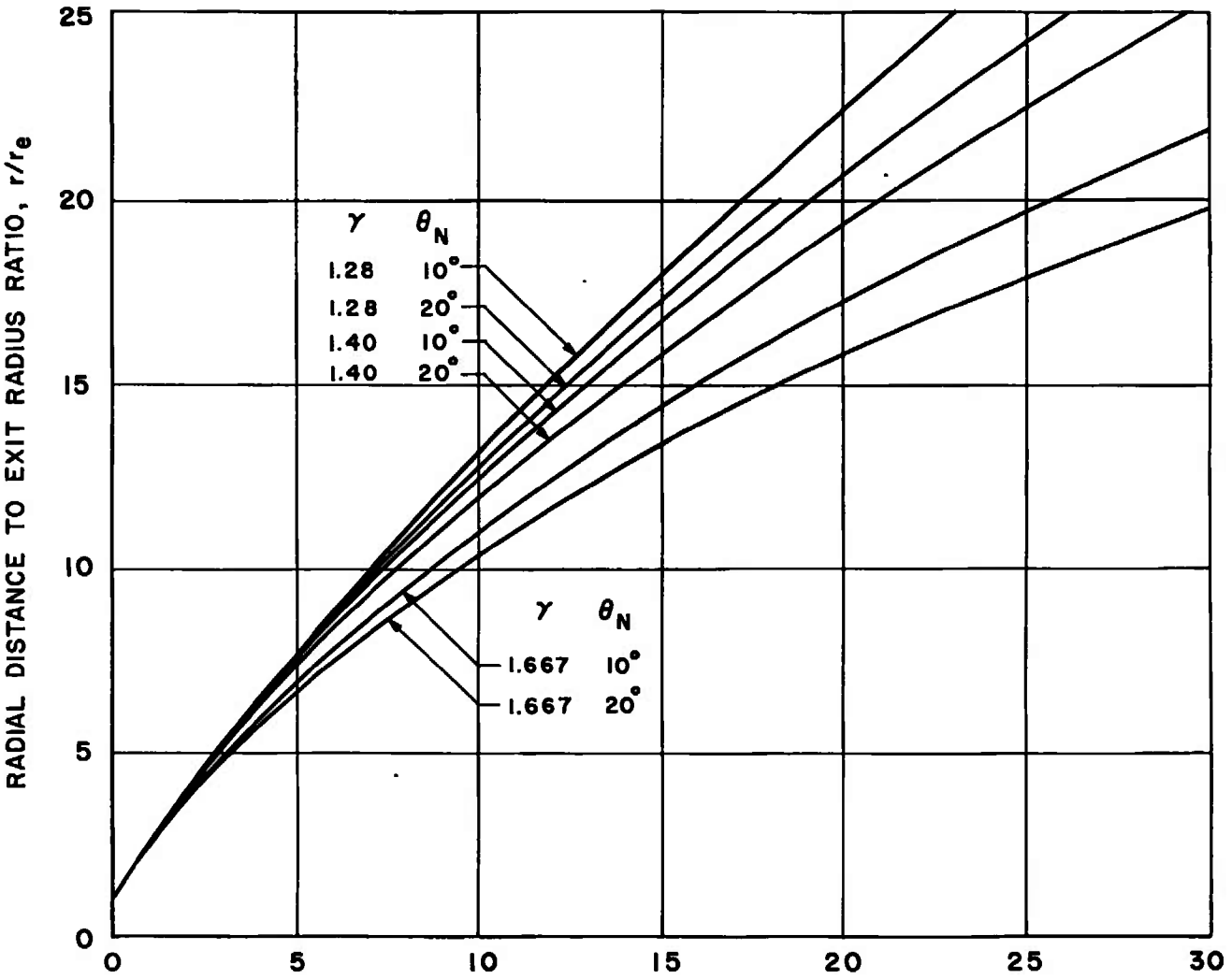

c. $\gamma M_1^2/\beta_1 = 18$, $\delta_1 = 60$ deg

Fig. 9 Continued

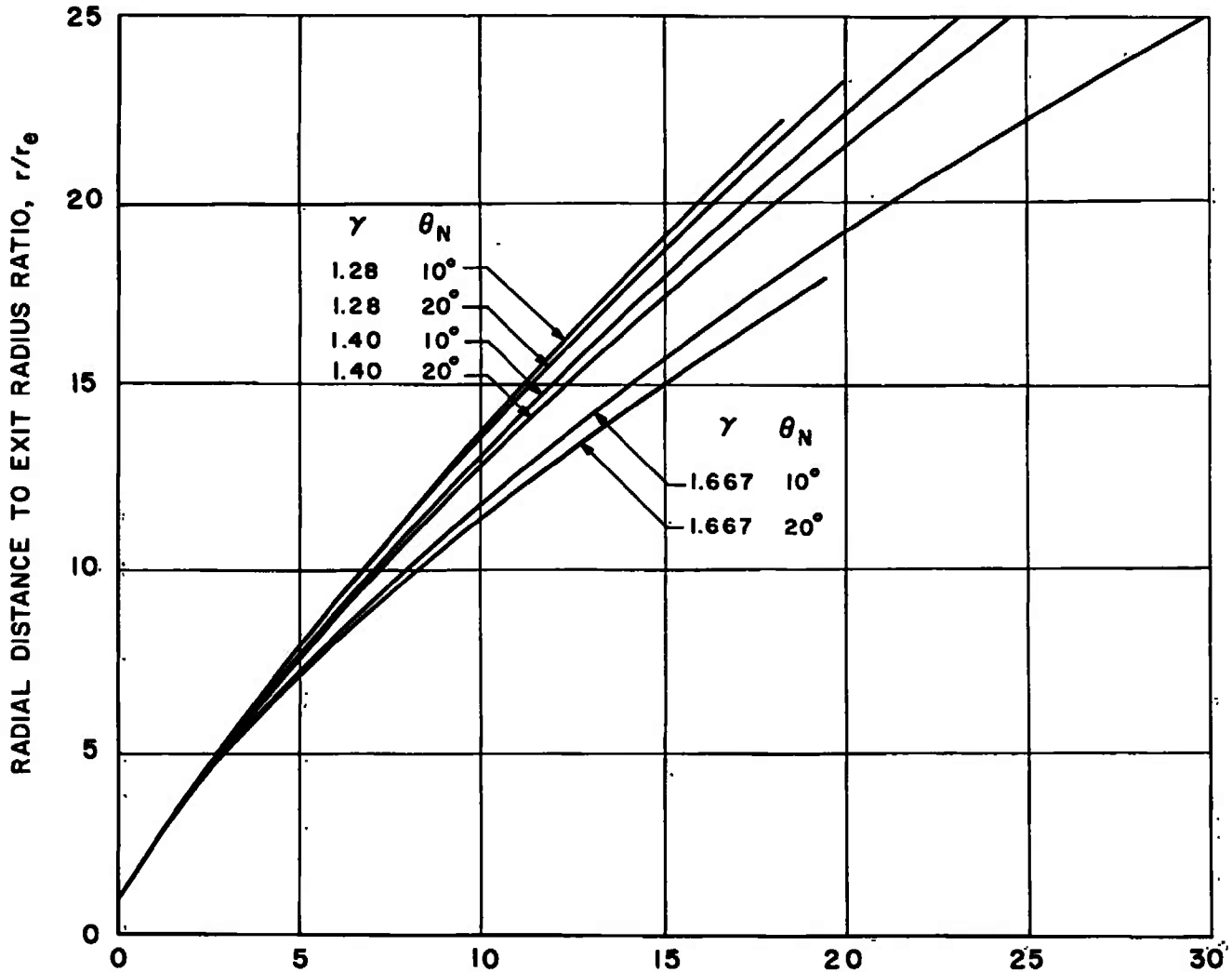

d. $\gamma M_1^2/\beta_1 = 22$, $\delta_1 = 60$ deg

Fig. 9 Concluded

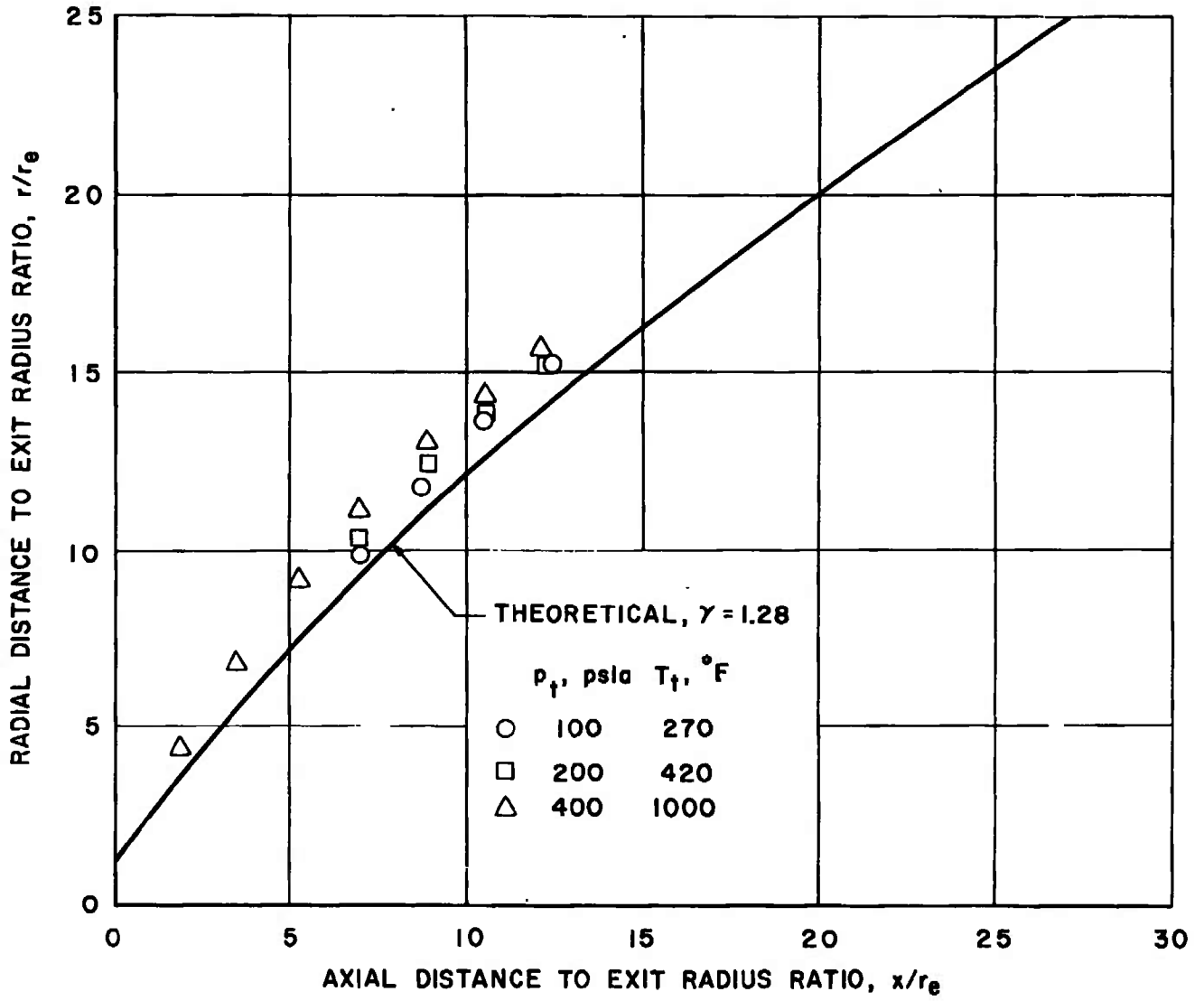

a. CO_2, θ_N = 10 deg, δ_1 = 60 deg

Fig. 10 A Comparison of Experimentally Determined Jet Boundaries with a Method-of-Characteristics Solution for $\gamma M_1^2/\beta_1 = 14$

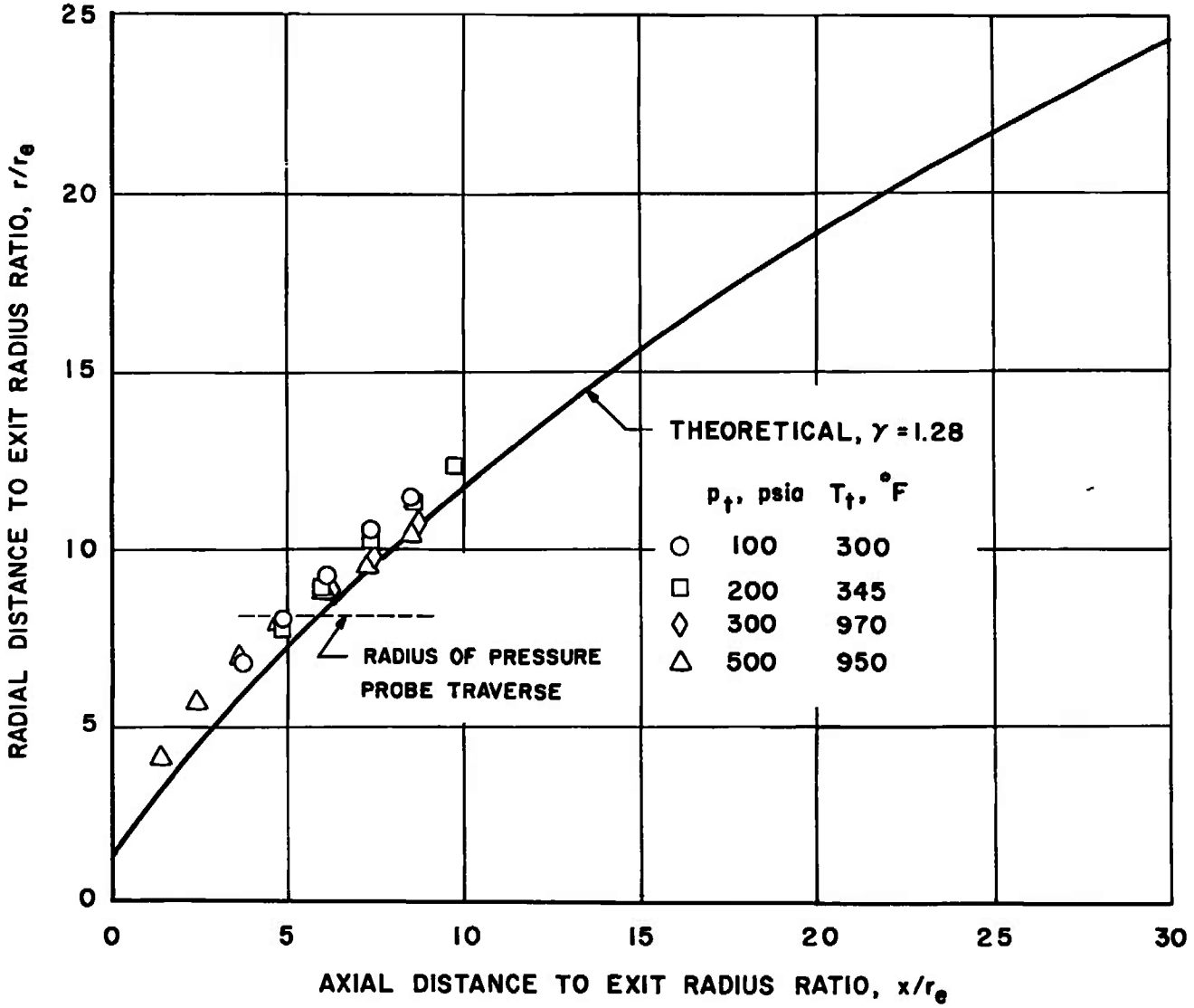

b. CO_2, θ_N = 20 deg 36 min, δ_l = 60 deg

Fig. 10 Continued

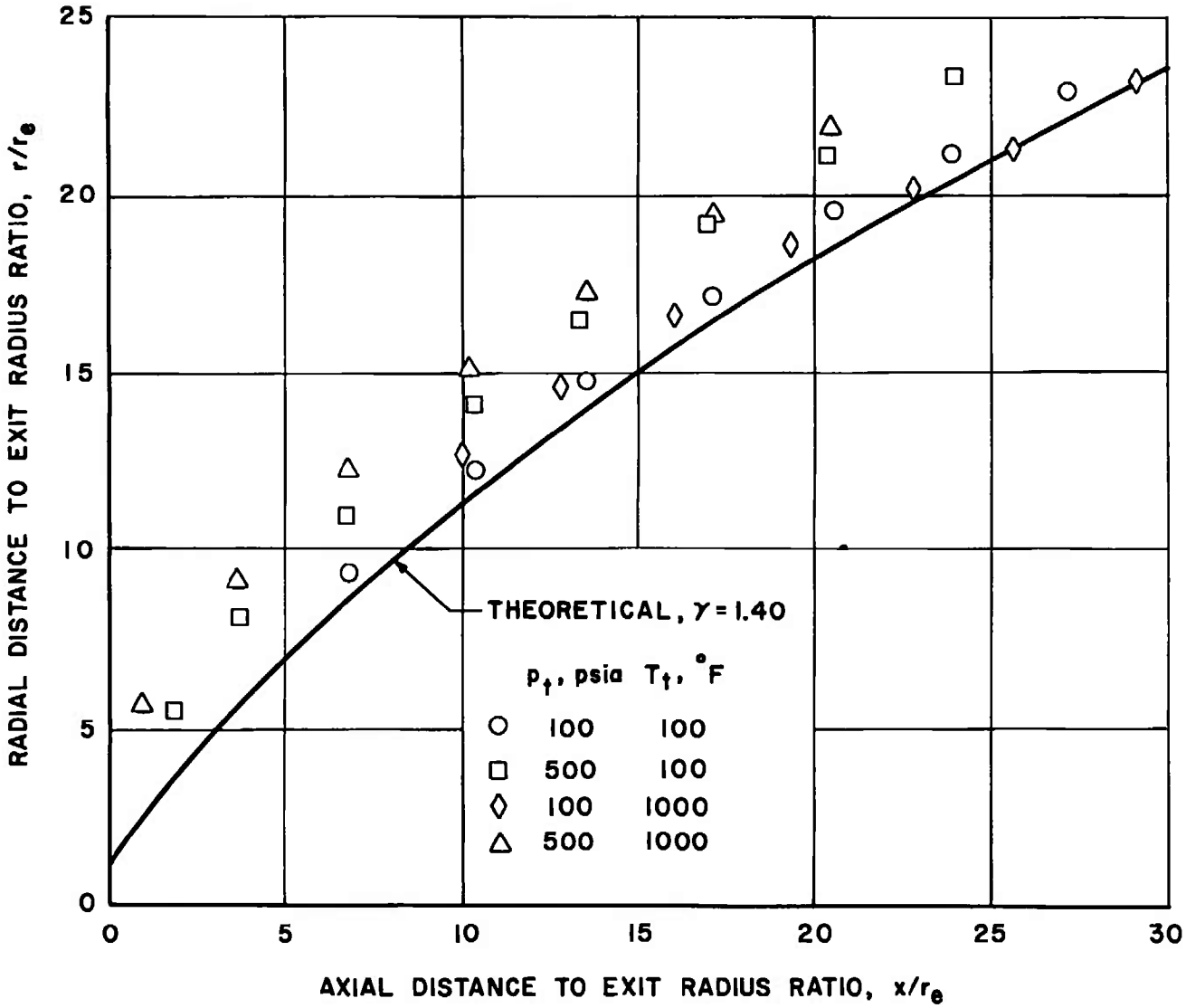

c. N_2, θ_N = 10 deg, δ_i = 60 deg

Fig. 10 Continued

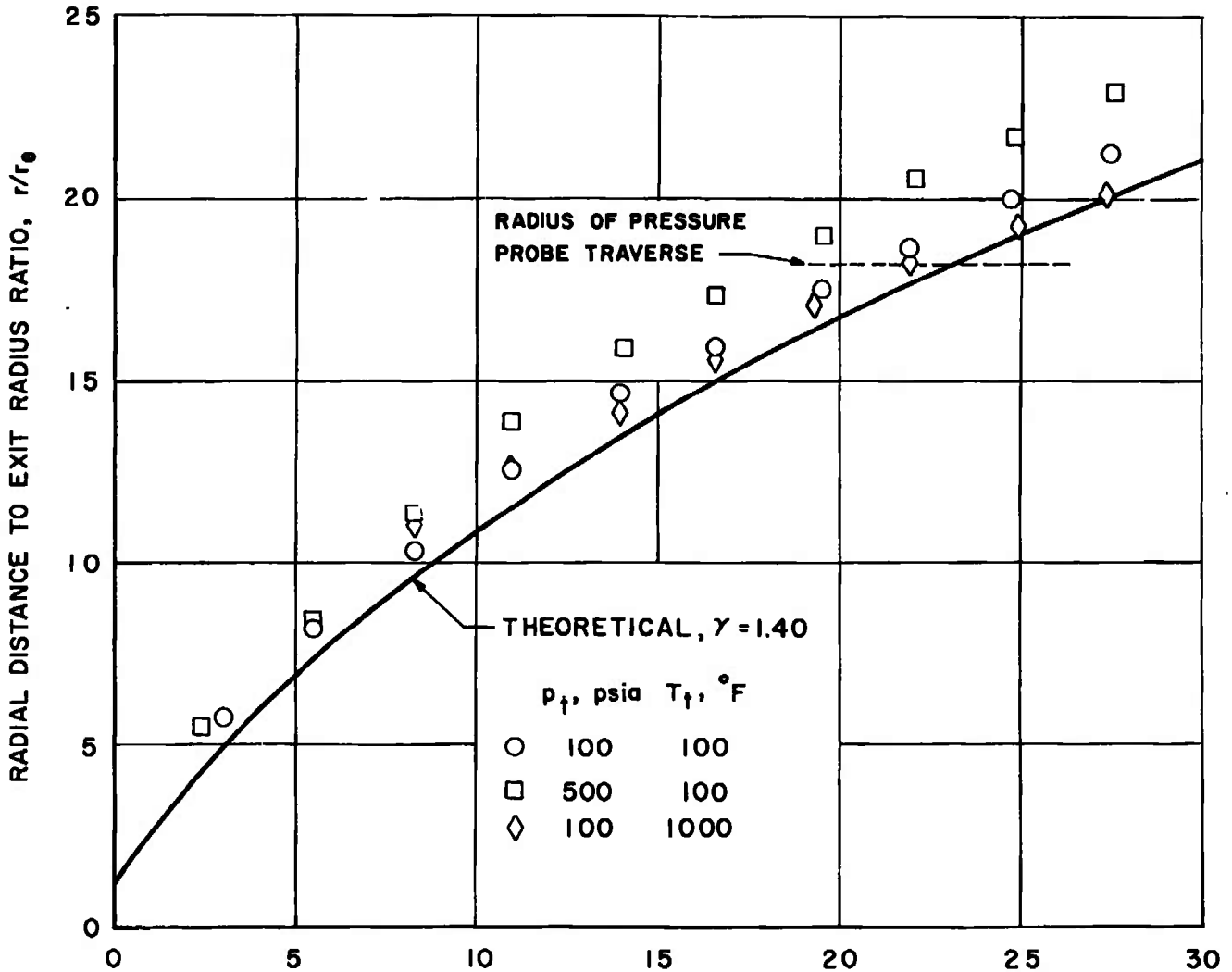

d. N_2, θ_N = 20 deg 36 min, δ_i = 60 deg

Fig. 10 Continued

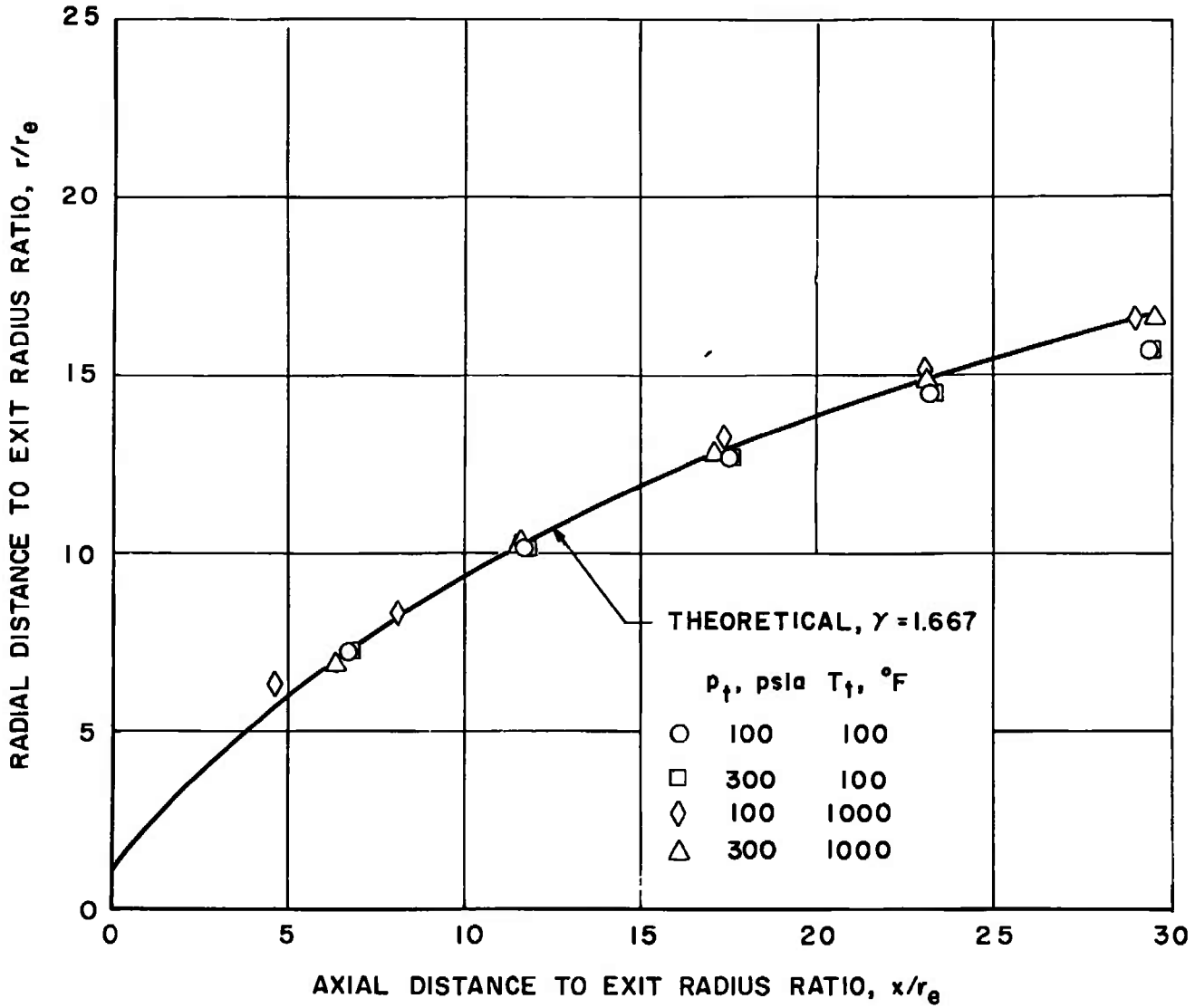

e. He, θ_N = 10 deg, δ_i = 58 deg 28 min

Fig. 10 Continued

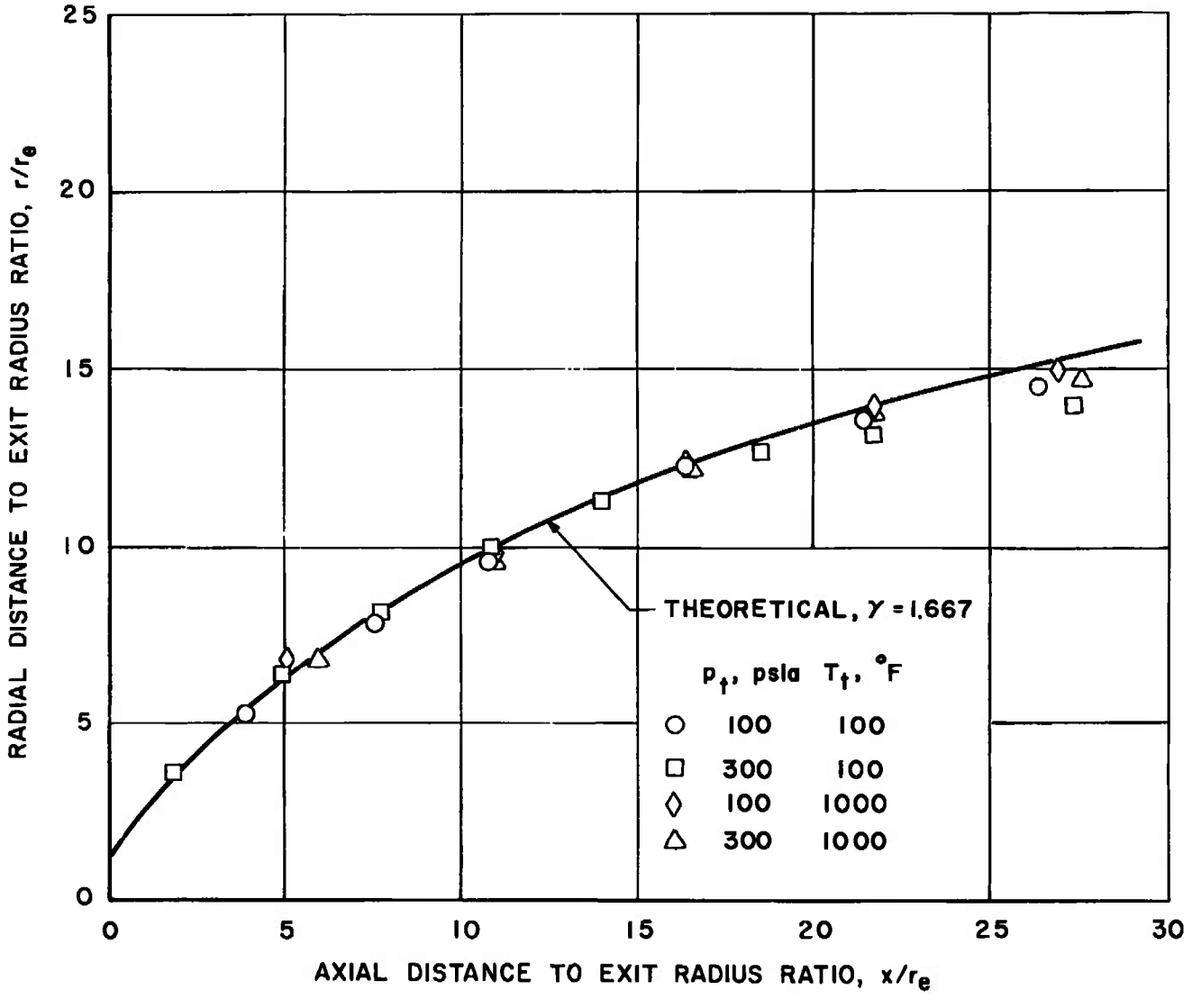

f. He, θ_N = 20 deg 36 min, δ_j = 61 deg 56 min

Fig. 10 Concluded

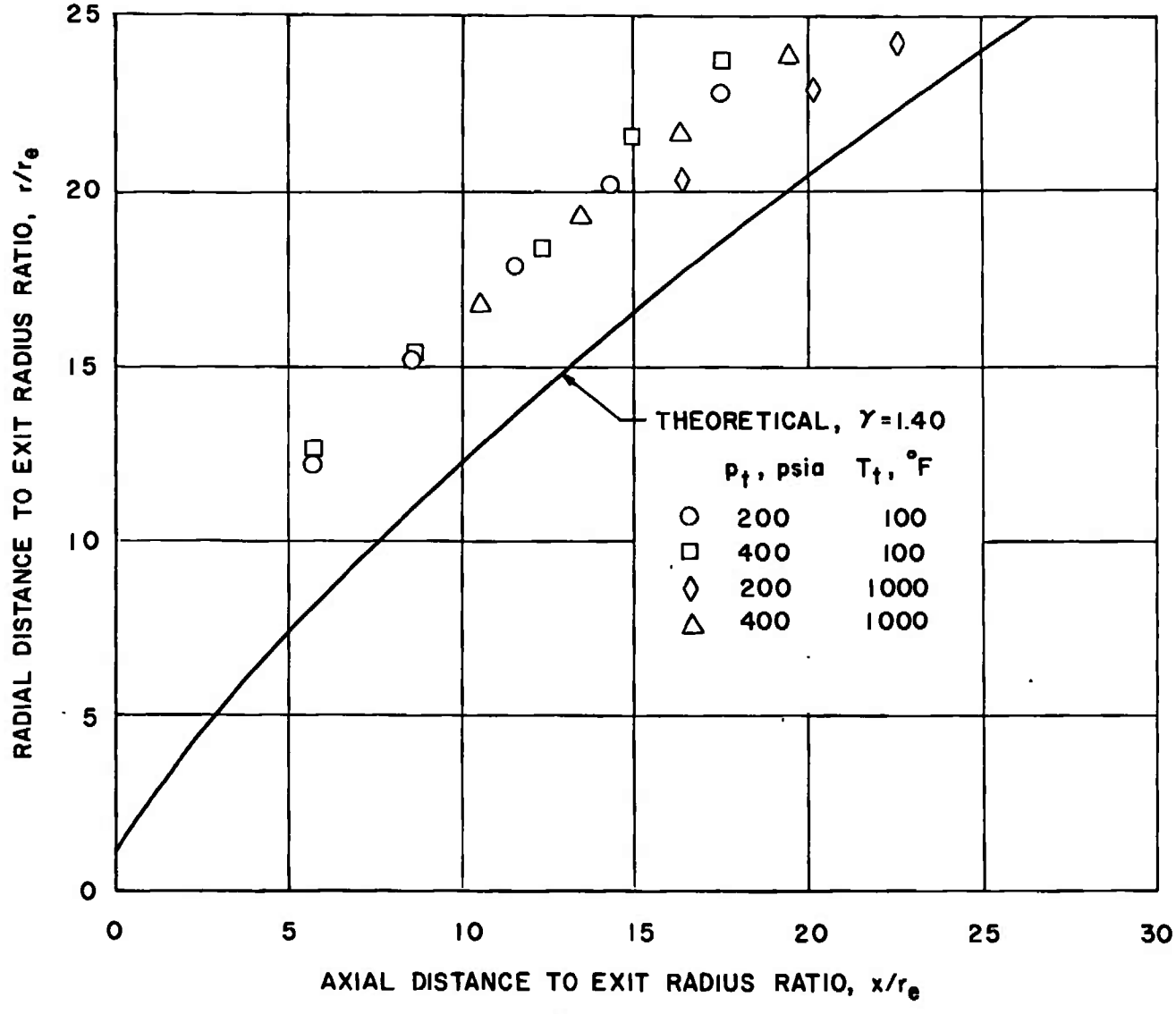

a. N_2, θ_N = 10 deg, δ_i 60 deg

Fig. 11 A Comparison of Experimentally Determined Jet Boundaries with a Method-of-Characteristics Solution for $\gamma M_1^2/\beta_1$ = 18

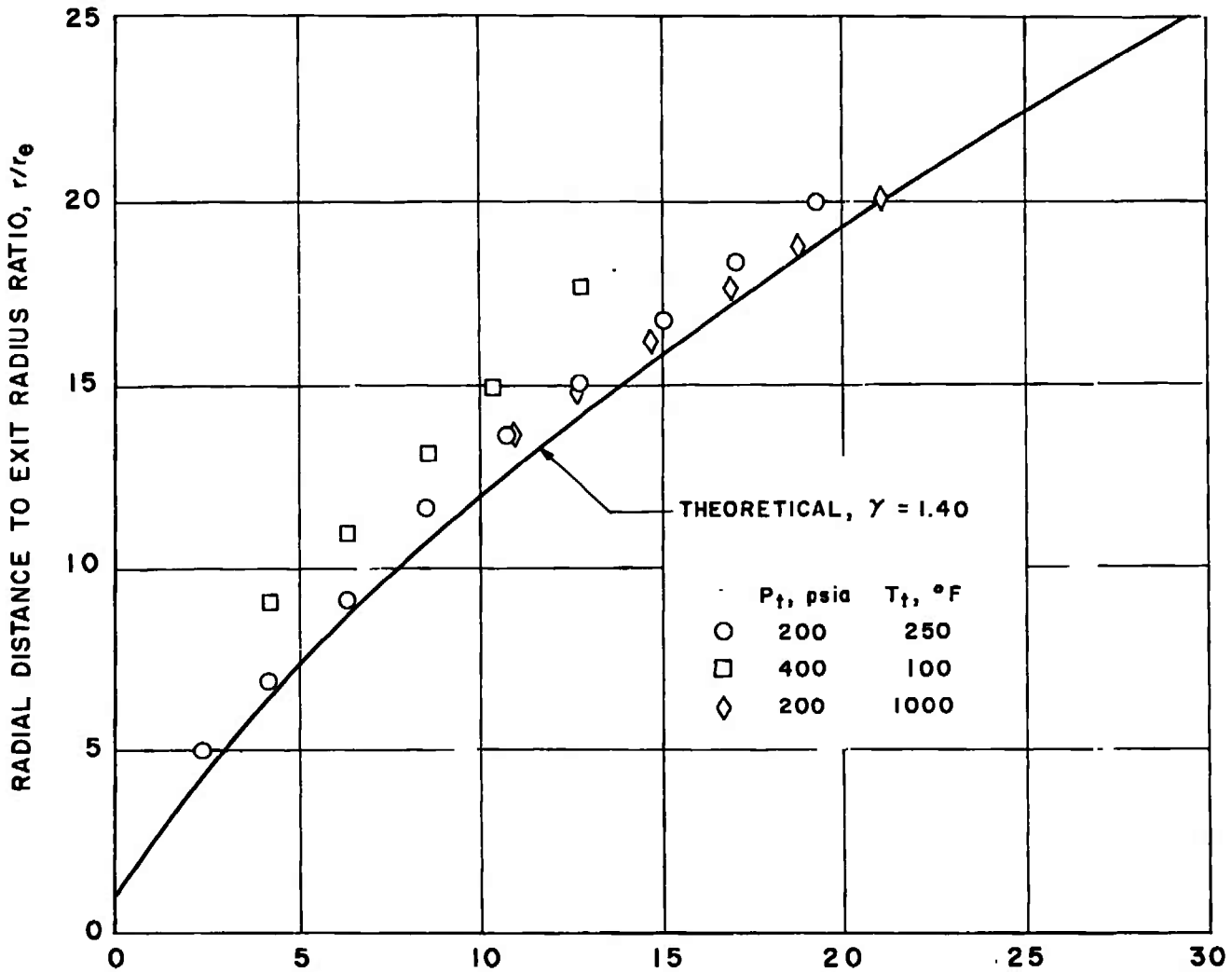

b. N_2, θ_N = 20 deg, δ_i = 60 deg

Fig. 11 Continued

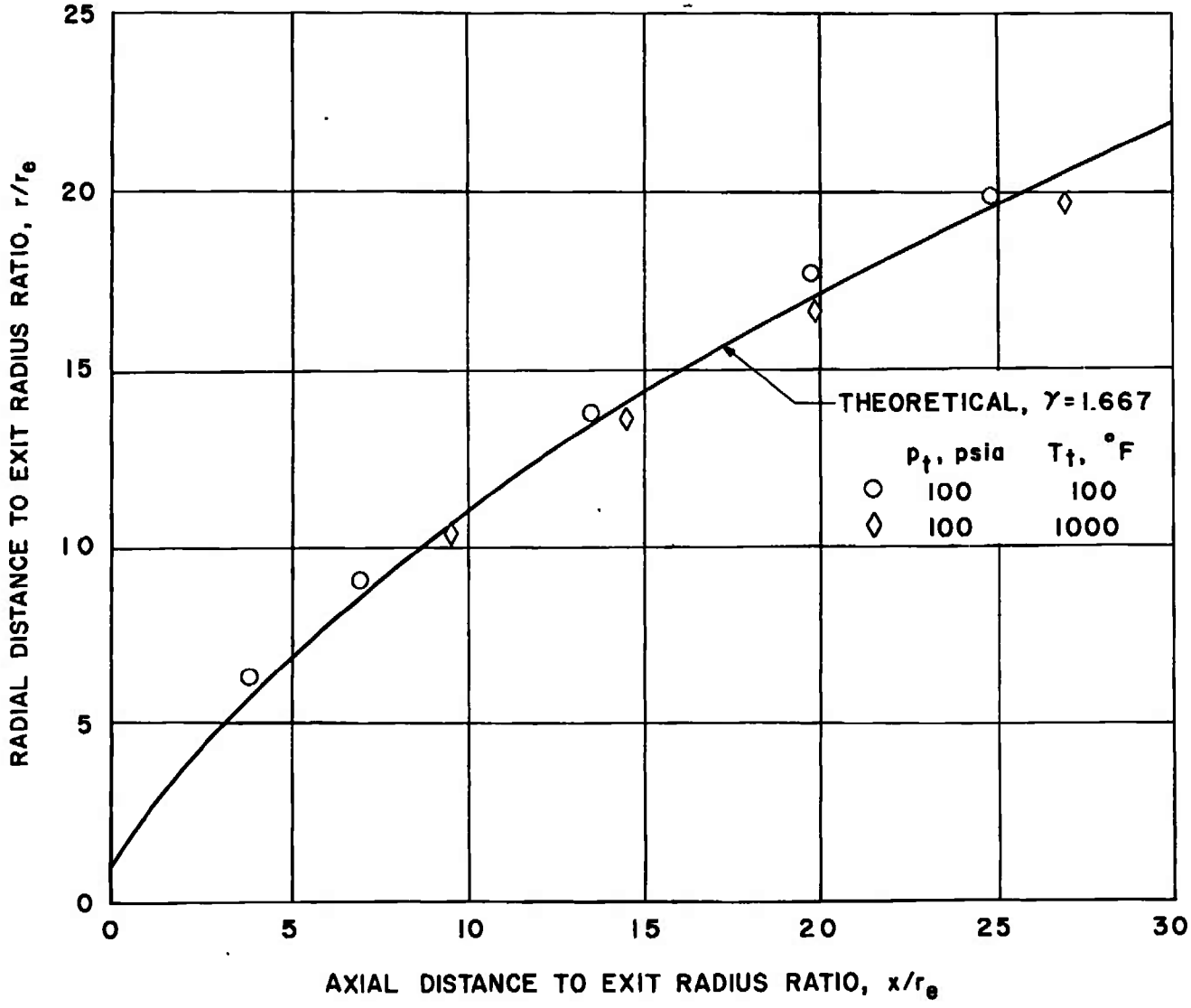

c. He, θ_N = 10 deg, δ_i = 60 deg

Fig. 11 Continued

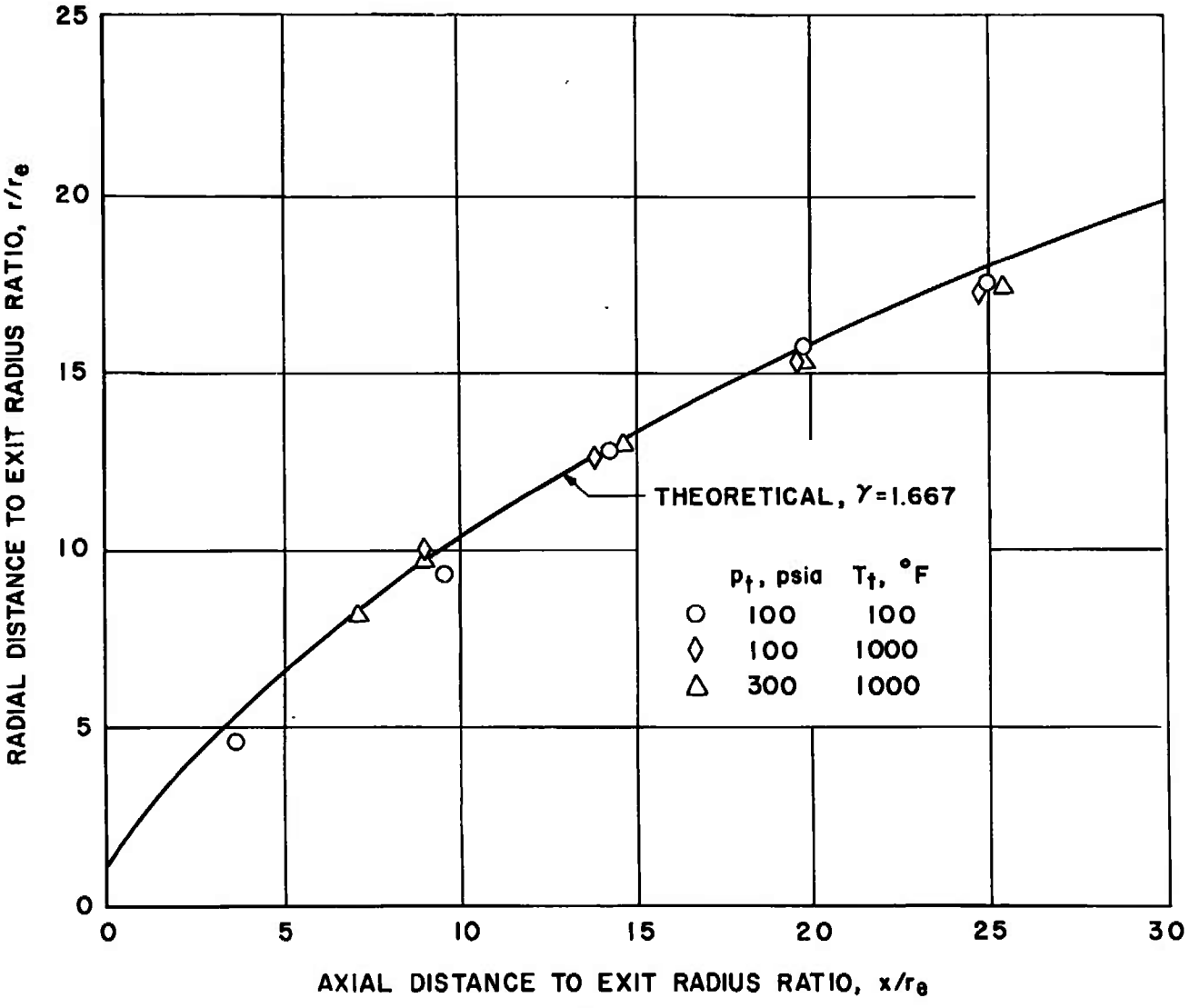

d. He, θ_N = 20 deg, δ_i = 60 deg

Fig. 11 Concluded

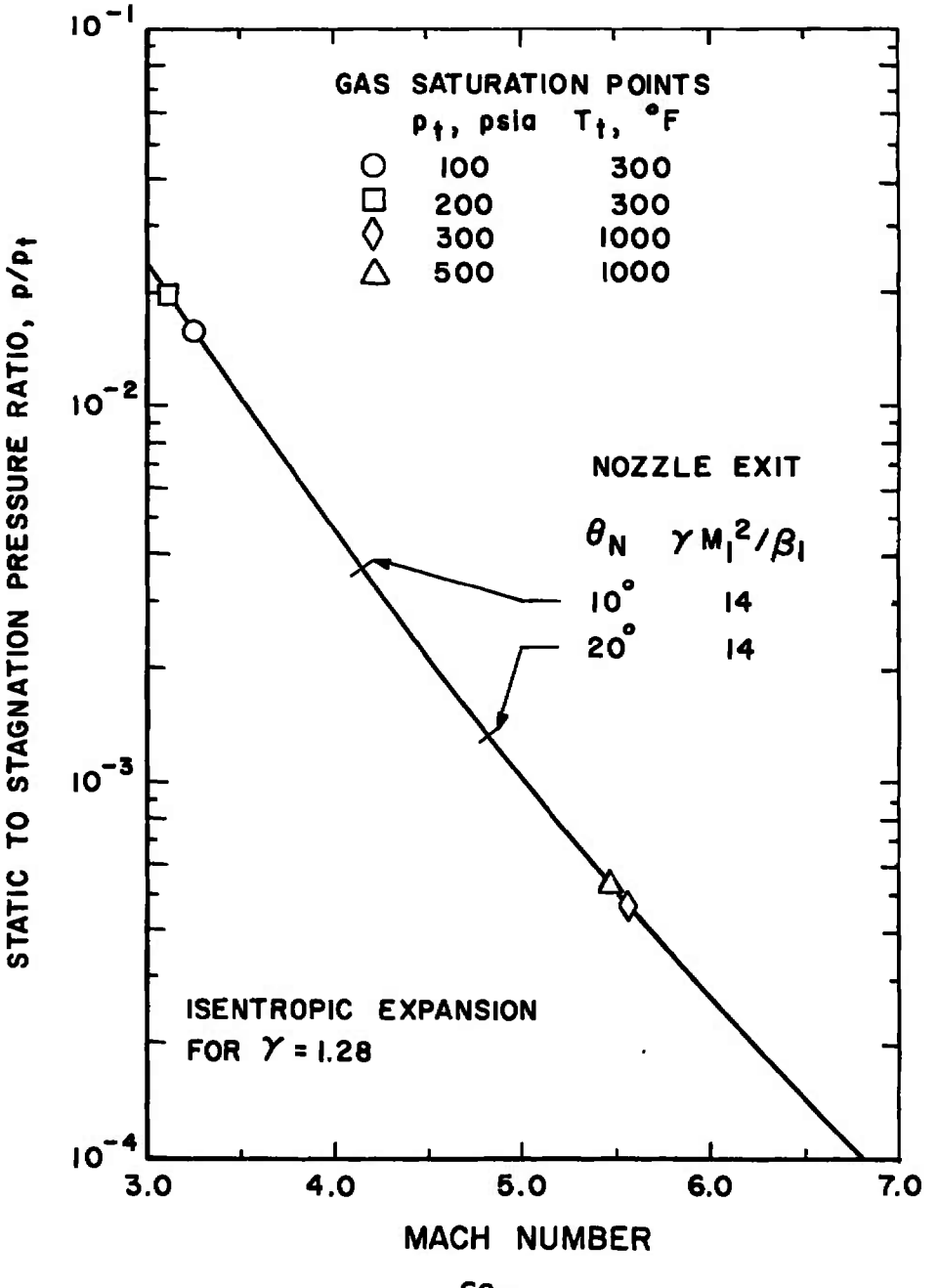

a. CO_2

Fig. 12 Location of Equilibrium Gas Saturation Conditions for an Expansion from the Experimental Stagnation Temperatures and Pressures

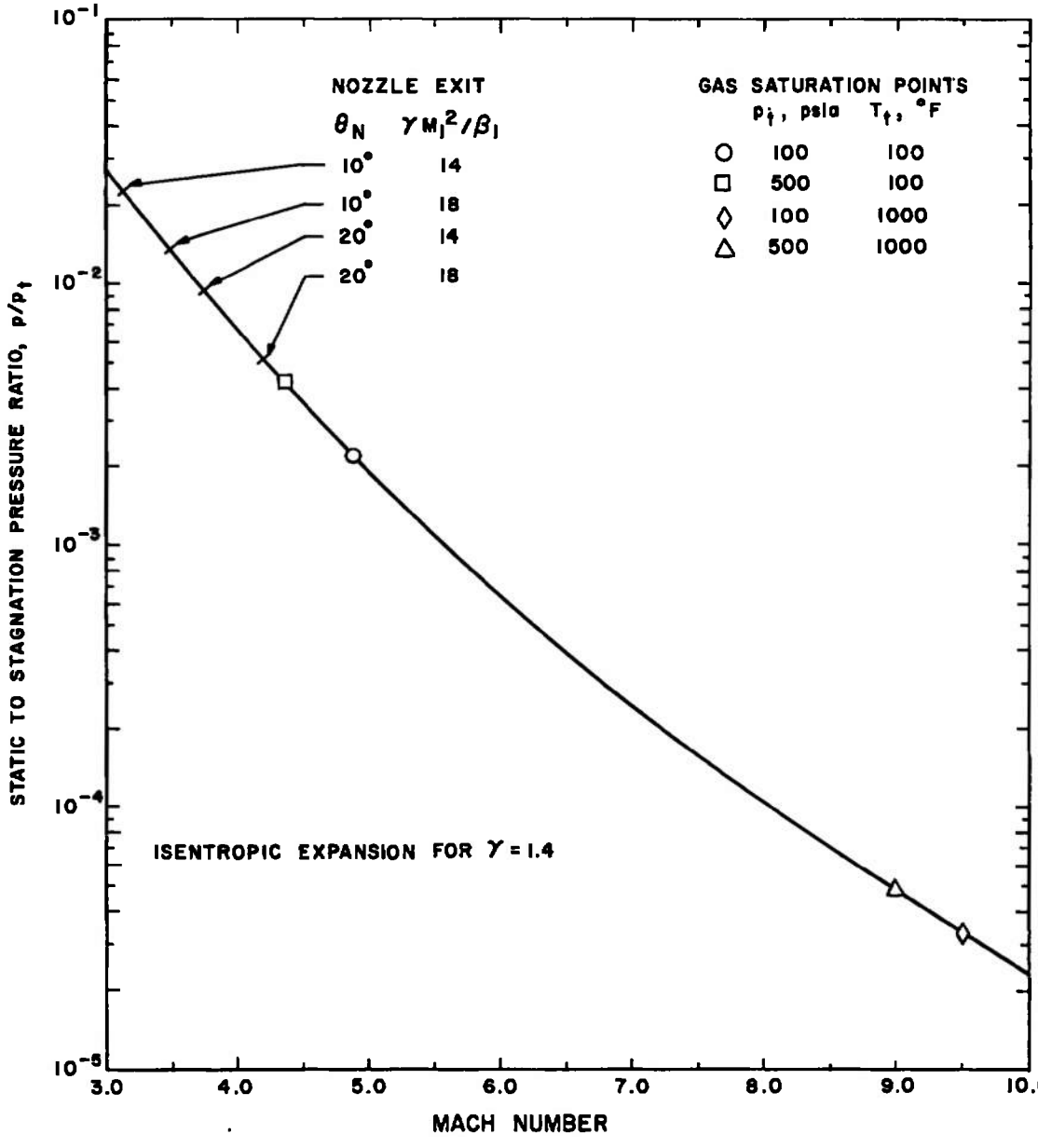

b. N_2

Fig. 12 Concluded

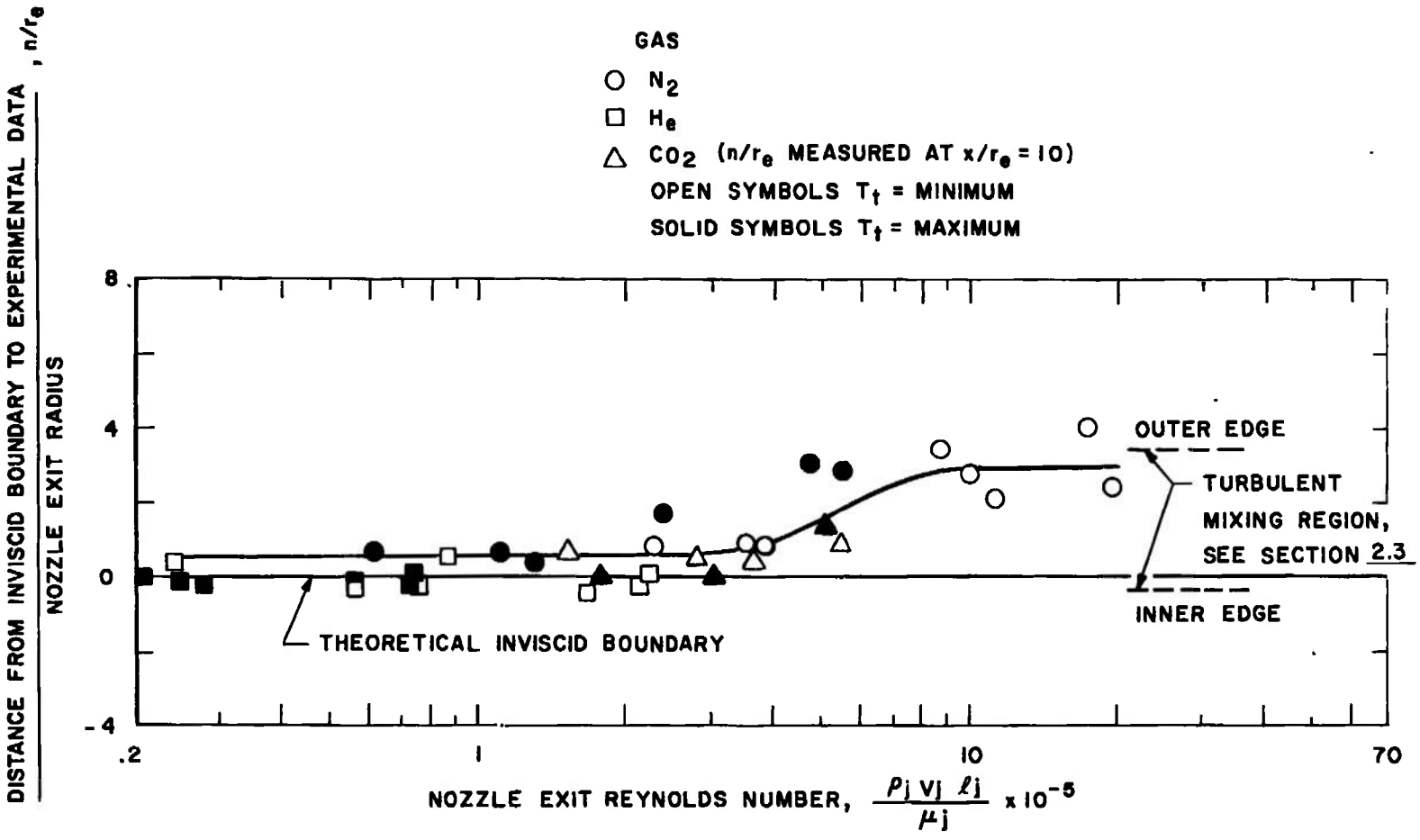

Fig. 13 Effect of the Nozzle Exit Reynolds Number on the Location of the Experimental Jet Boundary Relative to the Calculated Inviscid Boundary at $x/r_e = 20$

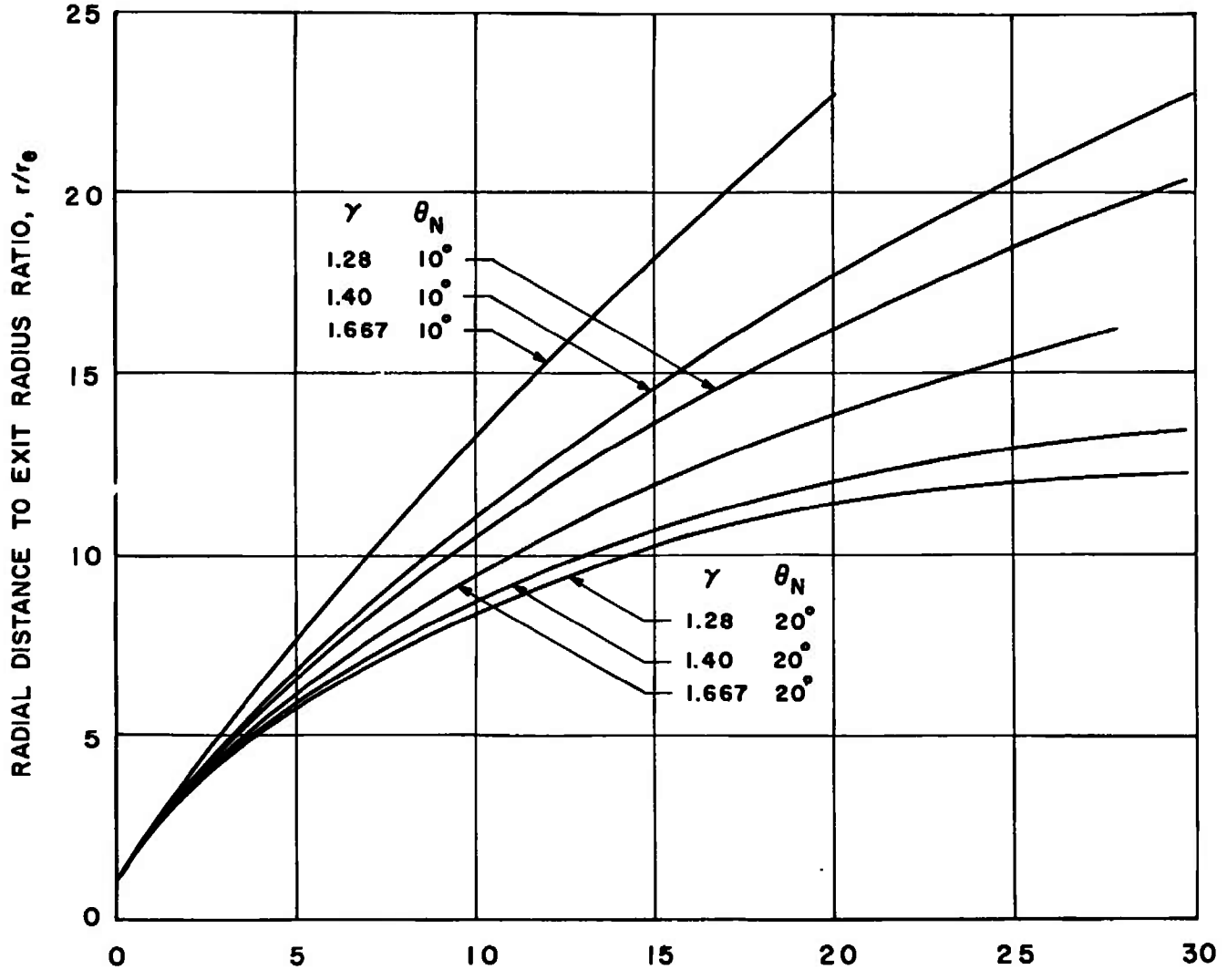

a. $\gamma M_i/\beta_i = 4.55$, δ_i - 60 deg

Fig. 14 Comparison of Jet Boundaries for Othor Proposed Simulation Parameters

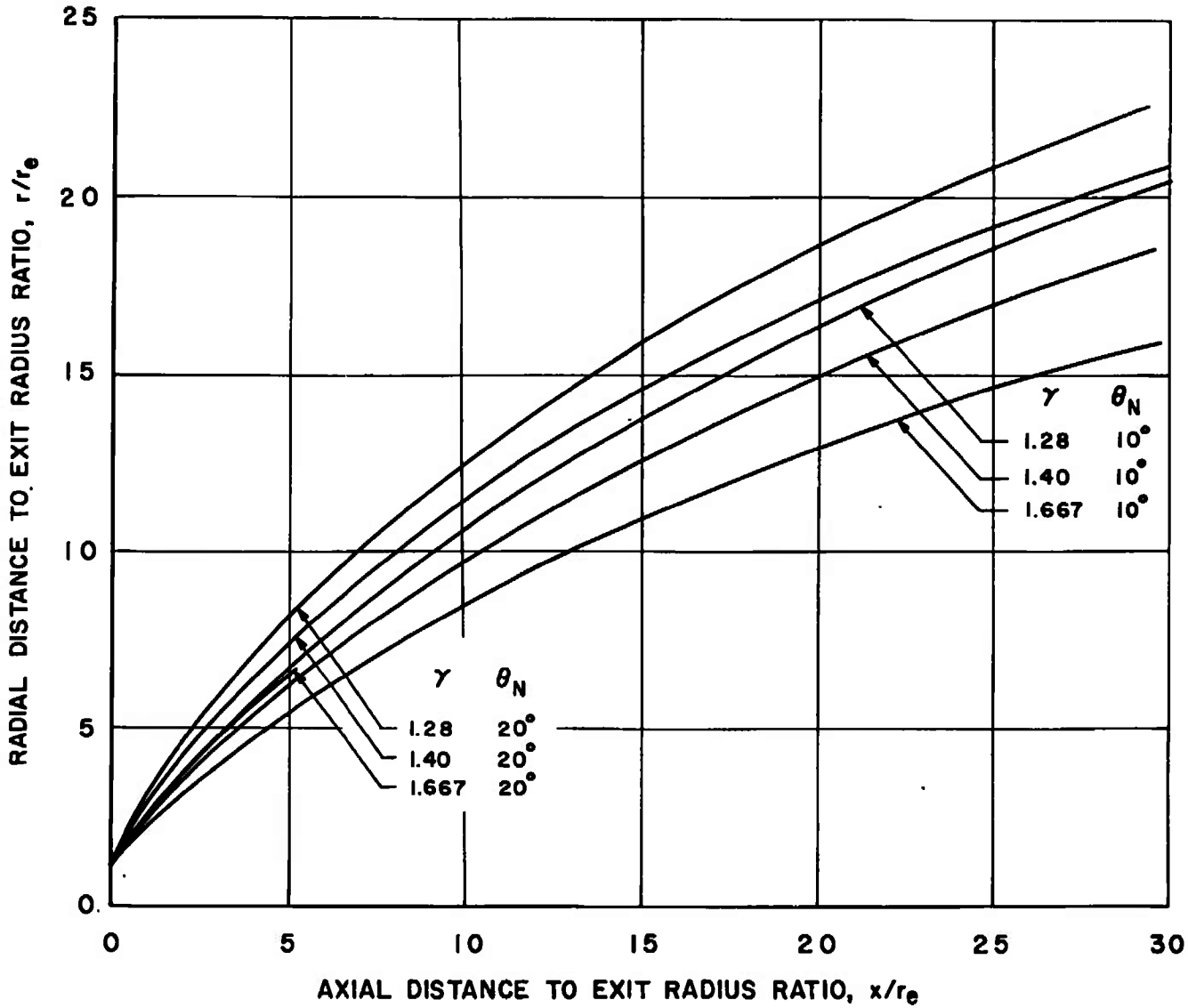

b. $\gamma M_i^2/\beta_i = 4.45$, $p_i/p_{\infty} = 345$

Fig. 14 Continued

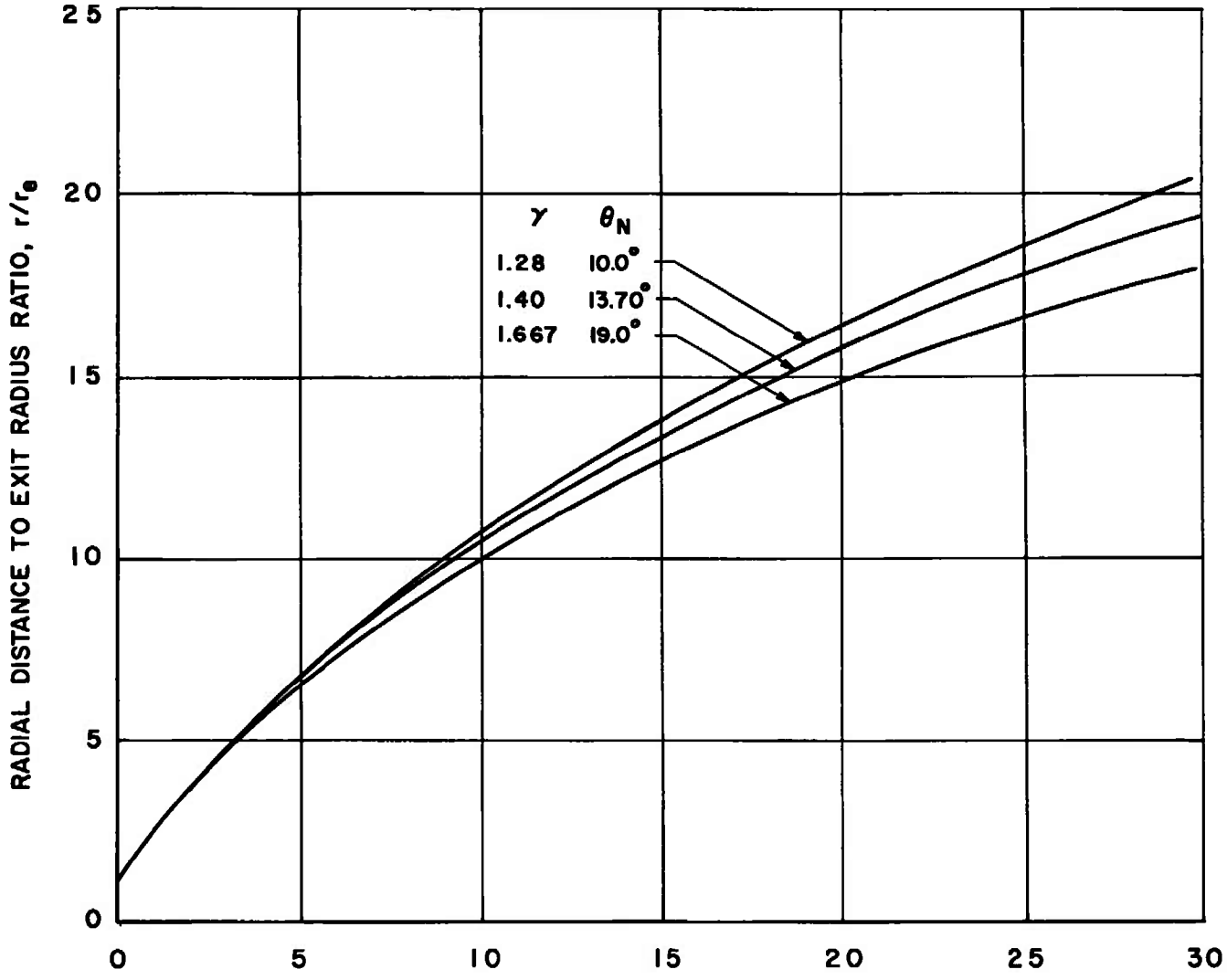

c. $\gamma M_i^2/\beta_i = 4.55$, $p_i/p_\infty = 345$, $\delta_i = 60$ deg

Fig. 14 Concluded

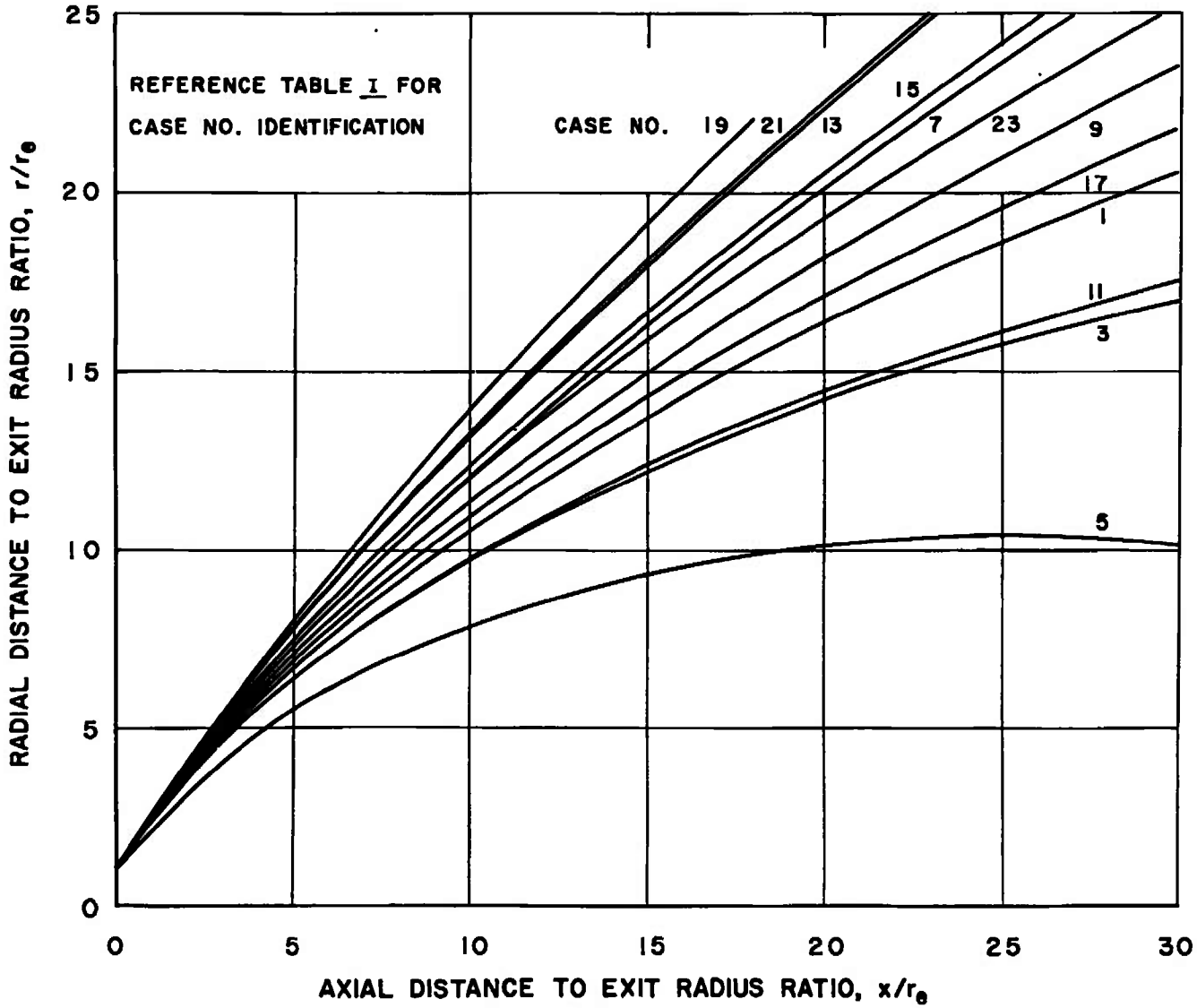

a. θ_N = 10 deg, δ_i = 60 deg

Fig. 15 Summary of Calculated Boundaries Presented in Figure 9

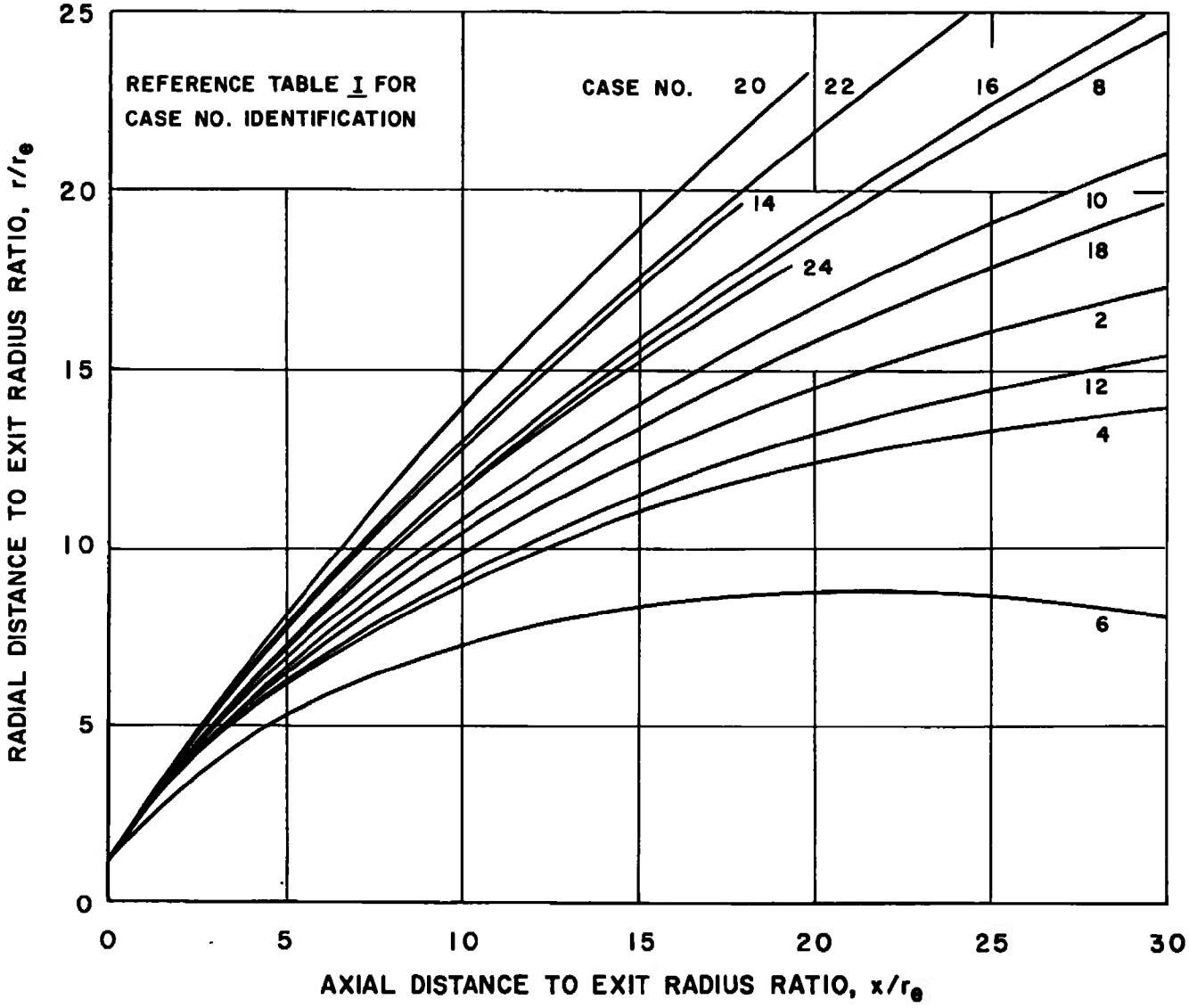

b. θ_N = 20 deg, δ_i = 60 deg

Fig. 15 Concluded

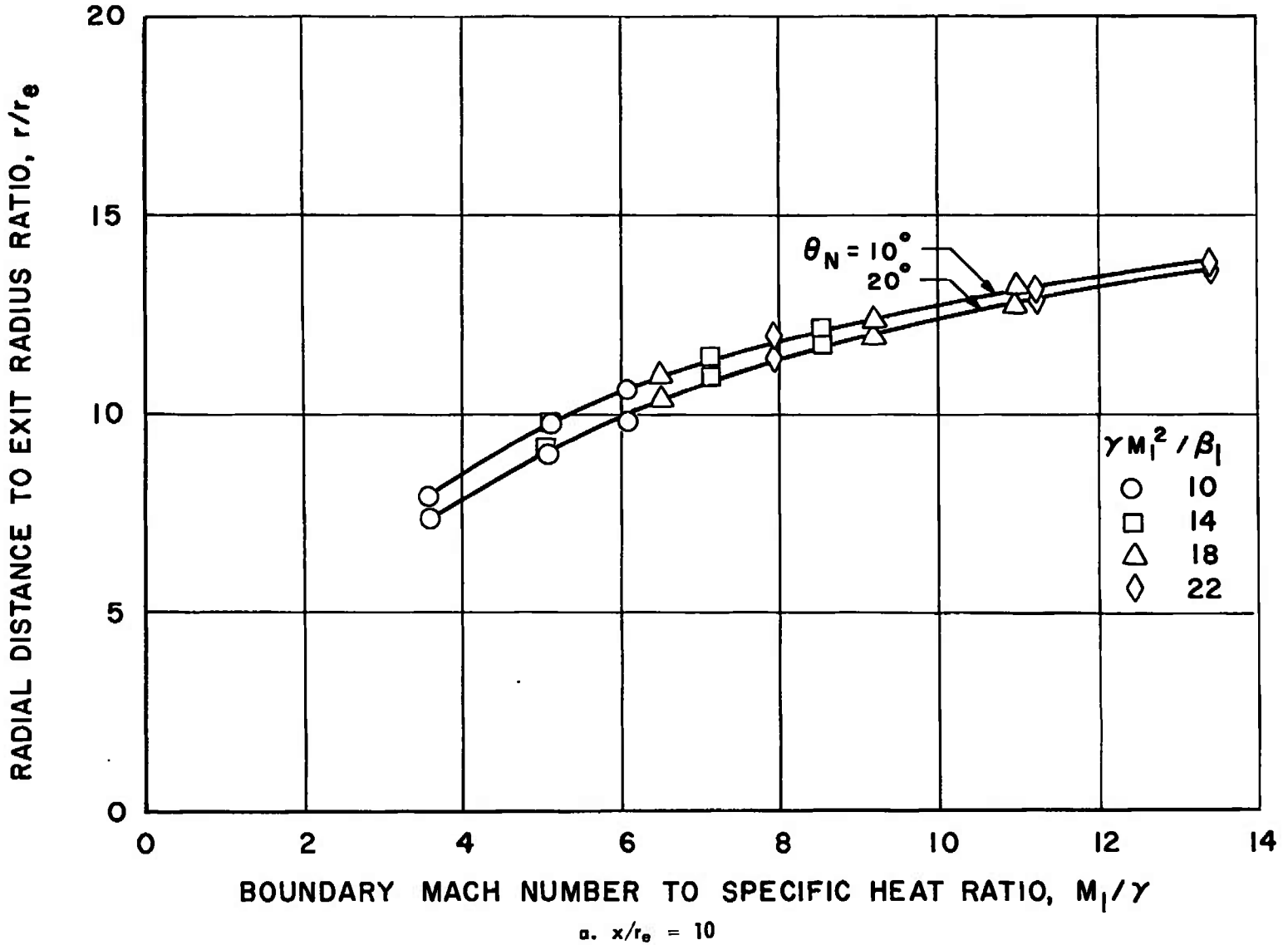

a. $x/r_e = 10$

Fig. 16 Correlation of Jet Radii from Figure 15 at a Fixed Axial Distance to Exit Radius Ratio

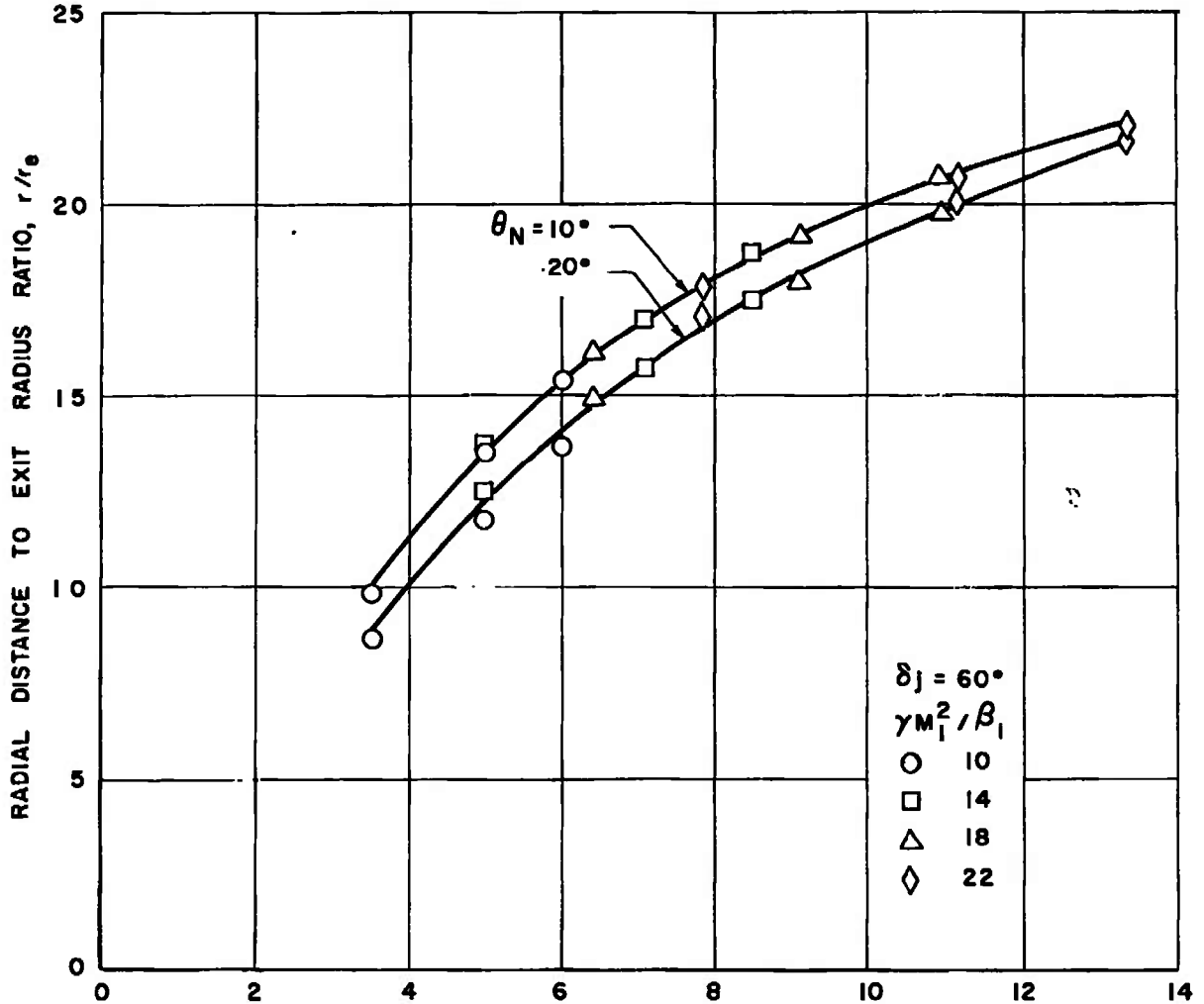

b. $x/r_e = 18$

Fig. 16 Concluded

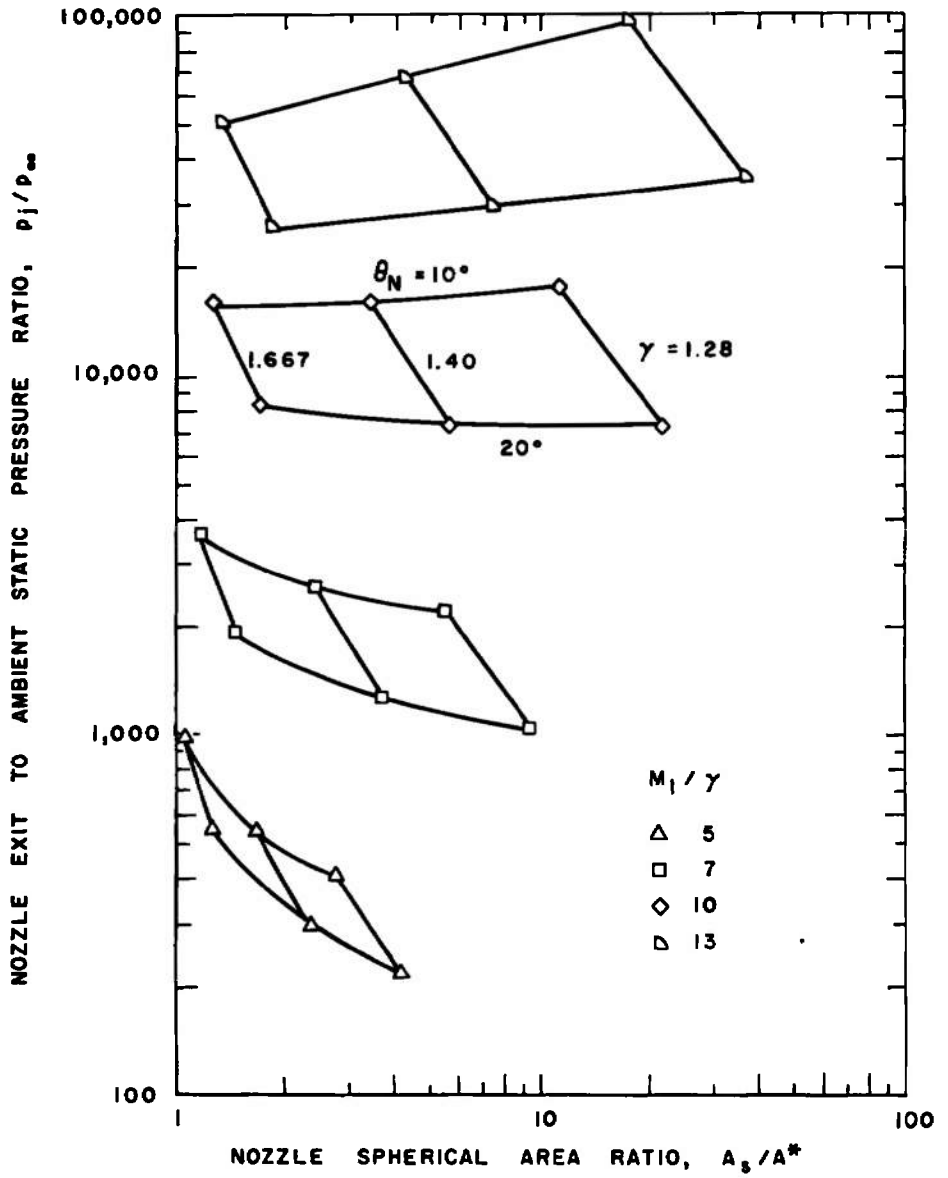

a. δ_j = 75 deg

Fig. 17 Range of Nozzle Area Ratio and Exit Pressure Ratio for Jets with Constant Values of M_1/γ

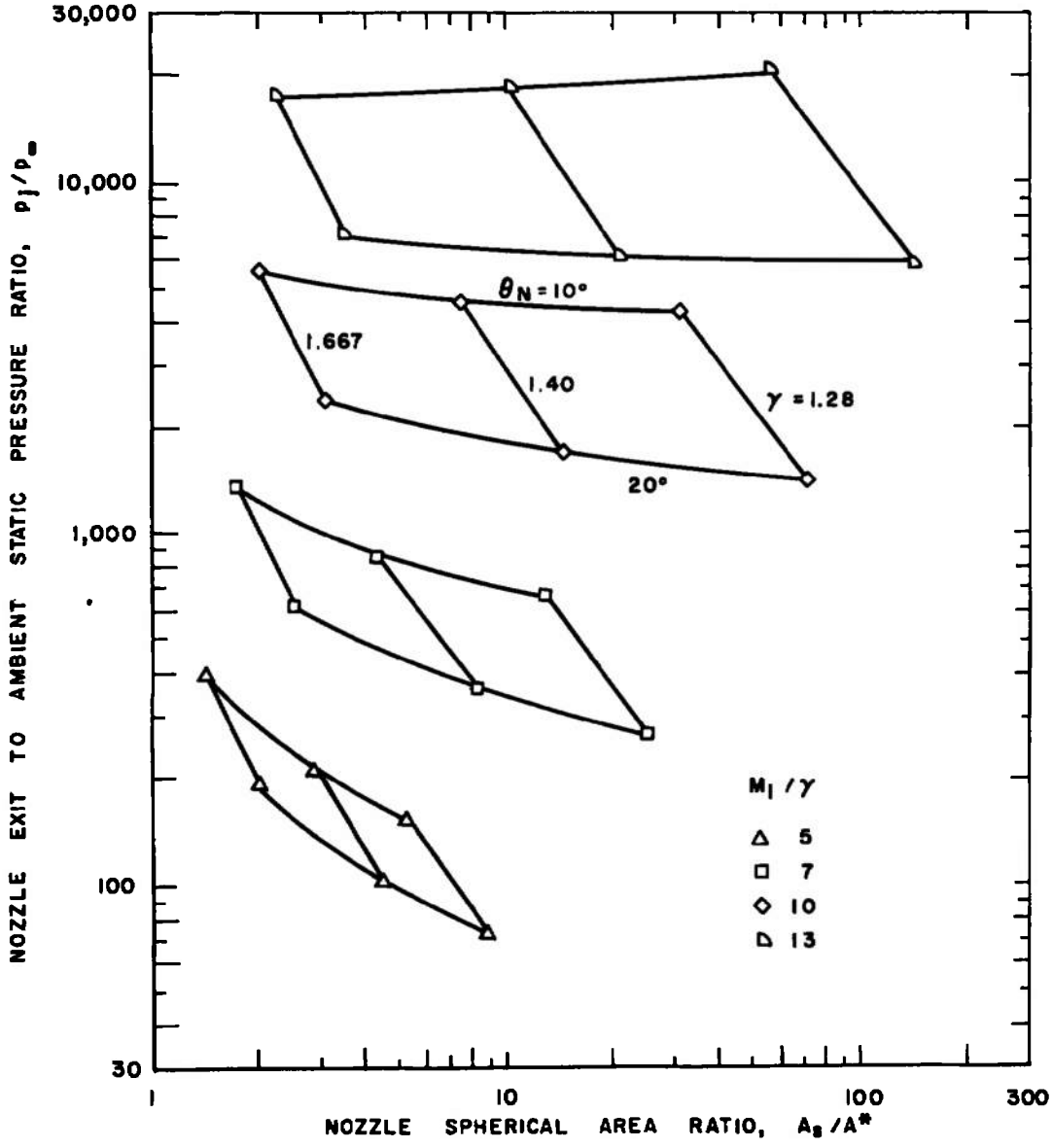

b. δ_i = 60 deg

Fig. 17 Continued

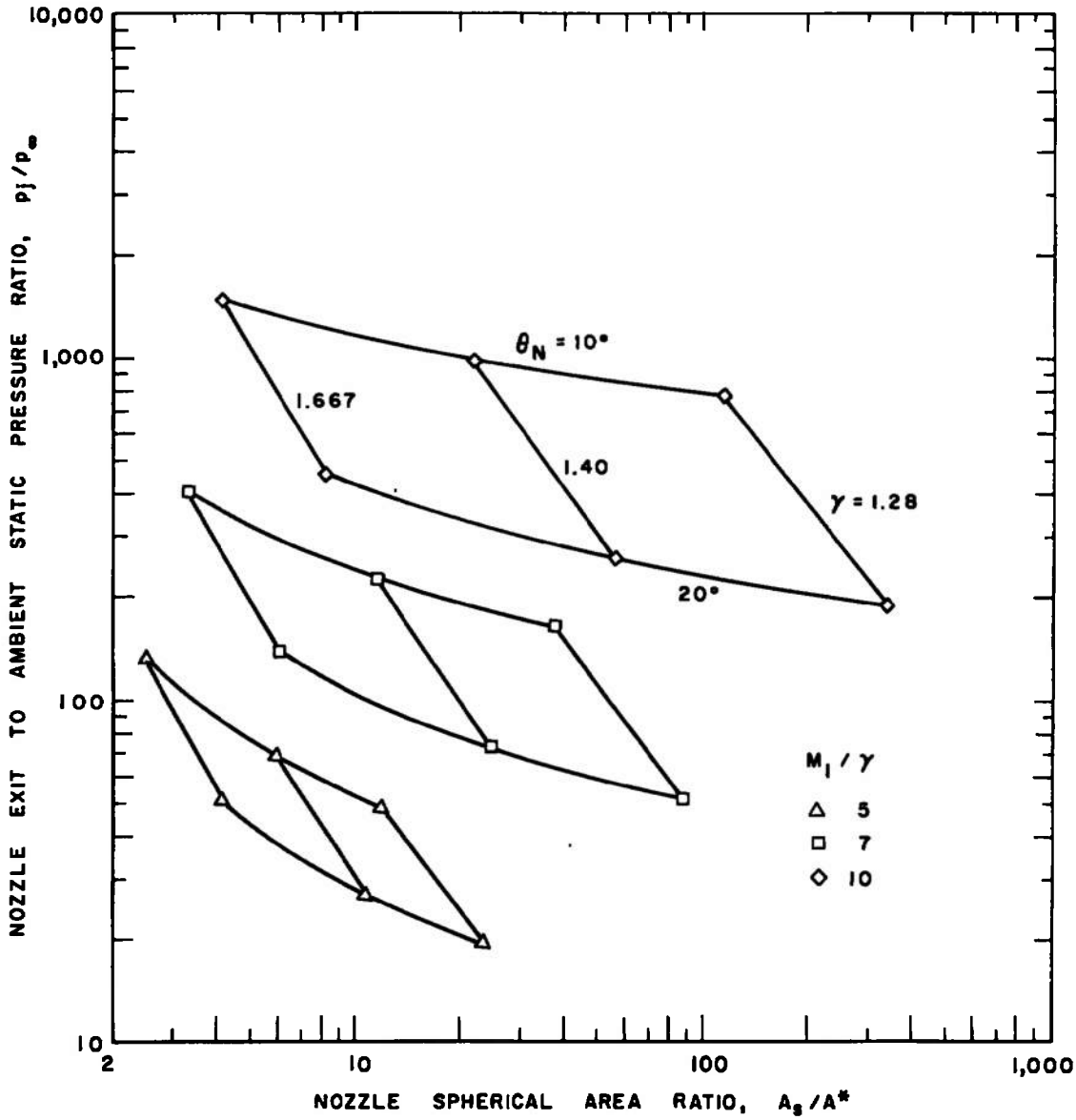

c. δ_j = 45 deg

Fig. 17 Concluded

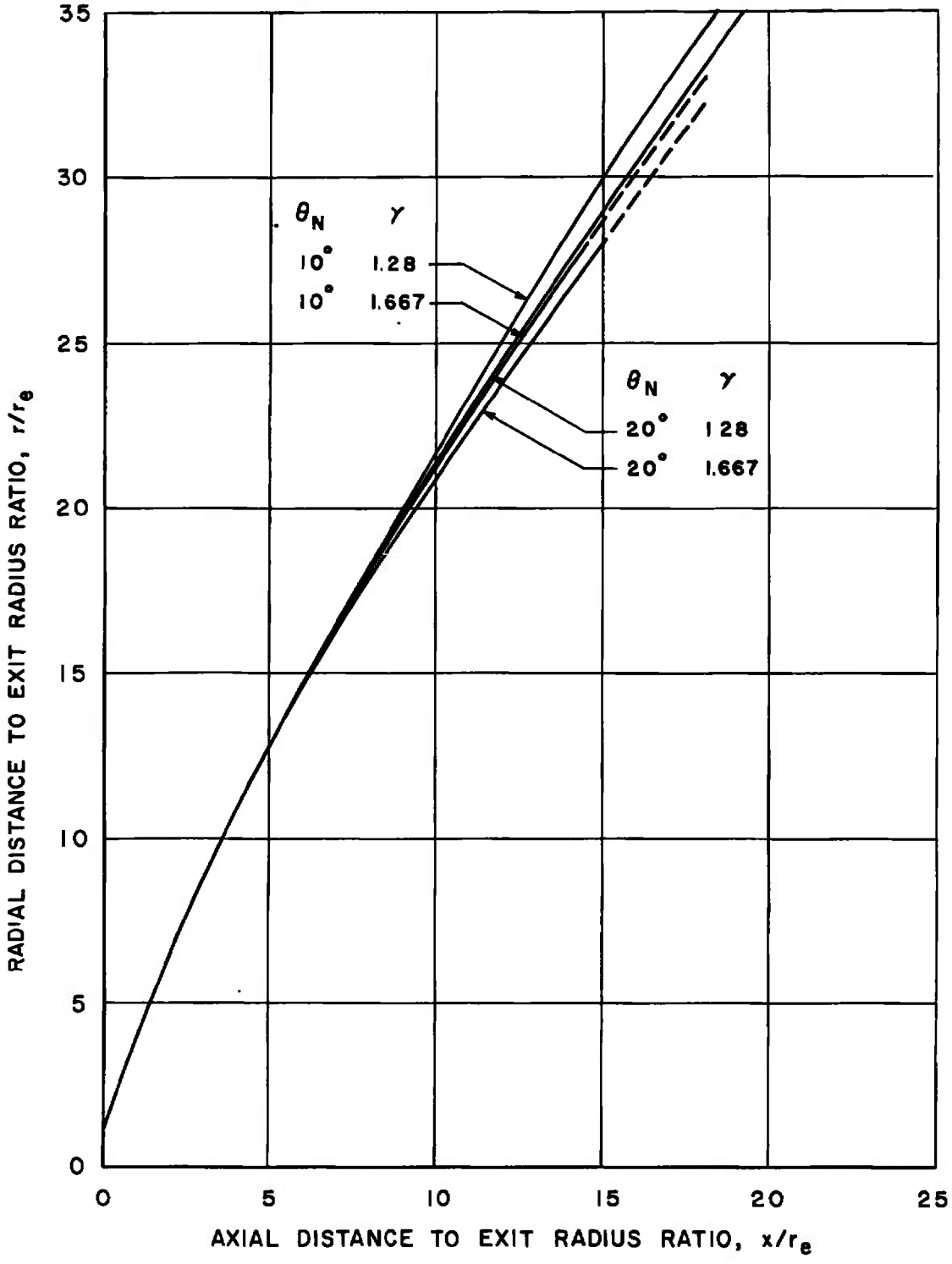

a. $M_1/y = 13$

Fig. 18 Comparison of Jet Boundaries as Determined by a Method-of-Characteristics Solution for $\delta_i = 75$ deg

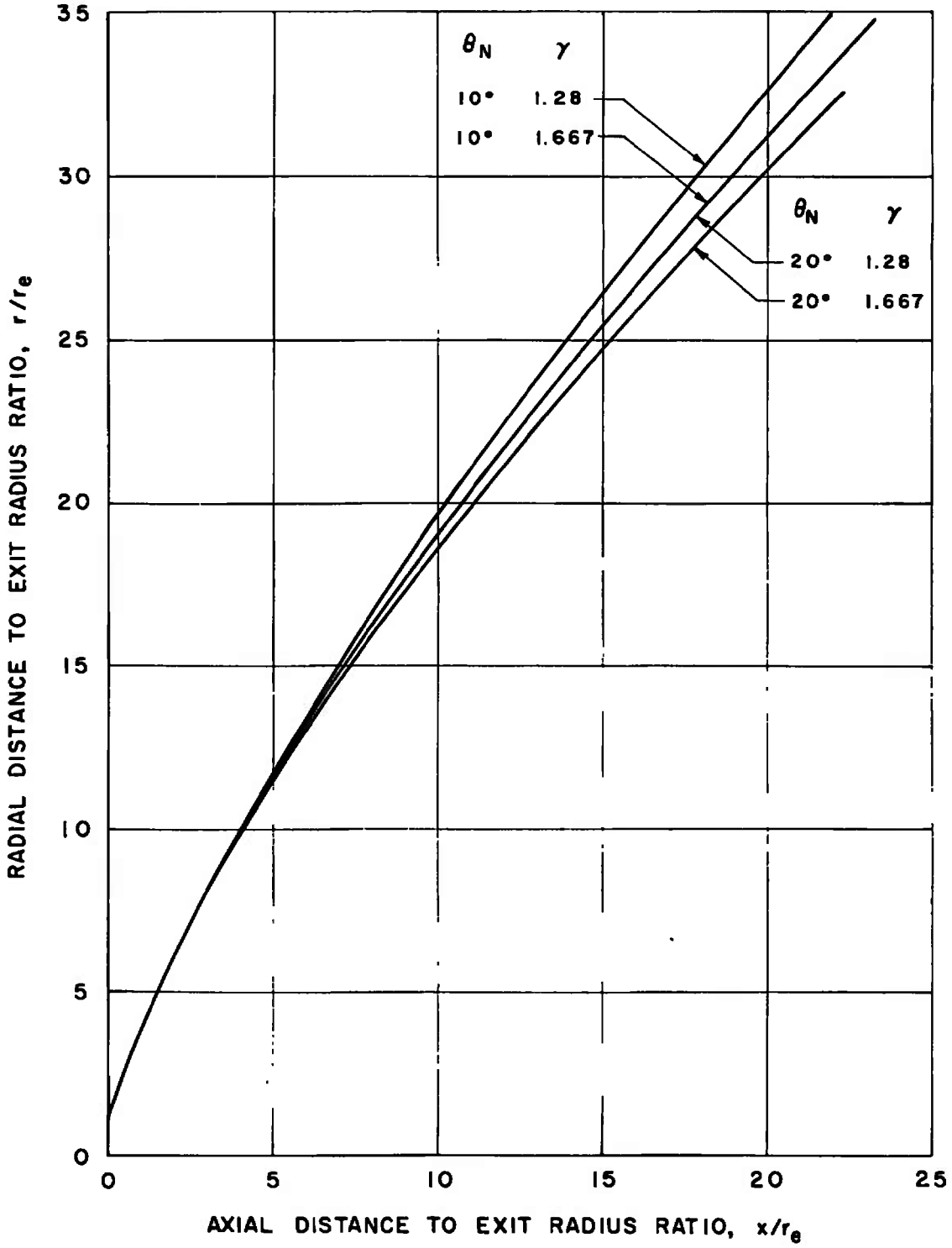

b. $M_1/\gamma = 10$

Fig. 18 Continued

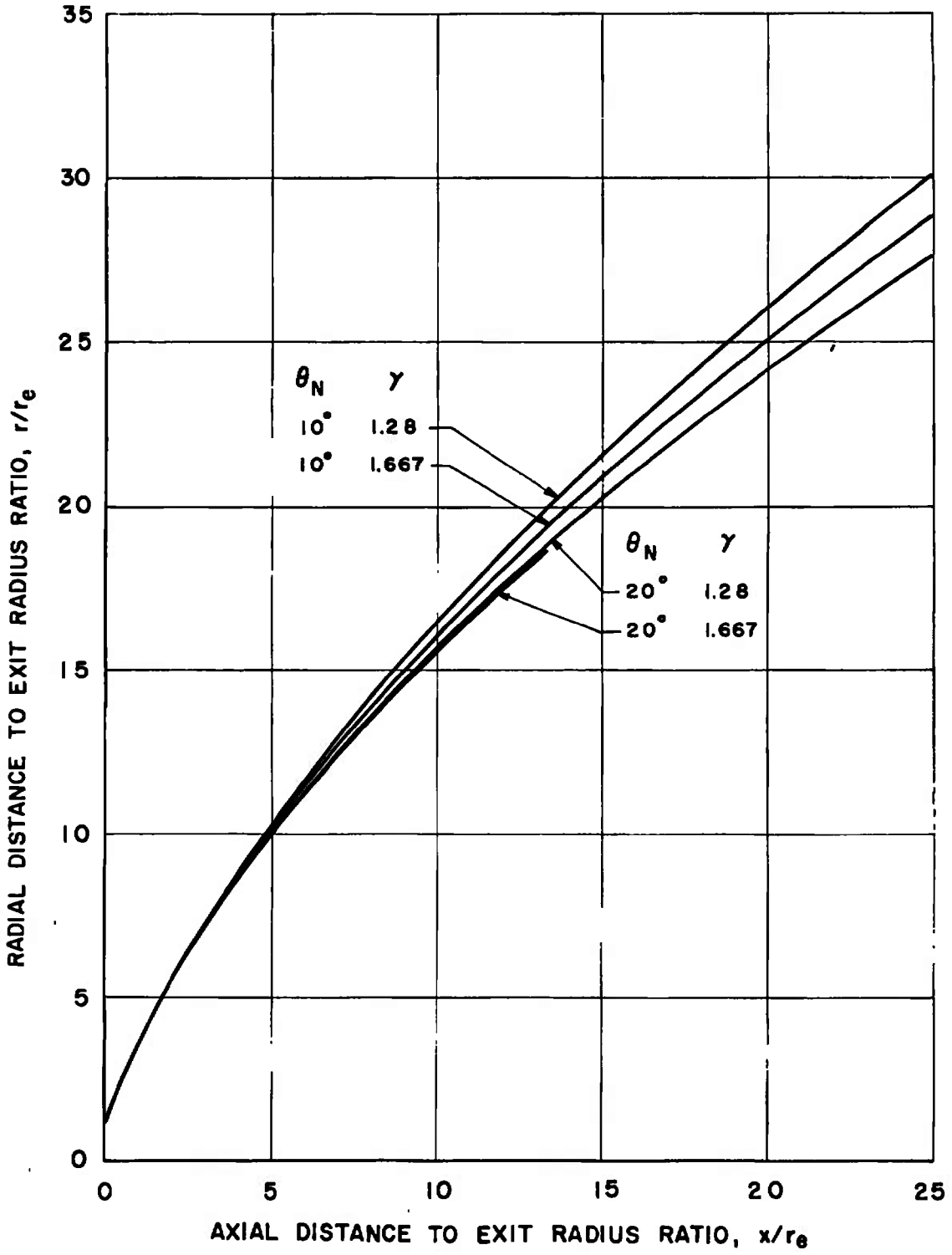

c. $M_1/y = 7$

Fig. 18 Continued

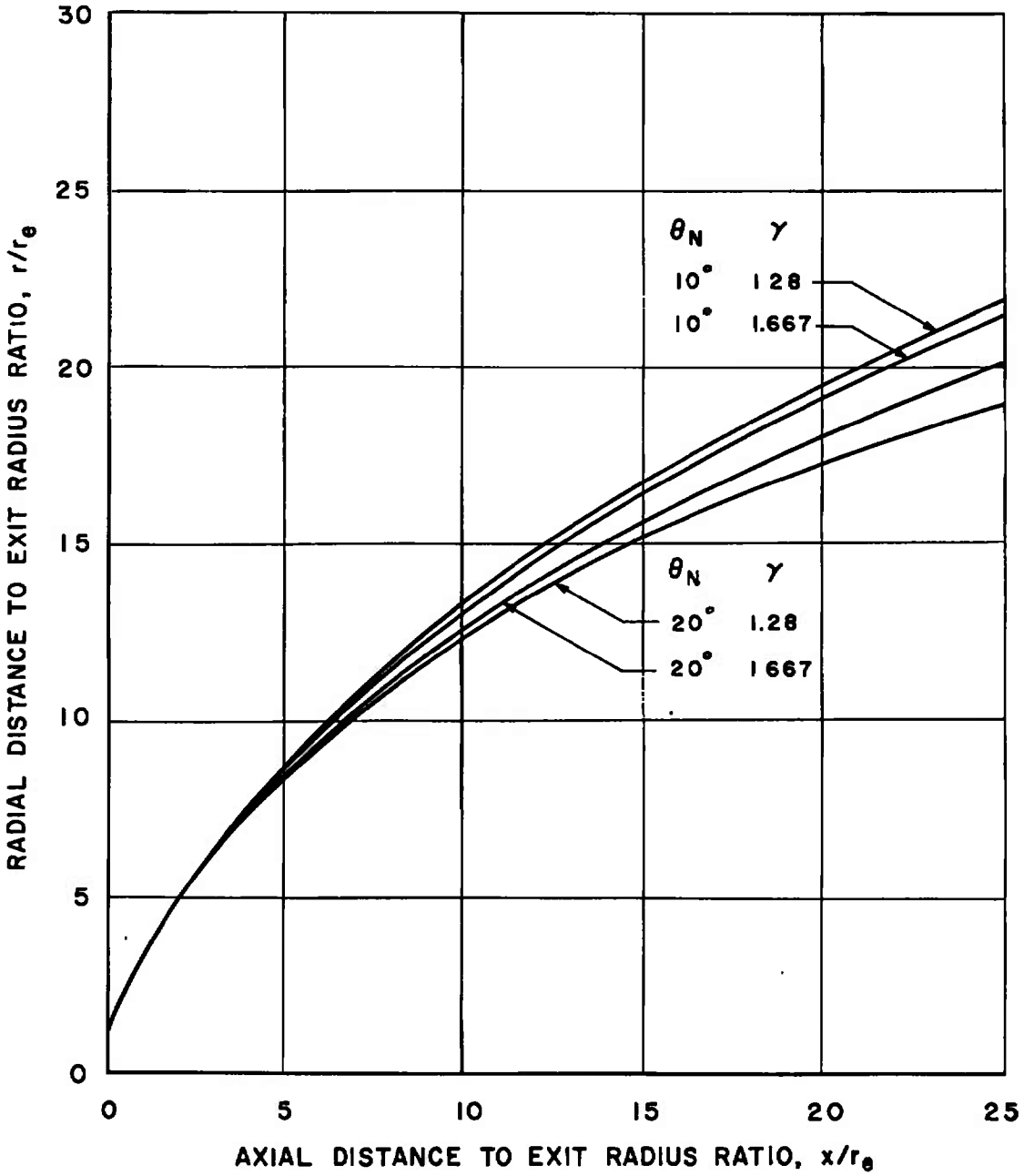

d. $M_1/\gamma = 5$

Fig. 18 Concluded

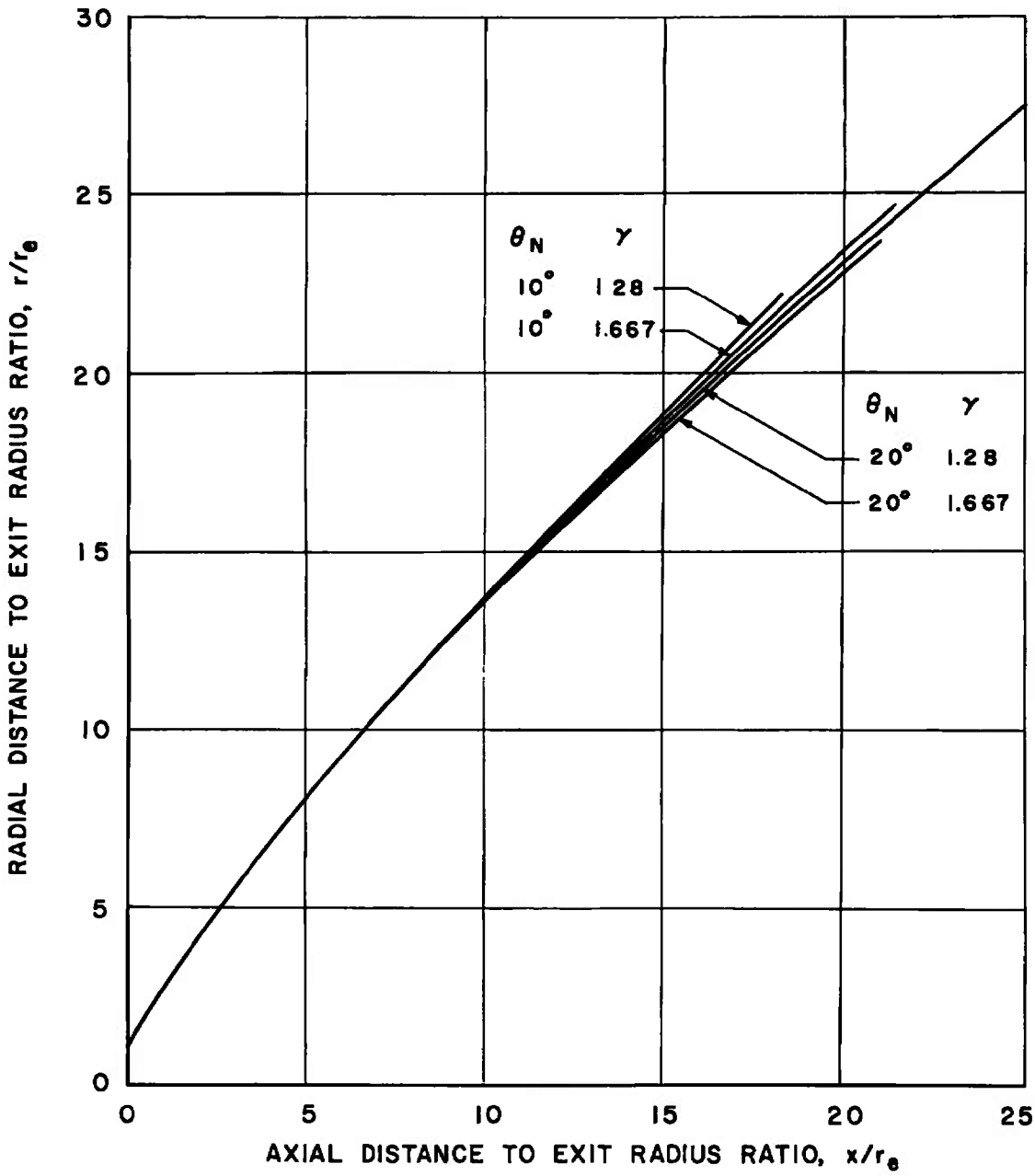

a. $M_1/\gamma = 13$

Fig. 19 Comparison of Jet Boundaries as Determined by a Method-of-Characteristics Solution for $\delta_j = 60$ deg

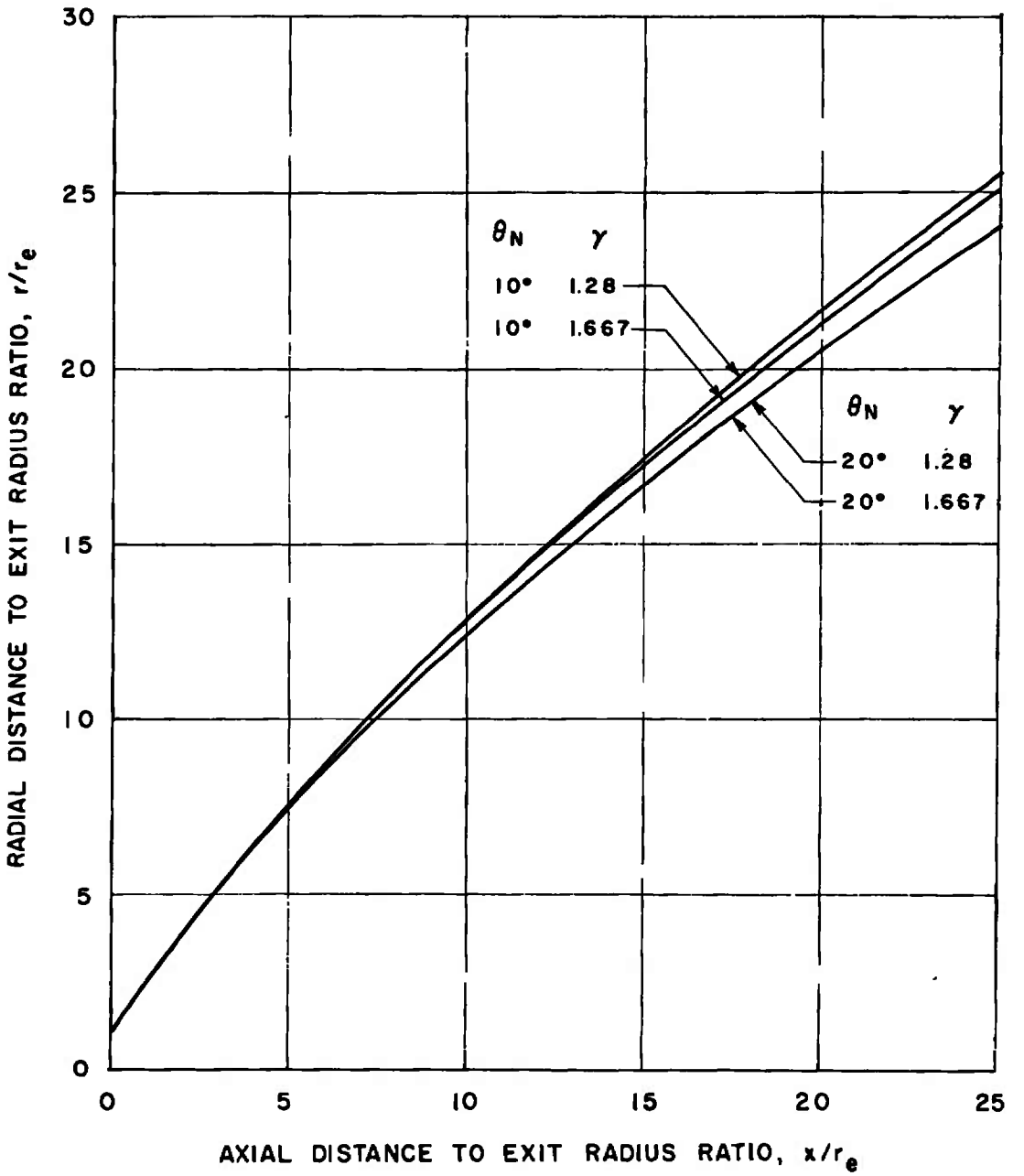

b. $M_1/y = 10$

Fig. 19 Continued

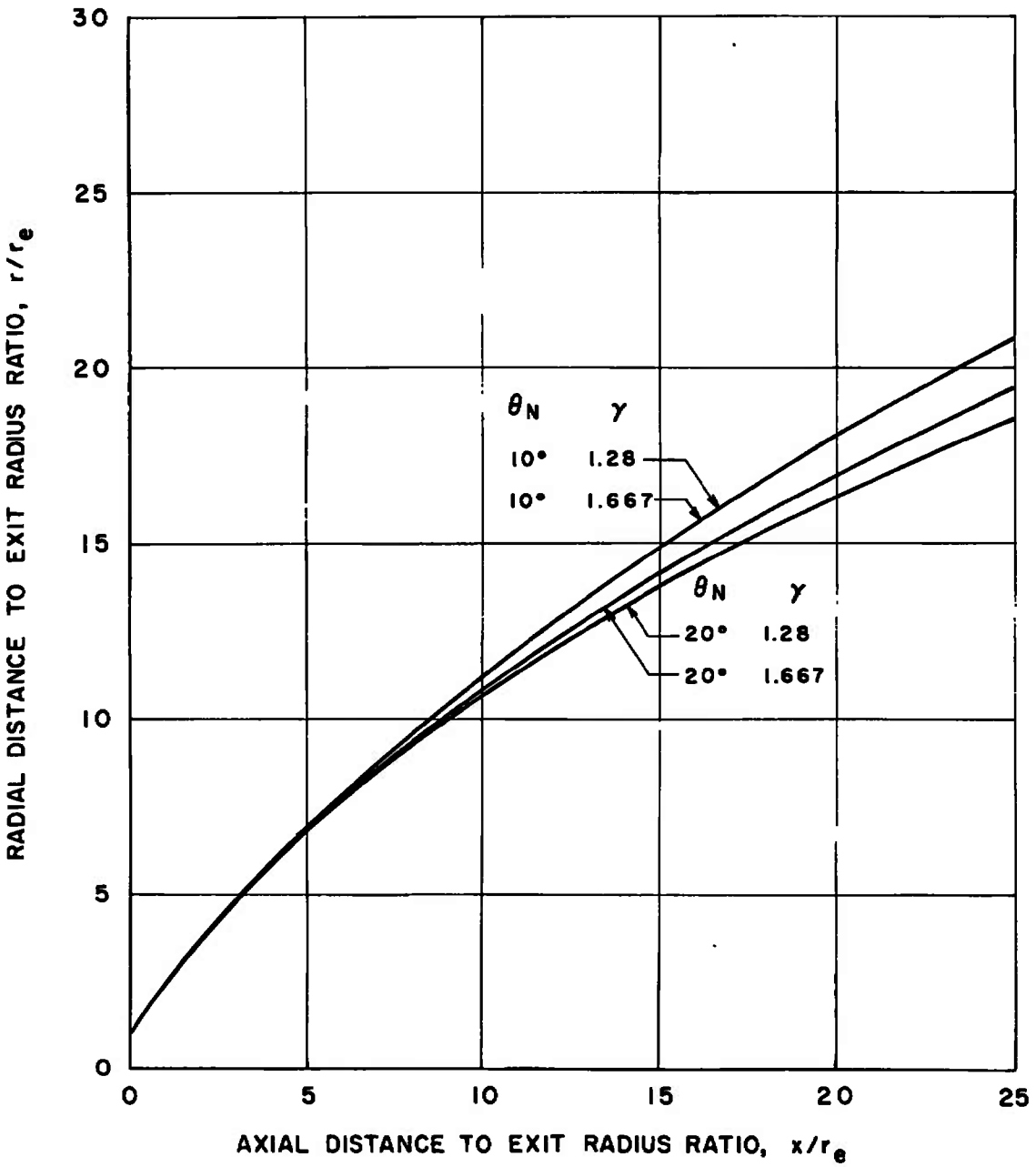

c. $M_1/\gamma = 7$

Fig. 19 Continued

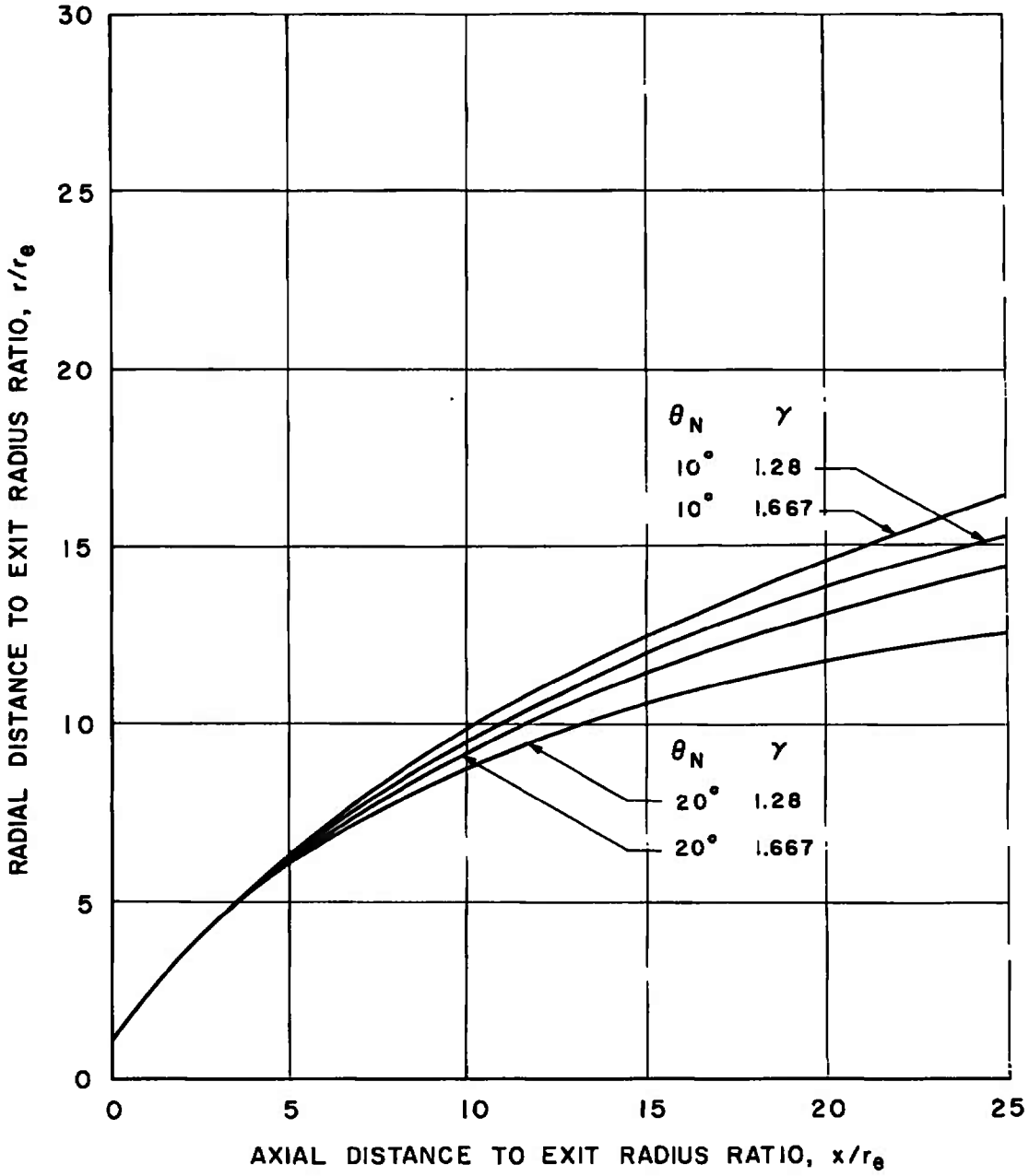

d. $M_1/\gamma = 5$

Fig. 19 Concluded

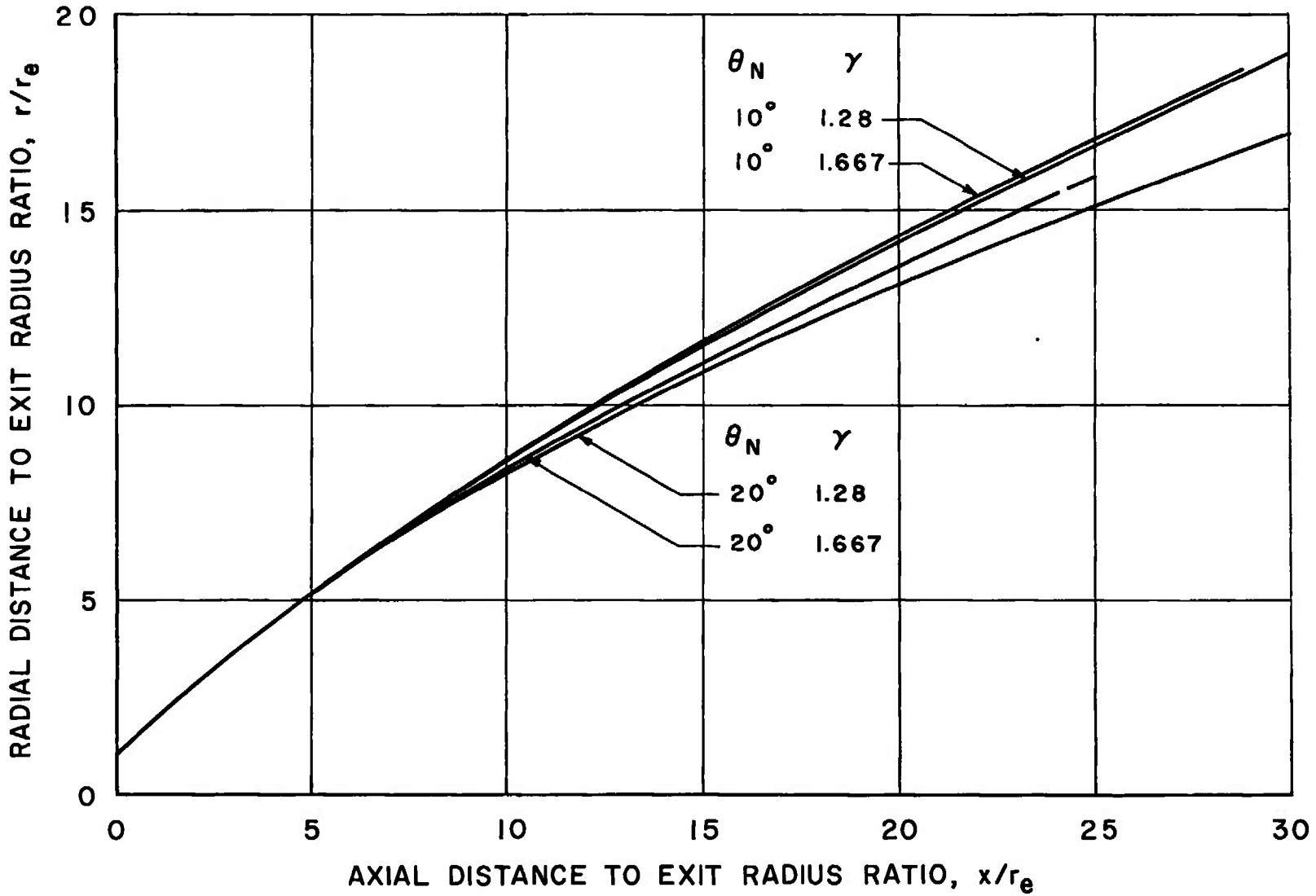

a. $M_1/\gamma = 10$

Fig. 20 Comparison of Jet Boundaries as Determined by a Method-of-Characteristics Solution for δ_i = 45 deg

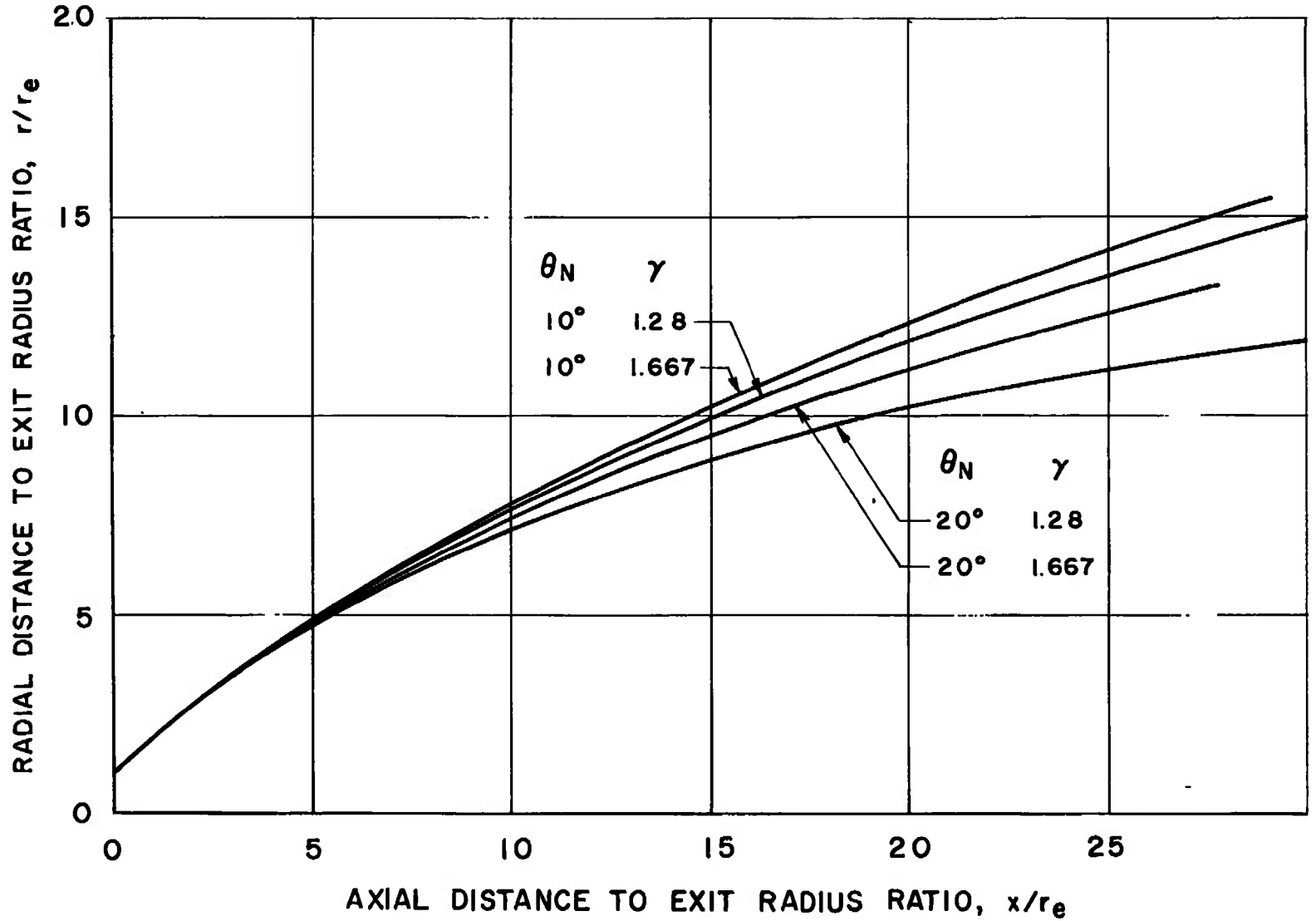

b. $M_1/\gamma = 7$

Fig. 20 Continued

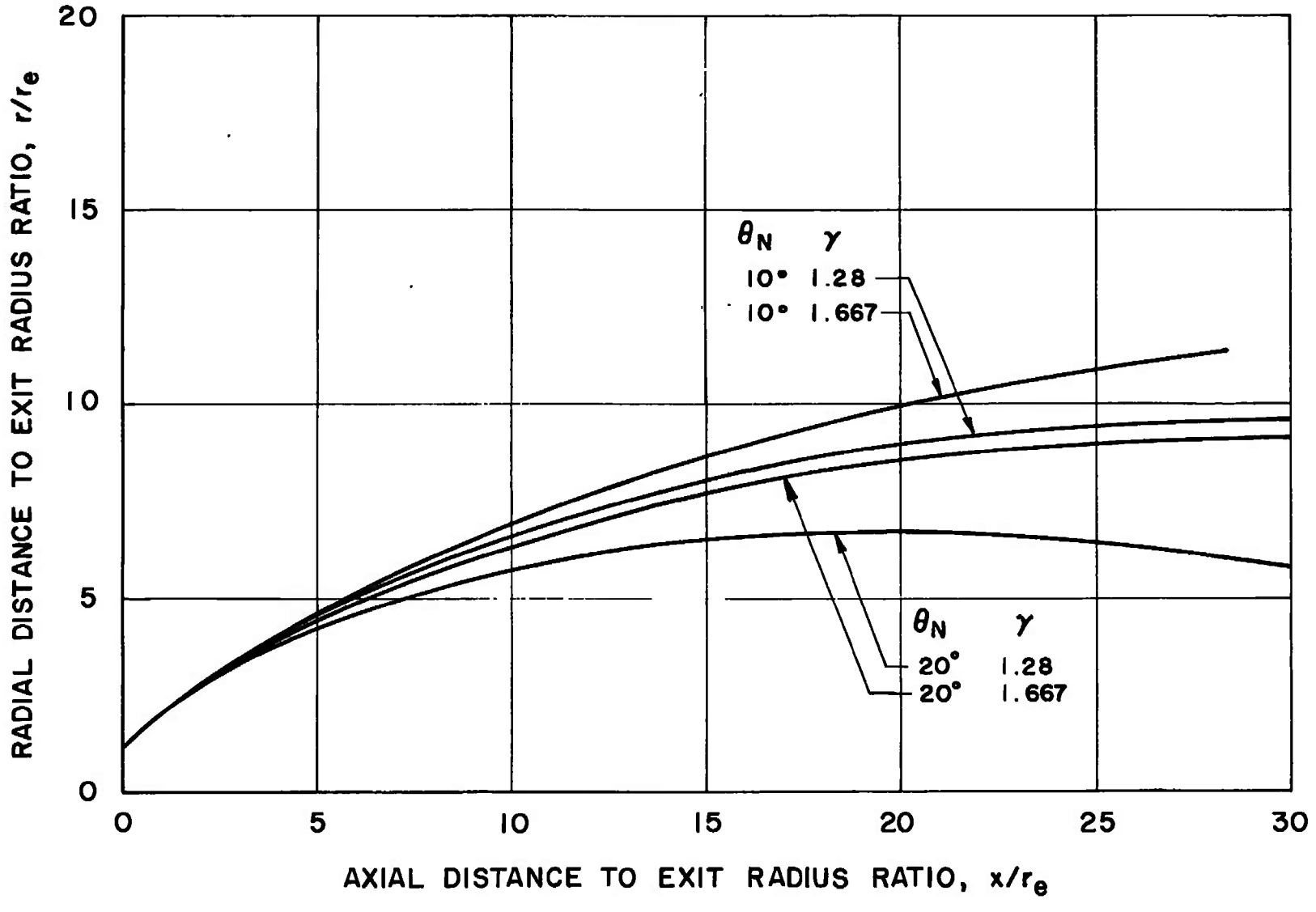

c. M_1/γ . 5

Fig. 20 Concluded

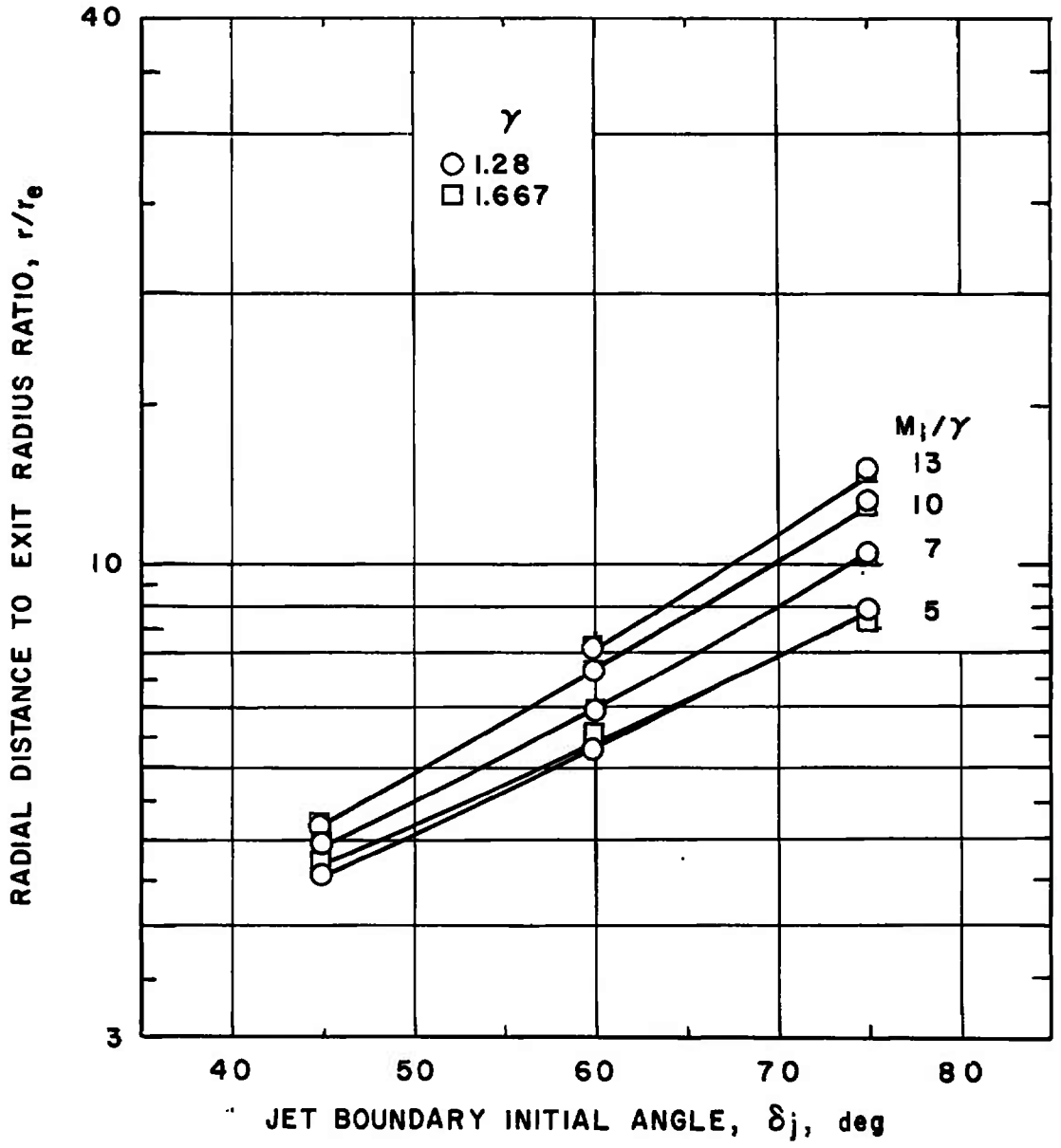

a. $x/r_e = 5$

Fig. 21 Effect of the Boundary Initial Angle on the Jet Radius at a Given Axial Distance for Nozzles with $\theta_N = 10$ deg

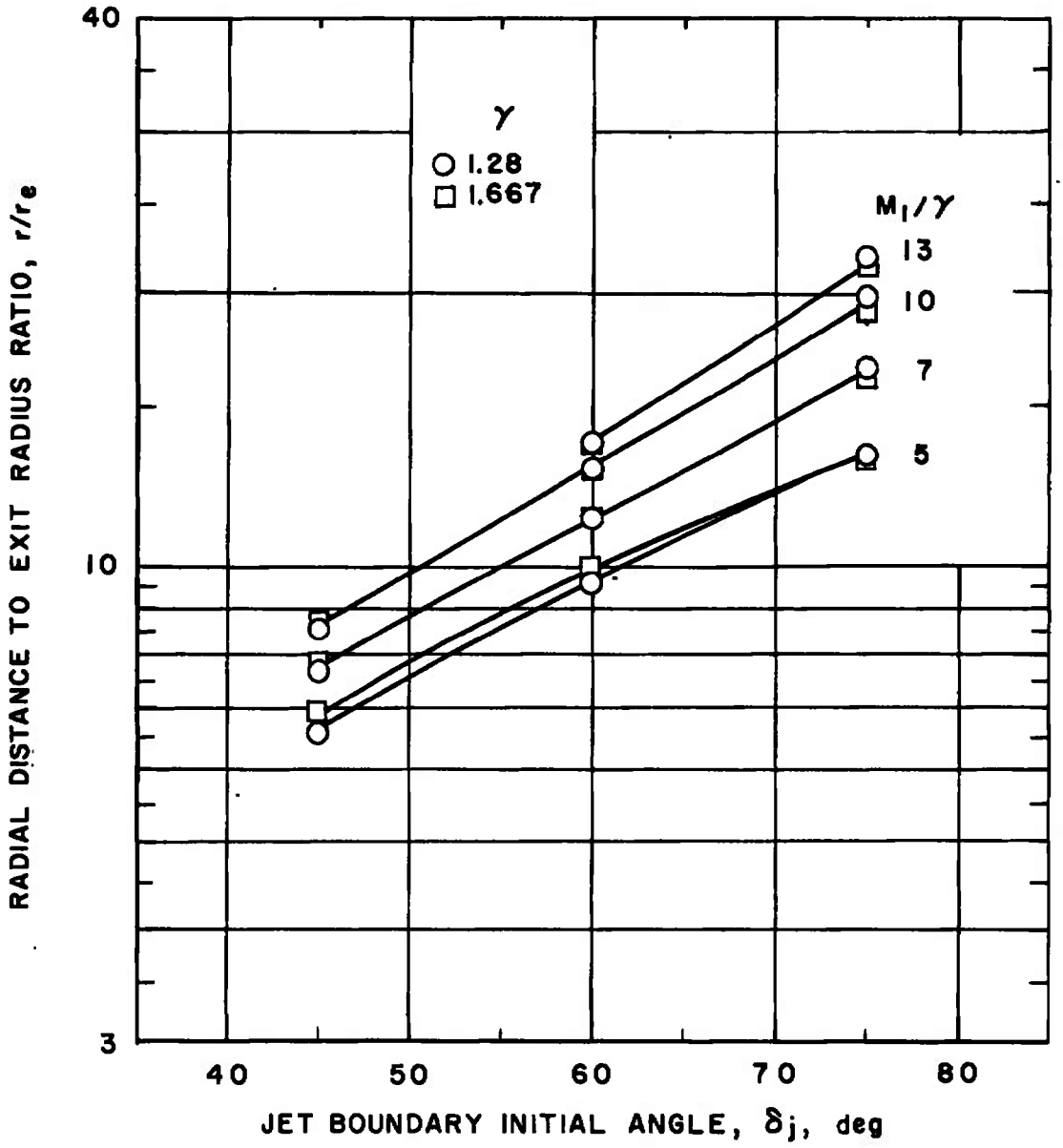

b. $x/r_e = 10$

Fig. 21 Continued

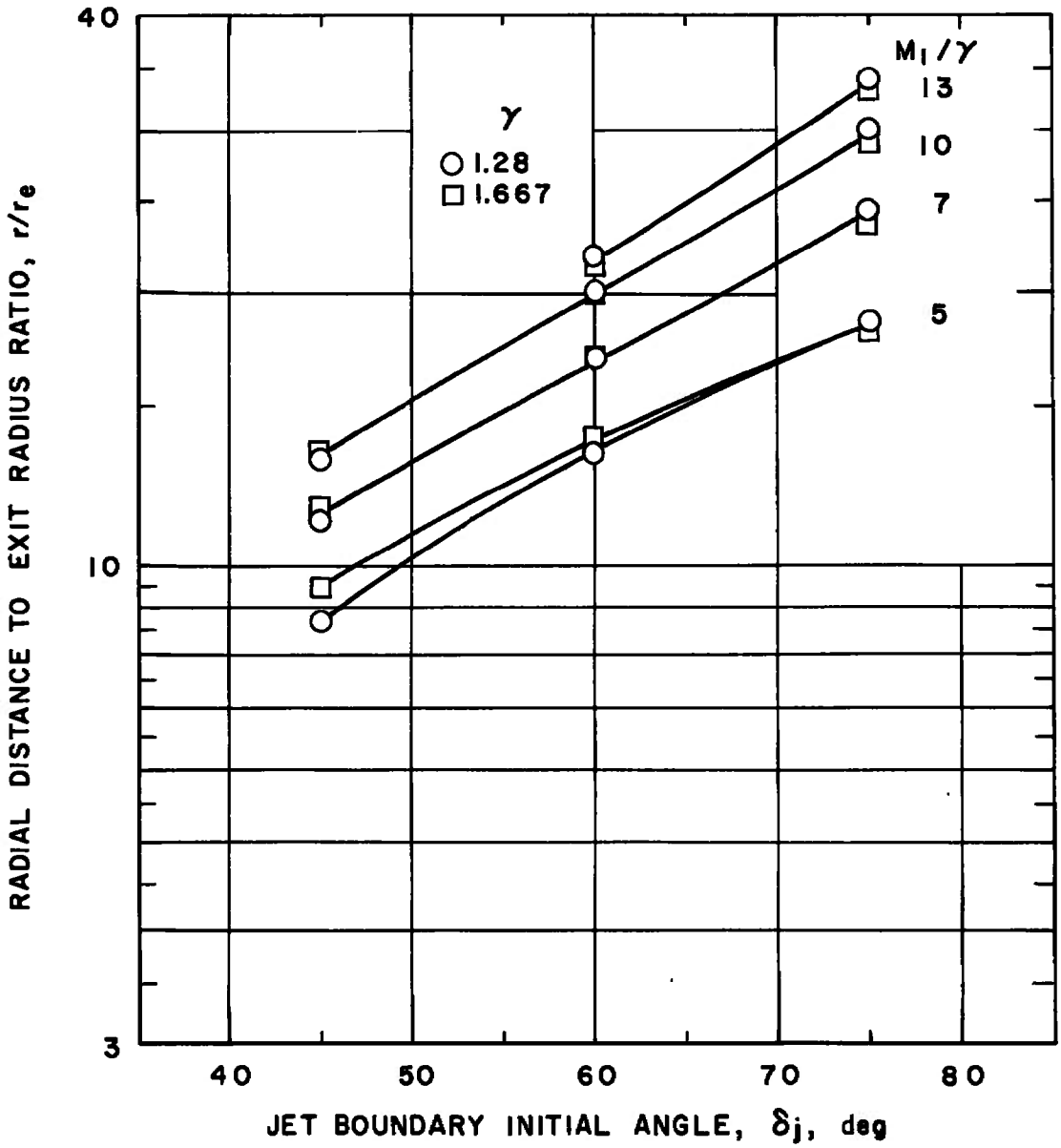

c. $x/r_e = 18$

Fig. 21 Continued

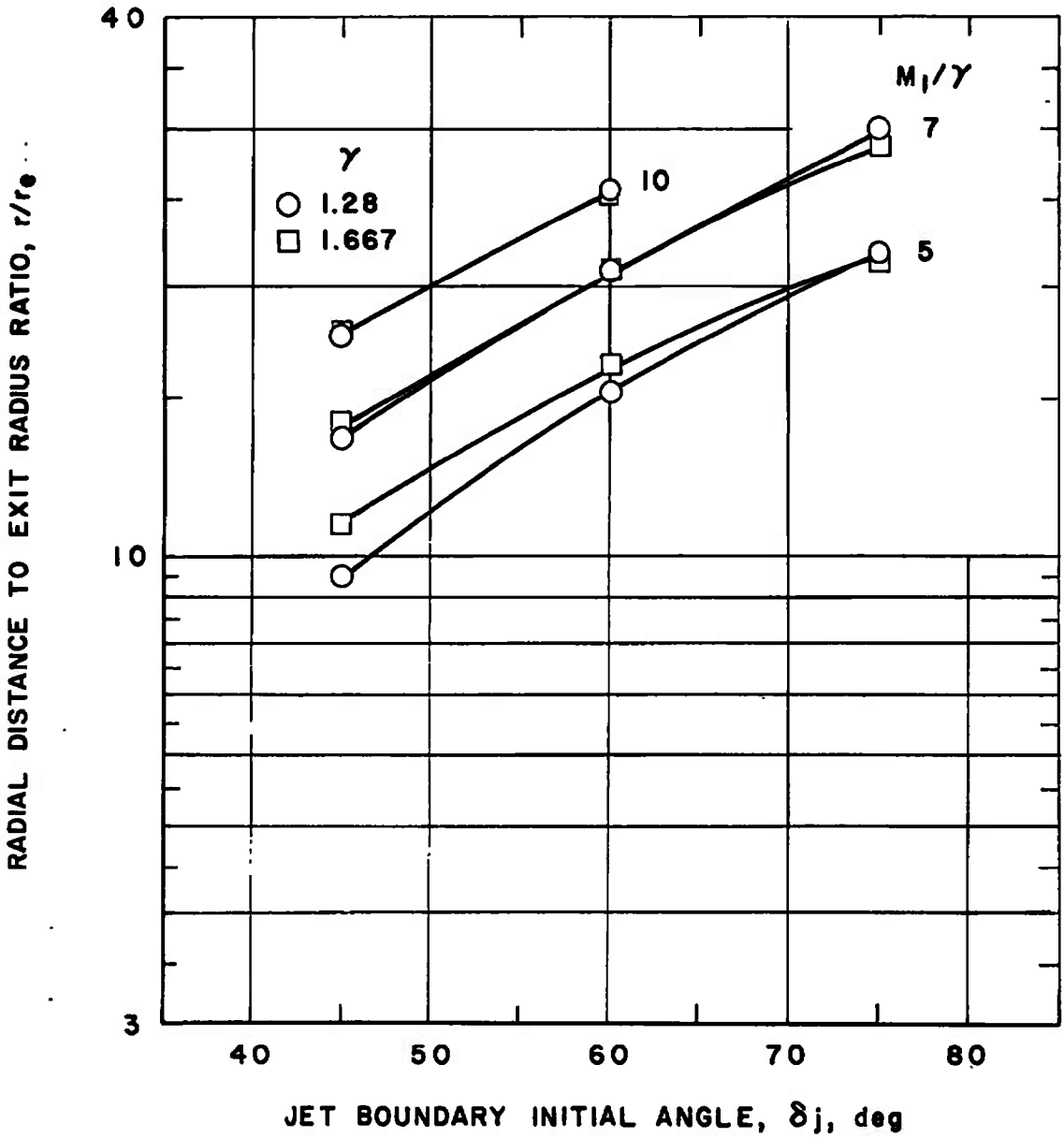

d. $x/r_e = 25$

Fig. 21 Concluded

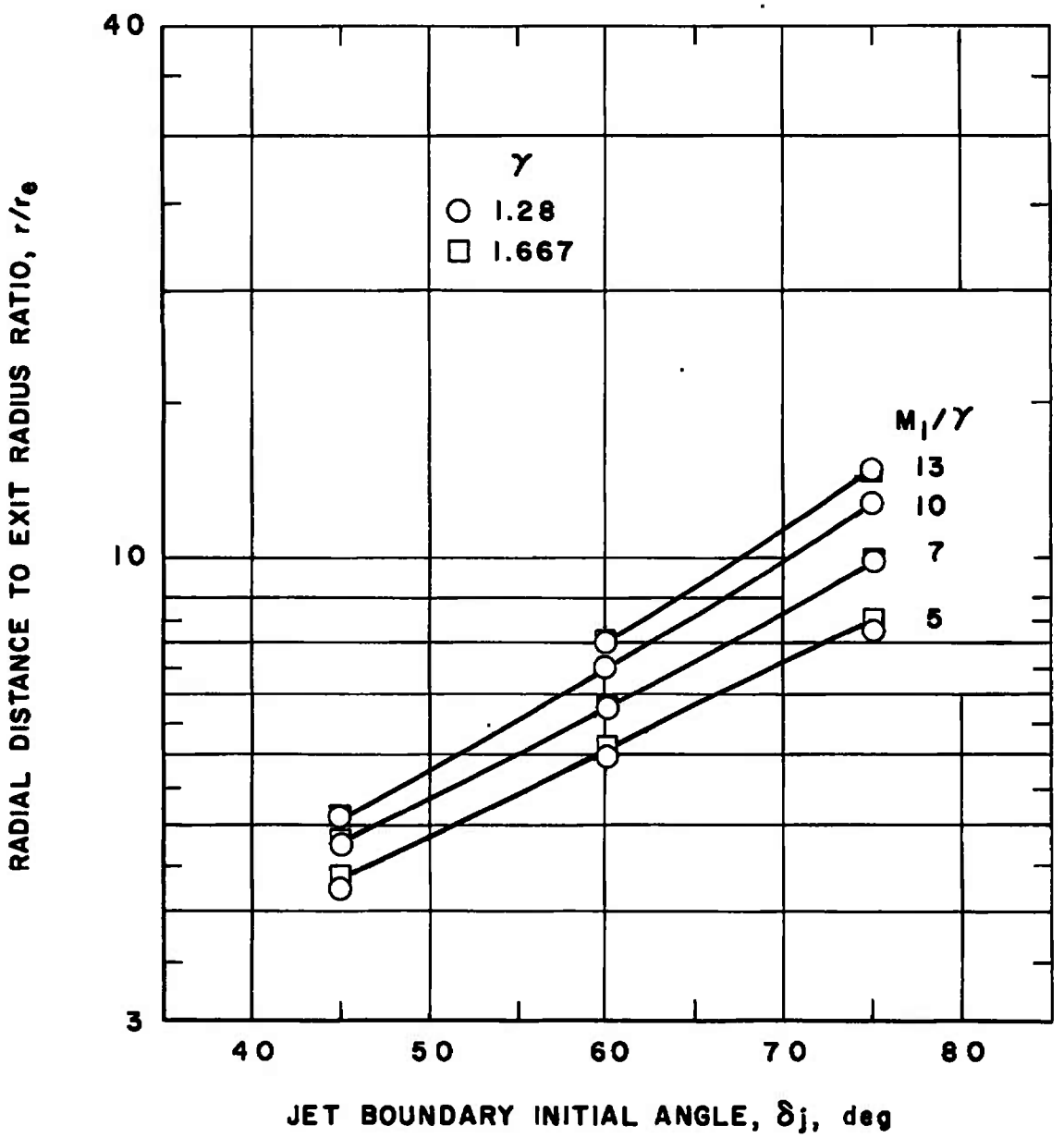

a, $x/r_e = 5$

Fig. 22 Effect of the Boundary Initial Angle on the Jet Radius at a Given Axial Distance for Nozzles with θ_N = 20 deg

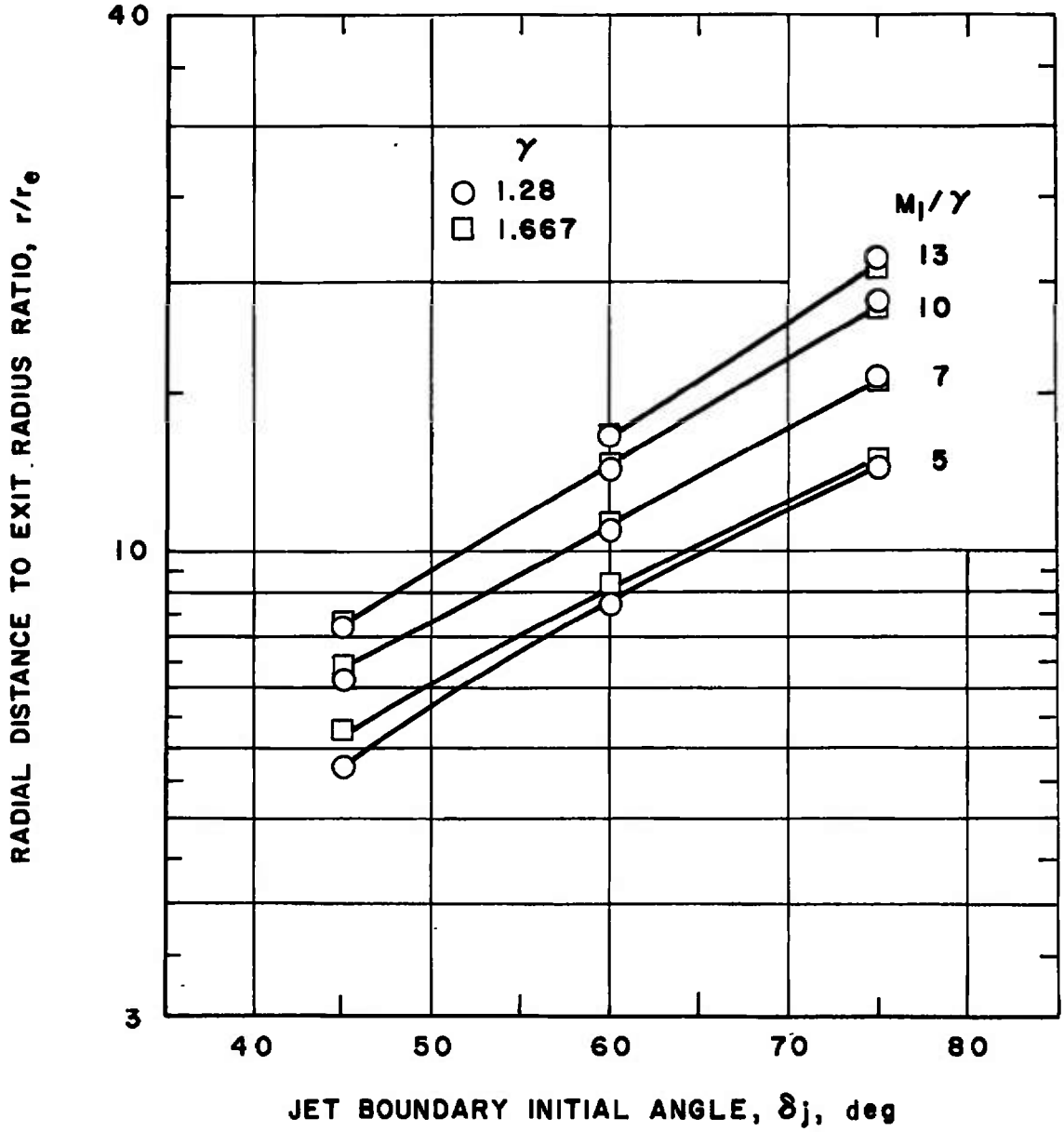

b. $x/r_e = 10$

Fig. 22 Continued

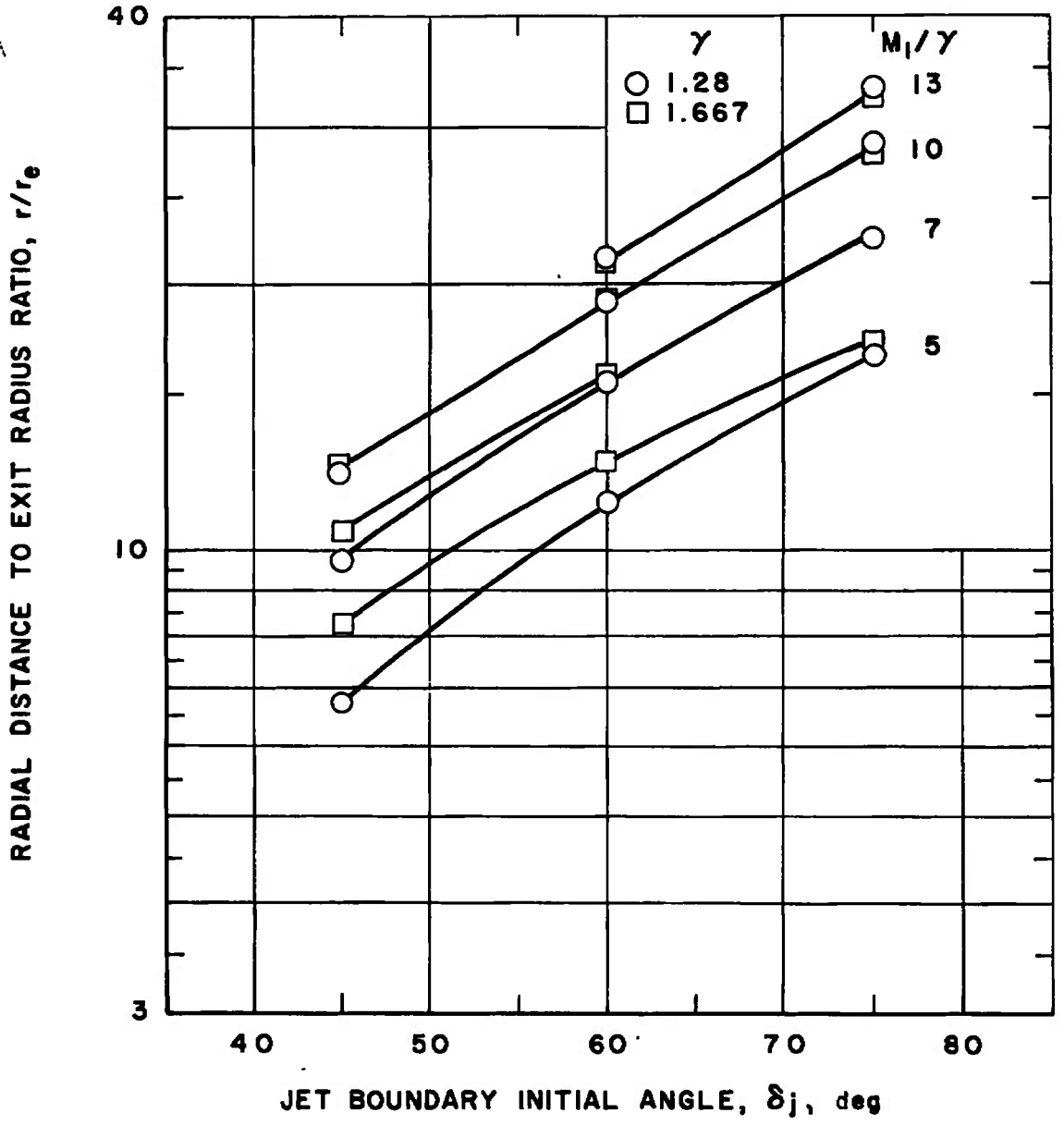

c. $x/r_e = 18$

Fig. 22 Continued

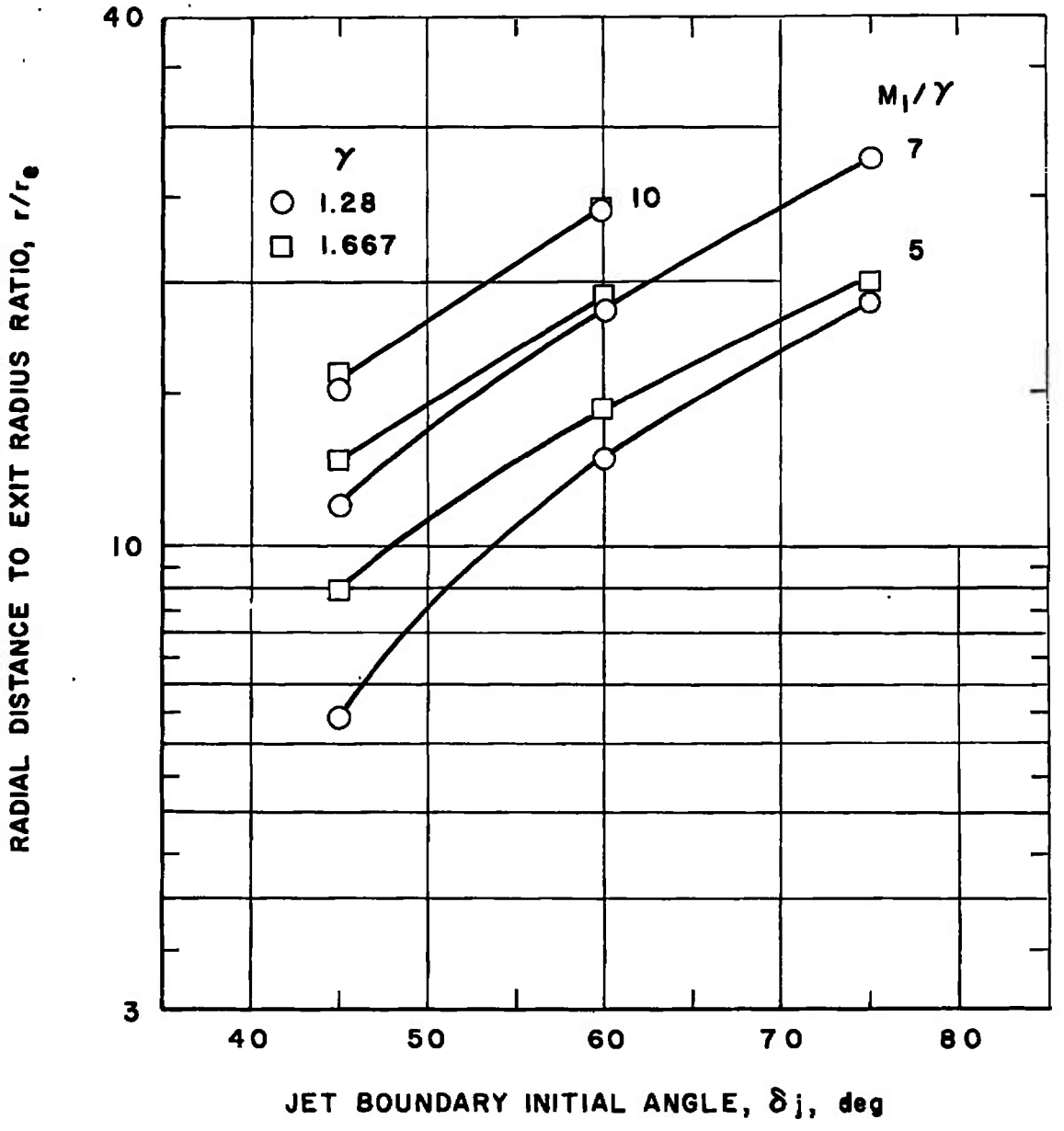

d. $x/r_e = 25$

Fig. 22 Concluded

TABLE I
FLOW PROPERTIES OF COMPUTED JETS MATCHING THE SIMULATION PARAMETERS $\gamma M_1^2/\beta_1$ AND δ_j

Case	δ_j, deg	$\gamma M_1^2/\beta_1$	θ_N, deg	γ	M_1	A_s/A^*	M_j	p_j/p_∞
1	60	10	10	1.28	7.747	8.677	3.399	345.5
2			20	1.28	7.747	16.016	3.920	147.8
3			10	1.40	7.071	2.887	2.597	222.4
4			20	1.40	7.071	4.585	3.083	106.1
5			10	1.667	5.912	1.187	1.566	127.7
6			20	1.667	5.912	1.533	2.002	68.2
7		14	10	1.28	10.891	20.946	4.152	1806
8			20	1.28	10.891	44.896	4.836	646.7
9			10	1.40	9.949	4.786	3.129	921.9
10			20	1.40	9.949	8.472	3.740	384.5
11			10	1.667	8.338	1.441	1.904	396.0
12			20	1.667	8.338	2.006	2.406	195.4
13		18	10	1.28	14.027	38.124	4.686	7331
14			20	1.28	14.027	90.935	5.509	2304
15			10	1.40	12.818	6.719	3.489	3010
16			20	1.40	12.818	12.807	4.201	1143
17			10	1.667	10.751	1.649	2.114	1003
18			20	1.667	10.751	2.404	2.672	467.3
19		22	10	1.28	17.158	58.573	5.084	24714
20			20	1.28	17.158	151.41	6.024	7033
21			10	1.40	15.682	8.549	3.750	8279
22			20	1.40	15.682	17.197	4.545	2927
23			10	1.667	13.159	1.816	2.259	2200
24			20	1.667	13.159	2.733	2.861	982.5

TABLE II
FLOW PROPERTIES OF COMPUTED JETS MATCHING THE SIMULATION PARAMETERS M_1/γ AND δ_j

Case	δ_j, deg	M_1/γ	θ_N, deg	γ	M_1	A_s/A^*	M_j	p_j/p_∞
25	75	5	10	1.28	6.400	2.728	2.405	406.6
26			20	1.28	6.400	4.135	2.771	217.3
27			10	1.667	8.335	1.047	1.270	976.9
28			20	1.667	8.335	1.265	1.685	541.5
29		7	10	1.28	8.960	5.504	3.015	2201.0
30			20	1.28	8.960	9.418	3.468	1029.0
31			10	1.667	11.669	1.152	1.506	3580.0
32			20	1.667	11.669	1.469	1.934	1933.0
33		10	10	1.28	12.800	11.123	3.609	17527.0
34			20	1.28	12.800	21.404	4.171	7144.0
35			10	1.667	16.670	1.265	1.686	15806.0
36			20	1.667	16.670	1.679	2.141	8227.0
37		13	10	1.28	16.640	17.541	3.998	95410.0
38			20	1.28	16.640	36.465	4.645	35450.0
39			10	1.667	21.671	1.341	1.787	50404.0
40			20	1.667	21.671	1.820	2.262	25621.0
41	60	5	10	1.28	6.400	5.230	2.972	154.1
42			20	1.28	6.400	8.810	3.412	73.2
43			10	1.667	8.335	1.410	1.940	395.6
44			20	1.667	8.335	2.005	2.406	195.1

TABLE II (Concluded)

Case	δ_j, deg	M_1/γ	θ_N, deg	γ	M_1	A_s/A^*	M_j	p_j/p_∞
45	60	7	10	1.28	8.960	12.729	3.723	677.6
46			20	1.28	8.960	25.054	4.310	268.8
47			10	1.667	11.669	1.717	2.175	1373.0
48			20	1.667	11.669	2.536	2.751	628.4
49		10	10	1.28	12.800	30.918	4.497	4345.0
50			20	1.28	12.800	70.991	5.268	1431.0
51			10	1.667	16.670	2.005	2.406	5694.0
52			20	1.667	16.670	3.116	3.057	2434.0
53		13	10	1.28	16.640	55.084	5.026	20419.0
54			20	1.28	16.640	140.680	5.948	5898.0
55			10	1.667	21.671	2.202	2.543	17450.0
56			20	1.667	21.671	3.536	3.250	7101.0
57	45	5	10	1.28	6.400	11.930	3.669	47.7
58			20	1.28	6.400	23.200	4.243	19.4
59			10	1.667	8.335	2.462	2.707	13.0
60			20	1.667	8.335	4.085	3.475	50.6
61		7	10	1.28	8.960	36.667	4.650	160.9
62			20	1.28	8.960	86.839	5.463	51.0
63			10	1.667	11.669	3.224	3.109	399.5
64			20	1.667	11.669	5.844	4.061	136.0
65		10	10	1.28	12.800	113.81	5.732	765.9
66			20	1.28	12.800	335.63	6.887	185.0
67			10	1.667	16.670	4.084	3.474	1479.0
68			20	1.667	16.670	8.035	4.625	443.7

UNCLASSIFIED
Security Classification

DOCUMENT CONTROL DATA - R & D

(Security classification of title, body of abstract and indexing annotation must be entered when the overall report is classified)

1 ORIGINATING ACTIVITY (Corporate author) Arnold Engineering Development Center ARO, Inc., Operating Contractor Arnold Air Force Station, Tennessee 37389	2a. REPORT SECURITY CLASSIFICATION UNCLASSIFIED 2b. GROUP N/A

3 REPORT TITLE
INVESTIGATION OF JET BOUNDARY SIMULATION PARAMETERS FOR UNDEREXPANDED JETS IN A QUIESCENT ATMOSPHERE

4 DESCRIPTIVE NOTES (Type of report and inclusive dates)
Final Report March 1965 to June 1967

5. AUTHOR(S) (First name, middle initial, last name)
R. D. Herron, ARO, Inc.

6. REPORT DATE September 1968	7a. TOTAL NO. OF PAGES 91	7b. NO. OF REFS 23

8a. CONTRACT OR GRANT NO. F40600-69-C-0001 b. PROJECT NO. Related to 8953, Task 895309 c. Program Element 6540223F d.	9a. ORIGINATOR'S REPORT NUMBER(S) AEDC-TR-68-108 9b. OTHER REPORT NO(S) (Any other numbers that may be assigned this report) N/A

10 DISTRIBUTION STATEMENT
This document has been approved for public release and sale; its distribution is unlimited.

11. SUPPLEMENTARY NOTES Available in DDC.	12. SPONSORING MILITARY ACTIVITY Arnold Engineering Development Center (AETS), Arnold Air Force Station, Tennessee 37389

13. ABSTRACT

An experimental and theoretical investigation was conducted to determine the degree of jet boundary simulation obtainable for underexpanded jets exhausting into a quiescent atmosphere. Tests were conducted with nitrogen, carbon dioxide, and helium gases, and theoretical boundaries were obtained by a method-of-characteristics solution. It was determined that the method-of-characteristics solution accurately represents the experimental jet boundaries and that the matching of the parameters δ_j and M_1/γ gives good boundary simulation for a wide range of jet conditions. Also a rapid, simple method for estimating jet boundary shape is developed from the method-of-characteristics results.

DD FORM 1 NOV 65 1473

UNCLASSIFIED
Security Classification

14 KEY WORDS	LINK A		LINK B		LINK C	
	ROLE	WT	ROLE	WT	ROLE	WT
boundaries, jet						
simulation techniques						
jets, cold						
jets, underexpanded						
nitrogen						
carbon dioxide						
helium						